Design, synthesis and characterization of artificial extracellular matrix proteins for tissue engineering.

DESIGN, SYNTHESIS AND CHARACTERIZATION OF ARTIFICIAL EXTRACELLULAR MATRIX PROTEINS FOR TISSUE ENGINEERING

A Dissertation Presented

by

ALYSSA PANITCH

Submitted to the Graduate School of the
University of Massachusetts Amherst in partial fulfillment
of the requirements for the degree of

DOCTOR OF PHILOSOPHY

September 1997

Department of Polymer Science and Engineering

DESIGN, SYNTHESIS AND CHARACTERIZATION OF ARTIFICIAL EXTRACELLULAR MATRIX PROTEINS FOR TISSUE ENGINEERING

A Dissertation Presented

by

ALYSSA PANITCH

Approved as to style and content by:

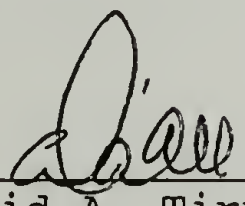

David A. Tirrell, Chair

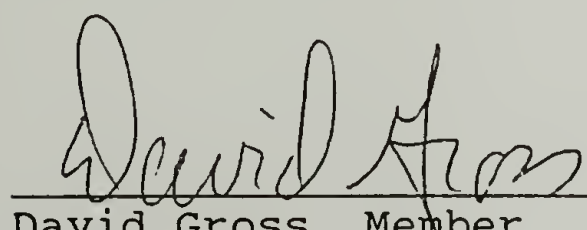

David Gross, Member

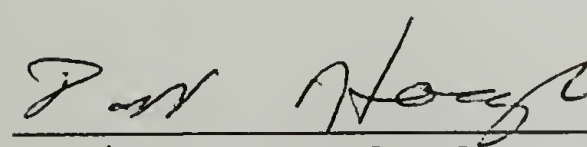

David A. Hoagland, Member

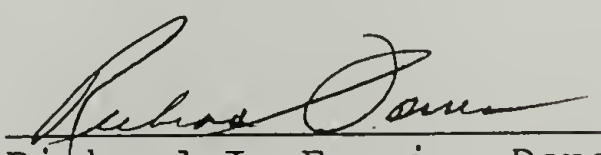

Richard J. Farris, Department Head
Department of Polymer Science and Engineering

ACKNOWLEDGMENTS

I am deeply indebted to my mentor, professor David A. Tirrell, for his guidance in my development as a scientist. He has bestowed in me a strong sense of confidence and independence as well as integrity which will carry me into the future.

I would like to thank my committee members for their suggestions and guidance. Their insights kept me from veering off course.

I owe a special thanks to my undergraduate advisor, Michael Malone, for his never ending belief in me and my ability, for his often sought after advice, and for instilling in me the belief that I could reach this goal.

My family has been a continual source of strength for me as I have strived to achieve my goals. Without endless rambling I wish to thank you. Your support has meant the world to me.

Special thanks to Linda Strzegowski who not only provided her secretarial expertise but her wisdom and friendship as well.

I wish to thank the support staff, technicians and secretaries of the Polymer Science and Engineering Department who were ever patient in their teachings and in ensuring that all of my requirements were fulfilled.

The publication containing my work on high cell density fermentation was a collaborative effort. Many thanks to

Eric Cantor and Kunio Matsuki for their work on the DNA construction and protein expression, to Ted Atkins and Sharon Cooper for their contributions to the solid state analysis, and to Dave Tirrell, Skip Fournier and Tom Mason for their many helpful suggestions and scientific interpretations throughout the duration of the work.

Many thanks to all of the members of the Tirrell group past and present for their help and advice. I wish to acknowledge specifically (soon to be Dr.)Karen Guhr and Dr. Jennifer Griffiths for scientific conversations and advice, but most of all for friendships that will span a life time. Dr. Tetsuji Yamaoka was especially helpful in teaching me cell culture techniques. I am greatly indebted to him for his time, patience, teachings and friendship. Kean Hock Yeap was a source of never ending optimism while he worked with me on the construction of genes encoding the artificial extracellular matrix proteins. His calming influence and his friendship were very important to me. Thank you all!

Finally, I wish to thank my friends outside of the scientific arena. Thank you for reminding me constantly that there is life outside of the lab, for understanding the demands of the goals I have set for myself, and for always being there for emotional support. You know who you are...

ABSTRACT

DESIGN, SYNTHESIS AND CHARACTERIZATION OF ARTIFICIAL EXTRACELLULAR MATRIX PROTEINS FOR TISSUE ENGINEERING

SEPTEMBER 1997

ALYSSA PANITCH, B.A., SMITH COLLEGE

B.S., UNIVERSITY OF MASSACHUSETTS AMHERST

Ph.D., UNIVERSITY OF MASSACHUSETTS AMHERST

Directed by: Professor David A. Tirrell

Artificial extracellular matrix proteins were synthesized using recombinant DNA technology. These proteins were meant to mimic the internal elastic lamina of the tunica intima of muscular arteries for use in the design of small diameter (<6 mm) vascular prostheses. These proteins are composed of two blocks, an elastin-like block made up of repeats of the pentapeptide (VPGIG) and a cell binding segment which is composed of the CS5 region of fibronectin. Proteins of the following sequence were designed, synthesized and characterized: $(CS5(VPGIG)_{40})_3$ and $(CS5(VPGIG)_{20})_5$. Successful synthesis and purification were confirmed by NMR spectroscopy and amino acid analysis.

These artificial extracellular matrix proteins were designed with both controlled structural integrity and endothelial cell binding ability. The presence of a lower critical solution temperature (LCST) for both proteins

suggests that the properties of the elastin like blocks were maintained. The endothelial cell binding ability of the CS5 region of fibronectin was also retained, as demonstrated through human umbilical vein endothelial cell (HUVEC) adhesion and spreading on the proteins, as well as through inhibition of this adhesion through preincubation of the HUVECs with soluble GREDVDY peptide which is known to inhibit $\alpha_4\beta_1$ integrin binding to CS5. Equivalent numbers of HUVECs adhered to $(CS5(VPGIG)_{20})_5$ and to fibronectin, although the number of cells well spread on the former was only approximately 55% of the number of those well spread on fibronectin.

TABLE OF CONTENTS

LIST OF TABLES

LIST OF FIGURES

LIST OF FIGURES

CHAPTER 1

INTRODUCTION

The field of tissue engineering draws upon multiple disciplines to achieve its goal of the design of new materials for tissue regeneration. It is a rapidly expanding field where knowledge about cell-cell and cell-material interactions, as well as about cell-protein, cell-chemical and cell-mechanical interactions are drawn upon to design materials that will optimize cell growth and differentiation and tissue regeneration both *in vitro* and *in vivo*. Extensive research is being conducted on materials for growth of new skin, liver, bone, cartilage and arteries, among other tissues.[1-3] These materials are often scaffolds that support cells and allow them to attach, proliferate, differentiate, and secrete their own scaffolding or extracellular matrix. Each organ has its own characteristics important in the successful design of synthetic materials for cell scaffolding; the composition of the extracellular matrix differs from tissue to tissue. While cartilage supports the weight of the body, blood vessels provide the transport network for nutrients and waste; in view of these differing functions, it is not surprising that cartilage is composed of more connective tissue, a collagen rich matrix, while muscular arteries are composed of more muscular tissue. Materials for

regeneration of any organ must provide the proper signals for the defined organ.

1.1 Vascular Grafts

Vascular grafts, or artificial blood conduits, are used to replace damaged or diseased vessels. New materials for small diameter vascular grafts are needed. The current gold standard for bypass surgery, autologous saphenous vein, has a 30% failure rate due to stenosis within five years.[4] Expanded polytetrafluoroethylene (PTFE) and polyethylene terephthalate (PET) are also available for vascular graft implantation; however, the patency rate of these materials is lower than that of saphenous vein[5]. Desirable materials would provide a vessel viable for the life of the patient.

Novel artificial extracellular matrix proteins can readily be designed and synthesized utilizing recombinant DNA technology. These proteins may contain isolated biological signals or a combination of signals. More specifically, cell adhesion domains such as the peptide Arg-Gly-Asp (RGD) can be designed into the backbone of the protein.[6] It is equally possible to synthesize materials which contain heparin binding domains, collagen binding domains, or protease degradation sites. Mechanical properties of the protein can also be controlled; one way to accomplish this is by designing an elastomeric-type protein endowed with mechanical properties similar to those of native elastin.[7-9] Elastin is an extracellular matrix

protein which composes the bulk of elastic fibers; these fibers are found, among other places, in the intima of muscular arteries.[10] We have synthesized an elastomeric protein containing (i) repeats of (VPGIG) (the single letter amino acid code is used in this and all subsequent protein sequences), and (ii) the CS5 domain of fibronectin, an integrin binding domain containing the REDV sequence.[11] This protein binds human umbilical vein endothelial cells (HUVECs) and is expected to exhibit mechanical properties similar to those seen in chemically synthesized repetitive polymers of (VPGVG), a pentapeptide repeat occurring up to 11 times consecutively in native elastin.[12]

In the case of vascular grafts it is likely that an elastic material will be better than a rigid material, as arteries are quite elastic. A material must be sufficiently viscoelastic to maintain flow during diastole[5] and must have sufficient structural integrity so that the new artery does not burst during systole. Materials must be porous enough (~100 μm) to allow diffusion of metabolites and migration of cells (such as smooth muscle cells to form a media), yet they must remain mechanically sound. The materials must be biocompatible if they are to be implanted in the body; a material that elicits a severe immune response will likely be rejected while those that elicit an inflammatory response may be "walled off" by fibrous tissue deposition.[13] In addition, these materials must interact favorably with the cells of the vasculature including endothelial cells, smooth

muscle cells and platelets. Materials should not promote thrombosis or intimal hyperplasia. To date, native tissue is optimal for its function. This knowledge must be utilized in the design of new materials. The ideal synthetic scaffold will support cell growth and differentiation as well as maintain mechanical integrity until the seeded or ingrowing cells secrete their own extracellular matrix. Finally, the synthetic material should degrade, leaving in its stead a native tissue.[1-3]

Selecting a suitable material for vascular graft fabrication is quite complex. Vascular grafts are immediately exposed to the blood, allowing for the rapid deposition of blood-borne proteins. These proteins are deposited on the graft surface. Proteins present in the bloodstream at the highest concentrations are initially deposited in the highest concentrations. Over time equilibrium prevails; those proteins which adhere most strongly to the vascular graft material will be present at higher concentration than seen initially.[14]

The adhesion of blood-borne proteins to foreign material, in particular fibrinogen,[15] often promotes platelet adhesion. This may trigger a cascade of events[16] leading to thrombosis, atherosclerosis and ultimately to graft failure. Exposure to the blood stream also invokes an immune or foreign body response. This response has been extensively studied and is found to be dependent on graft material. In general, bioresorbable materials[17] elicit a

greater foreign body response (which terminates after complete resorption) than nonresorbable materials, but the response to the nonresorbable material continues indefinitely. One approach to the problem of protein adhesion is the modification of surfaces to create nonadhesive interfaces. The modification of polyethylene terephthalate (PET) surfaces with polyethylene oxide (PEO)(which increases both the hydrophilicity and mobility of the surface by motion of the PEO) has been used to make surfaces less adhesive to proteins and cells,[18] hence, less thrombogenic. PTFE has been modified by plasma polymerization of tetrafluoroethylene to PTFE films followed by adhesion of albumin. Plasma polymerized PTFE shows an increased affinity for albumin.[19] Surfaces pretreated with albumin are less adhesive toward platelets. Conversely, plasma polymerized PTFE in the presence of oxygen has been shown to increase the retention of fibronectin and laminin, hence increasing the adhesion of HUVECs.[20]

Healthy vasculature is lined with a monolayer of endothelial cells which serves many functions including creating a naturally nonthrombogenic surface. It may be possible to achieve a monolayer of endothelial cells lining the luminal surface of a vascular graft via the growth of capillaries through the wall of the implant and the subsequent migration of endothelial cells to the graft surface. The use of highly porous (60μm internodal distance) ePTFE has been shown to allow capillary ingrowth

through the walls of the vessel and migration of capillary endothelial cells onto the graft to form a continuous layer of endothelial cells in both primates[21] and canines.[22] However, in humans the only endothelial cell migration in currently available vascular grafts occurs from the ends of the graft and proceeds for only 8-10mm before stopping, leaving the center of the graft devoid of endothelial cells.[21]

Another approach to designing patent vascular grafts is to preseed the graft with endothelial cells.[23] This is done to form a nonthrombogenic surface which appears, on the macroscopic level, to be similar to the native vessel. Preseeding of vascular material has not yet been shown to be an effective method for increasing the patency rate in humans. However, preliminary data from the labs of both Peter Zilla[24] and Stewart Williams (personal communication) suggest patency rates of autologously preseeded PTFE grafts are equal to autologous saphenous vein at 5 years post-implantation.

An alternative method for seeding of endothelial cells is the use of short peptide sequences for cell binding.[25] RGDS and related peptides have been shown to bind a variety of cell types through integrin receptors on the cell surface.[26] Grafting of RGD sequences to PTFE surfaces has shown an enhancement of endothelial cell binding to the graft material *in vitro* both in the absence and in the presence of flow.[27] Massia *et al.* covalently bound both

RGDS and REDV to glycophase glass, glass which has been treated with (3-glycidoxypropyl)trimethoxysilane followed by hydrolysis of the oxirane moieties to form diols, and demonstrated that cells would adhere to the peptide-modified surface of the glass.[28] They also found that endothelial cells, but not smooth muscle cells, platelets, or fibroblasts would adhere to the REDV modified glass surface.[29] This demonstrates the ability to adhere selectively certain cell types to surfaces through these peptides. In addition, it has been shown that cell adhesion and proliferation are dependent on the density of adhesion peptides.[30] The density of the peptides may be used to control the action of the adherent target cells. Although these peptides may be readily grafted to the surface of existing materials, making these materials more adherent toward cells, they do not alter the overall properties of the materials. Grafting peptides to PTFE and PET does not improve the mechanical properties of these materials, nor does it promote degradation.

A material which supports a monolayer of endothelial cells while inducing them to produce their own matrix, allows the endothelium to remain in an inactivated state, and is conducive to the development of an intima and a media comprises an optimal vascular graft material.

1.2 Material Design Through Genetic Engineering

Genetic engineering is a powerful technique that, when combined with ideas from polymer science, allows the researcher to design materials with precise molecular sequences and controlled architecture. We and others have previously reported the biosynthesis of highly repetitive, monodisperse, silk-like proteins, including derivatives containing non-proteinogenic amino acids or elastomeric domains.[31-37] The successful synthesis of elastin-like proteins by this method has also been reported.[7,8] In addition, we have described the successful synthesis of poly(alanylglycine) in multigram quantities,[38] and have subsequently applied the described technique to produce multigram quantities of a variety of recombinant proteins in our laboratory. The ability to synthesize multigram quantities of protein is critical for vascular graft design, as reasonable quantities of material must be readily available for mechanical testing and processing of prosthetic devices.

Due to the ability to control precisely the amino acid sequence of recombinant proteins, we felt it would be possible to design an elastomeric protein containing integrin binding domains that would bind endothelial cells while remaining nonadhesive toward smooth muscle cells, platelets and fibroblasts.[29] In addition to controlling the sequence of the domains, we are able to dictate the density of the domains, which has been shown to be important in cell

adhesion, spreading, focal adhesion contact formation,[39] and cell motility.[40] This elastin-like protein could be used as the innermost tunica of a vascular graft. Since this material is protein, it is thought that it will eventually be degraded by the body through natural processes which will result in nontoxic units that can be utilized by the body or cleared from the body through normal channels.

In the work reported herein, recombinant proteins were designed based on the pentapeptide repeat (VPGIG) which is known to form a beta turn structure and to have mechanical properties similar to those of native elastin.[12,41] Periodically interspersed with the pentapeptide repeat is the CS5 region of fibronectin, which has been shown to bind to the $\alpha_4\beta_1$ integrin receptor,[11,42-44] a receptor which is found on HUVECs but has not been found on smooth muscle cells, platelets or fibroblasts.[29,45,46] Scheme 1 shows the sequence of the CS5 region plus amino acids resulting from the linking of the segments at the DNA level.

Scheme 1.

CS5 = (*LD*GEEIQIGHIPREDVDYHLYP**GVP**)

GVP = insertion site for (VPGIG)
LD = amino acids resulting from DNA linking

The amino acid sequences of the complete proteins are:

$MG(CS5(VPGIG)_x)_yLE$

Where X, Y = 20, 5 or 40, 3

The entire CS5 region of fibronectin was incorporated into the protein because it was expected that conformation of the

REDV peptide was important for HUVEC binding. Hubbell *et al*. demonstrated that GREDVY peptide coupled to a surface through the amino terminus was recognized by HUVECs as an adhesion site, while the same peptide coupled through the carboxyl terminus did not appear to be recognized by the HUVECs as it did not promote adhesion.[29] This was further confirmed by Nicol *et al*. when short forms of the REDV peptide were incorporated, through chemical synthesis, into repeats of $(VPGVG)_x$ and no HUVEC binding was observed;[47] however, incorporation of short RGD peptides into proteins composed of (VPGVG) repeats does promote endothelial cell binding, indicating that the elastin backbone is compatible with cellular adhesion.[48]

The recombinant proteins, $(CS5(VPGIG)_{40})_3$ and $(CS5(VPGIG)_{20})_5$, serve two functions: the CS5 region provides the signals for cell adhesion while the (VPGIG) repeat provides the desired mechanical properties. The construction of the proteins was based on two DNA monomers that encode the CS5 region or the (VPGIG) repeats, respectively. These monomers were interconnected through cohesive ends to build the genes of interest, which were cloned into an *Escherichia coli* expression host.

1.3 Tissue and Organ Complexity

These novel extracellular matrix proteins are meant to serve as the internal elastic lamina of an artery. However, as with other organs, the arteries are composed of more than

one tissue. In most tissue engineering applications, it is likely that more than one material will be necessary to rebuild the tissue of interest. Different materials elicit different responses from cells. Chondrocytes cultured on type 1 collagen secrete large amounts of collagen, while the same chondrocytes cultured on polyglycolic acid secrete large quantities of proteoglycans.[49] Several signals may be necessary to create the optimal environment for tissue regeneration, while more than one material may be necessary to achieve the desired mechanical properties or even the desired structure.

Arteries are made up of three layers or tunicas.[10] The composition of each tunica is different, both in dominant cell type and in extracellular matrix composition. The three tunicas, as seen from the lumin outward, are the tunica intima, the tunica media, and the tunica adventitia. The muscular arteries are the vessels of interest for vascular graft design, for it is these arteries that fail.[5] The tunica intima of muscular arteries is lined with a monolayer of endothelial cells which lie on a basal lamina. Immediately juxtaposed to the endothelium is an internal elastic membrane.[10] Elastic, artificial extracellular matrix proteins such as those based on the (VPGIG) repeat may be able to mimic this tunica. The tunica media of these arteries consists largely of smooth muscle cells surrounded by collagen.[10] An artificial collagen which binds smooth muscle cells may be able to mimic the tunica media. The

adventitia consists of both elastic and collagen fibrils and fibroblasts.[10] It will be possible to blend the elastin like proteins with collagen analogues to mimic both the tunica media and the adventitia. Multilayered vascular grafts can then be fabricated to produce vascular prostheses.

1.4 High Cell Density Fermentation

In order to fabricate grafts it is necessary to produce the graft materials in large quantities. We have found through batch fermentation that it is possible to produce 10-100 mg/l of recombinant protein. Considering the best case where 100 mg/l of protein was produced, a 10 l fermentation is necessary to produce 1 g of recombinant protein. This is not time or cost effective. Through a fed batch fermentation process which is a modification of the process by Riesenburg *et al.*[50] we have been able to improve protein yields so that we can recover approximately 1 g/l of recombinant protein.

1.5 Dissertation Plan

Chapter 2 describes the high cell density fermentation procedure as well as the design, synthesis and characterization of poly(alanylglycine). Batch and fed batch fermentations are compared and the recombinant protein is evaluated by NMR spectroscopy, elemental analysis and

amino acid analysis, as well as Fourier transform infrared spectroscopy and x-ray diffraction.

The recombinant artificial extracellular matrix proteins are introduced in chapter 3. They are evaluated by amino acid analysis and NMR spectroscopy. The ability of HUVECs to adhere to the proteins and the number of cells attached to protein surfaces are also discussed.

The morphology of HUVECs on the protein surfaces and on glass is evaluated in chapter 4. LCST data of the proteins is presented as well as the stability of films of the proteins in aqueous solutions above the LCST.

The appendices contain more detailed information on DNA manipulations and on protein characterization.

CHAPTER 2

Poly(L-ALANYLGLYCINE): MULTIGRAM-SCALE BIOSYNTHESIS, CRYSTALLIZATION, AND STRUCTURAL ANALYSIS

2.1 Abstract

The biosynthesis of poly(L-alanylglycine) (poly(AG)) was performed in high cell density cultures of recombinant *Escherichia coli*. The purity of the material was determined by amino acid analysis, elemental analysis and ^{1}H NMR spectroscopy. Fed batch fermentation increased the yield of recombinant protein from levels of tens of milligrams per liter (typical of batch fermentation in rich media) to hundreds of milligrams per liter. Poly(AG) was recrystallized from dichloroacetic acid solutions in the form of texture-oriented chain-folded lamellae with a lamellar stacking periodicity of 3.2 nm. The crystal structure within the lamellar core is similar in general, but different in detail, to the antiparallel β-sheet structure previously reported for oriented films of poly(AG) and fibers of *Bombyx mori* silk fibroin (silk II). The structure consists of polar antiparallel (ap) β-sheets, with repetitive folding through γ-turns every eighth amino acid (including the fold), stacking with like surfaces together. The wide angle x-ray diffraction signals index on an orthorhombic unit cell with *a* (hydrogen bond direction) = 0.948 nm, *b* (sheet stacking direction) = 0.922 nm, and *c* (chain direction) = 0.695 nm. The stacking distance (*b*-

value) is increased by about 4% in comparison with the previously reported structure of poly(AG), owing, we believe, to steric interaction at the lamellar fold surfaces. Random shears of approximately ± *a*/4 and alternating shears of +*c*/2 and -*c*/2 in the *ac* plane are required to obtain a good fit between the calculated and measured x-ray structure factors.

2.2 Introduction

Recombinant DNA technology is a powerful tool for synthesis of novel proteins for pharmaceutical and biomedical applications[51,52] as well as for research in structural biology and protein folding. We and others have previously reported[31-37,53,54] the biosynthesis of highly repetitive, monodisperse, silk-like proteins, including derivatives containing non-proteinogenic amino acids[37] or elastomeric domains.[53,54] We describe herein the preparation, on a multigram scale, of two monodisperse variants of the "parent" polymer in this family of materials, poly(L-alanylglycine) (poly(AG)). These polymers can be crystallized to form silk II-like β-sheet structures, as shown by Fourier transform infrared spectroscopy (FTIR), small angle x-ray scattering (SAXS) and wide angle x-ray scattering (WAXS).

Poly(AG) (as prepared by chemical synthesis) has been studied previously.[55-57] Fraser *et al.* prepared poly(AG) by polymerization of an L-alanylglycine *p*-nitrophenyl ester

monomer, resulting in a degree of polymerization of about 40.[55] Lotz and Keith used the pentachlorophenyl ester as monomer and obtained molecular weights in the range of 15,000 to 20,000.[57] Infrared and x-ray scattering data indicated that such polymers form either the silk I (crankshaft geometry) or the silk II (β-sheet geometry) structures depending on sample preparation conditions.[57]

We have reported previously the use of genetic engineering to produce artificial proteins that adopt predictable, chain-folded antiparallel (ap) β-sheet structures in the solid state.[32,33,36] The chain-folded lamellar architecture[58-61] is a kinetic trap in the crystallization of all linear polymers sufficiently flexible to form hairpin-like folds, and it is known that protein chains in the β-conformation can make tight turns, with either one or two amide groups (two or three amino acid C_α-atoms) in the fold. The egg-stalk silk protein of the green-wing fly *Chrysopa flava* folds with a periodicity corresponding to eight amino acids to form lamellae of thickness ≅ 3 nm,[62] and nylons 4[63] and 4,6[64] crystallize with amide units, rather than polymethylene segments, in the turn. The biosynthesis of multigram quantities of poly(AG) with known chain lengths well in excess of the expected fold periodicity allowed us to search for chain-folding in poly(AG), and to compare the folded-chain structure with that previously reported by Fraser *et al.*[55,56]

The yield of a recombinant protein in bacterial fermentations is determined in part by the total number of cells in the culture. Traditional batch reactors yield approximately 1.5 g dry cell weight per liter. This low ratio of biomass to culture volume leads to low efficiency in terms of space, time, and cost. Alternatively, fed batch processes yield significantly greater cell densities; values up to approximately 100 g dry cell weight per liter have been reported.[65]

We describe in this chapter simple fed batch techniques with the addition of oxygen that have increased the yield of poly(AG) from tens of milligrams per liter (using batch techniques) to hundreds of milligrams per liter. We also discuss the structural analysis of poly(AG) by infrared and x-ray diffraction methods.

2.3 Experimental Section

2.3.1 Materials

T4 DNA ligase, T4 polynucleotide kinase, calf intestinal phosphatase, and all restriction enzymes were purchased from New England Biolabs. Ribonuclease A, Deoxyribonuclease I, Organic Antifoam, Ampicillin and chloramphenicol were purchased from Sigma Chemical Co. *Escherichia coli* strains DH5αF' and HB101 were purchased from Bethesda Research Laboratories. Plasmid p937.51 was a gift of Protein Polymer Technologies, Inc. The expression

plasmid pET-3b and *E. coli* strain BL21(DE3)pLysS[66] were obtained from Novagen.

2.3.2 General Methods

Bacterial growth in rich medium, DNA manipulations and transformation conditions were performed as described in Sambrook, Frisch and Maniatis.[67] Fourier transform infrared spectra were obtained from KBr pellets on a Perkin Elmer 1600 series FTIR spectrophotometer. ^{1}H NMR spectra were run on a Bruker AMX 500 MHZ spectrometer. Ultraviolet spectra were obtained in distilled water on a Hitachi U2000 spectrophotometer in quartz cuvettes with a path length of 1 cm, while cell density measurements were done in plastic cuvettes at λ=600 nm. High cell density medium for fermentations was adapted from Riesenberg *et al.*[50] with the addition of 100% O_2 once an optical density (OD_{600}) of 10 was reached. A New Brunswick 80L mobile pilot plant (MPP-80) was used for high cell density fermentation. Centrifugation was performed using a Cepa Z41 continuous centrifuge. Amino acid analyses were obtained from an Applied Biosystems 420/130A derivatizer-analyzer following hydrolysis and derivatization with phenylisothiocyanate; data were analyzed with the Applied Biosystems 920A data module.

2.3.3 Preparation of Synthetic DNA

Oligonucleotides (**1**) were synthesized on a 1 μmol scale on a Biosearch Model 8700 DNA synthesizer using phosphoramidite chemistry.[68] Crude oligonucleotides were purified by denaturing polyacrylamide gel electrophoresis and eluted using the "crush and soak" method.[67] Purified oligonucleotides were annealed at 80 °C and allowed to cool to room temperature over several hours. The annealed duplex (**1**) was phosphorylated with T4 polynucleotide kinase, ethanol precipitated and dried *in vacuo*.

```
          Stop Gly Ala Gly Ala Gly Ala Gly Ala Gly
AAT TCG TAA GGT GCC GGT GCG GGT GCA GGT GCG GGT GCC GGC      (1)
    ATT CCA CGG CCA CGC CCA CGT CCA CGC CCA CGG CCG AG
     |          |                       |       |
Eco RI        Ban I                   Ban I   Bam HI
```

2.3.4 Cloning and Amplification of Synthetic DNA

The purified synthetic duplex was ligated into Eco RI/Bam HI digested pUC18[69] and used to transform *E. coli* strain DH5αF'. Cells were grown at 37 °C overnight on 2xYT solid medium containing 200 μg/ml ampicillin, 25 μg/ml β-isopropylthiogalactoside (IPTG) and 40 μg/ml of the chromogenic substrate 5-bromo-4-chloro-3-indolyl-β-D-galactopyranoside (X-Gal) for blue-white screening. Plasmid DNA from white transformants was sequenced using Sequenase 2.0 (Amersham Life Sciences) to verify the identity of the insert. After isolation of the recombinant plasmid from a 1

liter 2xYT culture, the DNA was digested with Ban I and the fragments were separated by nondenaturing polyacrylamide gel electrophoresis. The DNA monomer was eluted from the polyacrylamide slice using the "crush and soak" method.[67]

2.3.5 Polymerization of the DNA Monomer and Cloning of DNA Multimers

Purified monomeric DNA was self-ligated with T4 DNA ligase to form a population of multimers. Multimers were resolved by electrophoresis and ligated into Ban I digested, dephosphorylated p937.51, a small, high copy number cloning vector that carries an origin of replication from pBR322 and a gene encoding chloramphenicol acetyltransferase.[70] The recombinant plasmids were used to transform *E. coli* strain HB101. Transformants were screened by restriction enzyme digest analysis and clones encoding 16 and 60 repeats of the monomer were selected. The recombinant plasmids were designated p937.51-$(AG)_{64}$ or p937.51-$(AG)_{240}$ respectively.

2.3.6 Construction of Bacterial Expression Vector

Recombinant p937.51-$(AG)_{240}$ or p937.51-$(AG)_{64}$ was digested with Bam HI to release the multimer. The fragments were separated by 1% low melting point agarose gel electrophoresis and recovered by extraction with phenol and with phenol/chloroform, and finally by ethanol precipitation. The recovered DNA was ligated into Bam HI digested, dephosphorylated pET-3b and used to transform

E. coli strain HB101. Transformants were screened for the presence and orientation of each multimer by Ava I digestion. Recombinant plasmids, designated pET3b-$(AG)_{240}$ and pET3b-$(AG)_{64}$ respectively, containing inserts in the correct orientation were used to transform the expression host, *E. coli* strain BL21(DE3)pLysS.

2.3.7 Protein Expression, Batch Phase, Rich Medium

Single colonies of BL21(DE3)pLysS containing recombinant pET3b-$(AG)_{240}$ or pET3b-$(AG)_{64}$ were used to inoculate 5 ml of LB medium containing chloramphenicol (34 μg/ml) and ampicillin (200 μg/ml). The cultures were grown to saturation and used to inoculate 750 ml volumes of LB medium containing chloramphenicol (34 μg/ml) and ampicillin (200 μg/ml). The cultures were grown to OD_{600} = 1 at 37 °C and protein expression was induced by the addition of IPTG to a final concentration of 0.4 mM. Cells were harvested after 2 hours by centrifugation (2,520 x g, 15 min at 4 °C). The cell pellets were resuspended in 10 mL of water and stored at -20 °C.

2.3.8 Protein Purification

Frozen cells were thawed and phenylmethyl sulfonyl fluoride (PMSF) (1 mM), $MgCl_2$ (5 mM), RNAse (20 μg/ml) and DNAse (20 μg/ml) were added. The solutions were incubated at 37 °C for 30 min and the insoluble portion was recovered by centrifugation (10,000 x g, 4 °C, 15 min). The pellets

were resuspended in 10 ml TENT solution (50 mM Tris-Cl (pH 8.0), 10 mM EDTA, 100 mM NaCl, 0.5-0.7% Triton X-100) and incubated with shaking at room temperature for 30 min. The insoluble portion was recovered by centrifugation (10,000 x g, 4 °C) for 15 minutes. The pellets were resuspended in 10 ml of TENS (50 mM Tris-Cl (pH 8.0), 10 mM EDTA, 100 mM NaCl, 0.5% sodium dodecylsulfate (SDS)) and incubated at room temperature with shaking for 60 min. The insoluble portion was recovered by centrifugation (10,000 x g, 4 °C, 15 min) and the TENS treatment was repeated. The resulting pellet was resuspended in TEN plus porcine pancreatic lipase (20 μg/mL) and incubated at 37 °C for 30 minutes. The insoluble portion was recovered by centrifugation (10,000 x g, 4 °C, 15 min). The pellet was then washed sequentially with 10 mL TENT, 10 mL water, 10 mL chloroform:methanol:acetone 40:30:30, 10 mL of acetone, 10 mL water and 10 mL water. The insoluble portion was recovered by centrifugation (10,000 x g, 4 °C, 15 min) after each wash. The recovered fusion protein was then dried and weighed.

2.3.9 Cleavage of Fusion Protein

Cyanogen bromide cleavage of the fusion proteins was accomplished by the method of Smith.[71] Approximately 35 mg of fusion protein was dissolved in 5.5 mL of 98% formic acid and diluted to 70% formic acid with distilled water. The solution was deoxygenated with nitrogen and 50 mg of CNBr

crystals was added. The solution was stirred at room temperature for 24 hr and the solvent was removed by rotary evaporation. The residue was washed with distilled water several times and the insoluble portion was recovered by centrifugation and dried by lyophilization.

2.3.10 High Cell Density Fermentation and Protein Expression

A 5 ml volume of 2xYT medium containing chloramphenicol (34 μg/ml) and ampicillin (200 μg/ml) was inoculated with a single colony of BL21(DE3)pLysS pET-3b$(AG)_{240}$. The culture was incubated in a rotary shaker at 37°C until visible turbidity was reached (approximately 6 hrs), and then used to inoculate 100 mL of 2xYT medium containing chloramphenicol (34 μg/ml) and ampicillin (200 μg/ml). This was grown to visual turbidity at 37 °C, and then used to inoculate 2 liters of 2xYT medium containing chloramphenicol (34 μg/ml) and ampicillin (200 μg/ml). The culture was grown to saturation overnight and the cells were harvested by centrifugation at 4,000 rpm for 10 min. The resulting pellet was used to inoculate 35 liters of the minimal medium[50] specified in Table 2.1. ampicillin and chloramphenicol were added to final concentrations of 200 μg/mL and 34 μg/mL respectively. Ammonium hydroxide (25%) was used as the base (which was fed through the base pump of the pH controller), both to control pH and to provide a nitrogen source. The culture was grown in an 80 liter New Brunswick fermentor until the glucose was depleted as

determined by a rise in pH above the set point, pH 6.8. At this time a glucose feed (50% w/v glucose/water) was established. Glucose was fed through the acid pump of the pH controller; pH was maintained at 6.8.[50] Pure O_2 was used to ensure aerobic conditions when air was insufficient to maintain the dissolved oxygen concentration above 20%. Induction was achieved by the addition of 1.0 mM IPTG when the OD_{600} reached 25-30. Cultures were grown for 4 hr prior to harvesting by centrifugation with a Cepa Z41 continuous centrifuge. Cells were weighed and resuspended in 4 mL of water per gram of cells (wet weight). Protein purification was performed as described above.

2.3.11 Infrared Spectroscopy

Poly(AG) comprising 64 dyads ($(AG)_{64}$) was prepared for crystallization by dissolving 30 mg of protein in 1 mL of 98% formic acid. The solution was diluted to 70% formic acid by addition of distilled water, and stirred until a gel formed (about 10 hr). The gel was washed with methanol, dried and crushed to form a KBr pellet for infrared analysis.

2.3.12 X-ray Diffraction

Poly(AG), in the form of a white powder, was continuously added to a mixture of dichloroacetic acid and 10% aqueous lithium hydroxide at 60°C and stirred until a gel formed. The gel was compressed between two filters at

50°C until dry (approximately 4 h). X-ray diffraction photographs from these compressed crystalline mats were obtained using a Statton-type x-ray camera, evacuated to backing pump pressure to reduce air scatter. The nickel-filtered CuKα sealed beam source was collimated with a system of 200 μm pinholes. The diffraction photographs were recorded on x-ray film with specimen-to-film distances of 50-100 mm. X-ray diffraction photographs of the mats were obtained with the x-ray beam directed either parallel or perpendicular to the surface of the mat.

2.3.13 Computer Modeling and Simulated X-ray Diffraction Patterns

Molecular modeling was performed on a Silicon Graphics Iris 4D20 workstation using the following software packages: Discover 2.9 (Biosym Technologies) and Cerius 2, Release 1.6 (Molecular Simulations, Inc.). The simulated x-ray diffraction patterns were created on a Silicon Graphics Indigo R4000 using the Diffraction 1 module of the Cerius 2, Release 1.6, program. The appropriate Lorentz and polarization correction factors are incorporated in the displayed intensities. The degree of arcing and the temperature factor were chosen to match the observed x-ray diffraction photographs.

2.4 Results and Discussion

2.4.1 Gene Construction

The strategy used in our laboratory to prepare artificial proteins has been described previously.[32] In this work, DNAs encoding two chain-length variants of poly(AG) were ligated into the Bam HI site of the expression plasmid pET-3b. The resulting recombinant plasmids encode either 16 or 60 repeats of the alanylglycine tetramer, flanked by N- and C- terminal extensions of 23 and 33 amino acids respectively (**2**). These terminal regions are derived from the transfer and expression vectors and can be removed by CNBr cleavage at flanking methionine residues.

M A S M T G G Q Q M G R D P M F K Y S R D P M G-$[(AG)_4]_n$

2

-A R M H I R P G A Y Q L D P A A N K A R K E A G L A A A T A E Q

n = 16 or 60

2.4.2 Protein Expression

The host used for protein expression was *E. coli* strain BL21(DE3)pLysS.[66] In this strain, a gene encoding T7 RNA polymerase is incorporated into the bacterial chromosome under *lacUV5* control, and protein production is induced by the addition of IPTG. The pLysS plasmid provides low levels of T7 lysozyme, which inhibits T7 RNA polymerase and suppresses the basal level of protein expression.

Protein expression in rich medium was performed as described in the Experimental Section. Aliquots of cultures representing approximately equal numbers of cells (as determined by the optical density at 600 nm) were removed periodically after induction of protein synthesis (t= 0, 30, 60, 120, 180 min). Samples were loaded onto a 12.5% polyacrylamide gel and separated by electrophoresis. Protein bands were stained with Coomassie Brilliant Blue R-250. The recombinant protein was insoluble in SDS and did not migrate during SDS-PAGE; however, increased stain intensity following induction could be seen in the wells of the stacking gel (data not shown) indicating inducible protein production.

Protein production in minimal medium was carried out in a New Brunswick 80L Mobile pilot plant as described above. The growth medium (Table 2.1) was adapted from that reported by Riesenburg *et al.*[50] Oxygenation of the culture must be maintained in order to insure aerobic growth during the induction period; otherwise no recombinant protein is

produced. Oxygen was bubbled through the medium at a flow rate which maintained the dissolved oxygen content approximately 20% above the O_2 level obtained when the medium was deoxygenated with N_2. After the termination of batch phase growth (OD_{600} = 21) a 50% (w/v) glucose solution was fed on demand through the pH pump. Upon depletion of glucose as the carbon source, the culture begins to metabolize acetic acid previously produced as a result of glucose metabolism. Depletion of acetic acid results in an increase in pH; the acid pump is turned on and glucose is fed to the culture. Acetic acid is then produced, and again lowers the pH. This allows both the carbon source (glucose) and the nitrogen source (ammonium hydroxide) to be fed on demand through the pH control mechanism of the system. The addition of glucose by pH control is similar to the method used by Frude *et al.*,[72] except that in the present work the base source is also the nitrogen source.

2.4.3 Protein Purification and Analysis

Table 2.2 shows the weight of recombinant protein produced per gram wet cell weight for cultures of BL21(DE3)pLysS pET-3b-$(AG)_{240}$ grown to optical densities (600 nm) of 1, 10, or 25 prior to protein induction with IPTG. An optical density of 25 corresponds to approximately 10 cell doublings of the inoculum. There is no loss of protein produced per gram of wet cell weight (WCW) as the cell density is increased from 3-4 g WCW/L to 64 g WCW/L prior to

protein induction. This result indicates that we are not at the limit of the method, and suggests that these cultures might be grown to still higher densities with further increase in the amount of recombinant protein produced per liter of culture.

Amino acid analyses for both $(AG)_{64}$ and $(AG)_{240}$ are shown in Table 2.3. The $(AG)_{240}$ product was found to contain approximately 5% valine. Two-dimensional NOSY NMR spectra of the recombinant protein confirmed the presence of valine in the polymer (Appendix F), suggesting mutation of the coding sequence subsequent to sequencing of the DNA monomer. Conversion of alanine to valine was observed previously in our work on the related polypeptide $((AG)_4PEG)_{14}$.[73] The shorter recombinant molecule does not appear to contain these changes to valine as determined by amino acid analysis (Table 2.3).

The ^1H NMR spectrum of $(AG)_{64}$ in formic acid (Figure 2.1) shows the alanine α-proton multiplet at 4.45 ppm and the CH_3 doublet at 1.36 ppm. The glycine α-CH_2 signal occurs at 4.05 ppm. The absence of other signals indicates sample purity, consistent with the results of amino acid analysis reported in Table 2.3.

The results of elemental analysis are shown in Table 2.4, and are compared with the theoretical analysis for the product containing 3% water. Addition of 3% water gives good agreement with the experimental results for carbon and hydrogen content; we find nitrogen analysis consistently

lower than theoretical predictions for these kinds of artificial proteins.[32,36]

2.4.4 Solid State Properties

Crystalline samples of $(AG)_{64}$ were prepared as described in the Experimental Section. The infrared spectrum of the crystalline polymer, shown in Figure 2.2, exhibits amide I and amide II vibrational modes at 1629 and 1529 cm^{-1} respectively, characteristic of the β-sheet conformation.

The wide angle x-ray diffraction photograph, taken with the x-ray beam directed parallel to the plane of the compressed mat and with the mat normal horizontal, is shown in Figure 2.3a. The diffraction photograph exhibits discrete Bragg diffraction signals consistent with an oriented crystalline polymer, and all observed signals index on an orthorhombic unit cell with dimensions a = 0.948 nm, b = 0.922 nm and c = 0.695 nm. The measured and calculated inter-planar spacings are listed for comparison in Table 2.5 together with an estimate of the observed intensities. In addition a set of low angle equatorial diffraction arcs, orders of 3.2 nm, were seen. This set of diffraction signals is noticeably different in character from the wide-angle diffraction signals; the degree of arcing is less by about a factor of two and they vary in intensity relative to the wide angle signals in different samples; indeed, in some cases they are so weak that they are barely detectable,

except for a diffuse first order at a spacing ≅3.6 nm. Their appearance or non-appearance did not change the nature of spacings of the other diffraction signals.

The orientation direction is along *a*. Thus the directionally coincident *a* and *a** axes lie along the meridian line (vertical bisector), and therefore, the *h*00 diffraction signals, the easily seen 200 and 400 in particular, appear as arcs centered on that meridian. The families of 0*k*0 and 00*l* diffraction signals appear on the equator (horizontal bisector). This type of texture-oriented x-ray diffraction pattern is similar to that reported previously for poly$(AG)_3$EG.[36,64]

Differences in the line broadening of the various diffraction signals, which relate in a consistent way to their assigned Miller indices, are observed in Figure 2.3a. The 200 and 400 diffraction arcs are particularly sharp, and demand long range correlational order along the *a*-axis. Diffraction signals with indices of the general *hkl* type are considerably broader than those with indices *hk*0; this comparison leads us to the conclusion that the coherent scattering length in the *c* direction is small. We estimate a length of 2 to 4 nm (allowing for instrumental line broadening); this is ca. 16 times less than the length of the protein chain. The coherent scattering length in the *b* direction is intermediate between those in the *a* and *c* directions.[32]

The wide-angle x-ray photograph taken with the x-ray beam directed orthogonal to the compressed mat is shown in Figure 2.3b. The diffraction signals appear as a set of concentric rings, which index on the orthorhombic lattice deduced from analysis of the oriented pattern.

The texture-oriented wide-angle x-ray diffraction photograph shown in Figure 2.3a, obtained with the x-ray beam parallel to the surface of the mat, is similar to that previously reported for oriented films of poly(AG) by Fraser *et al.*;[55,56] however, that paper contained no report of any x-ray diffraction photographs taken with the x-ray beam orthogonal to the films. The films were stroked during drying and it was implied that the a-axis is a unique direction;[55,56] as a consequence, their structure analysis assumed cylindrical averaging (fiber symmetry) about the *a*-axis. In our samples, prepared by compression into mats, the *a*-axis is merely confined to the plane of the mat, with random rotation about the mat normal.[37] It is vital to recognize there is a texture and to establish its nature if the x-ray structure analysis is to be performed correctly.[37] The overall features of our x-ray diffraction pattern are sufficiently similar to those of Fraser *et al.*[55,56] that we are confident that we have the same basic crystalline structure, even if our texture is different.

Fraser *et al.*,[55,56] proposed the following model. The structure consists of polar apβ-sheets, stacked in pairs with alanyl faces together and glycyl surfaces together,

respectively. The stacking direction is parallel to the *b* axis; the unequal packing of the apβ-sheets is responsible for the appearance of the 010 diffraction signal. Successive sheets shear ±*a*/4 parallel to the *a* axis (hydrogen bond direction) in the *ac* plane. The *c* axis is parallel to the chain axis. The only difference between our unit cell and that reported by Fraser *et al.*[55,56] is the value of *b*, the sheet stacking parameter; their reported value of 0.887 nm is 3.8% less than our 0.922 nm-value. A perspective view of the structure and the unit cell is shown in Figure 2.4 and a simulated x-ray diffraction pattern (SXDP) of this structure generated for comparison with the observed x-ray data is shown in Figure 2.3c. Comparison of Figures 2.3a and 2.3c shows that although the match between the observed and calculated diffraction patterns is reasonably good overall, there are noticeable discrepancies, the most obvious of which is the unwanted 1*kl* diffraction signals on the first layer line. Unwanted first layer line diffraction occurs even if fiber symmetry is assumed (although, of course, the relative intensities will be different). It can be removed by random shears of ±*a*/4 in the *ac* plane; thus, the model proposed by Fraser *et al.*[55,56] is not correct in detail. In addition there are other discrepancies between the calculated and experimental x-ray diffraction patterns; there are unwanted 0*kl* equatorial diffraction signals in the region between the 010 and 020

and there is poor agreement with the observed *h*00 intensities.

The low-angle equatorial diffraction pattern (which consists of orders of 3.2 nm), and the relative broadening of selected wide-angle diffraction signals favor a chain-folded lamellar structure for the poly(AG) crystals prepared in this work. Our interpretation of the poly(AG) x-ray diffraction results has benefited from the detailed analysis of poly$(AG)_3EG$.[36] The appearance of the first few orders of the 3.2 nm on the equator indicate that the lamellae are stacking reasonably well at the stacking periodicity of 3.2 nm. In a number of crystal preparations only a diffuse first order at spacing 3.6 nm (12% greater) was observed. This is consistent with poorly stacked lamellae. Figure 2.5 shows an orthogonal view (parallel to *b*-axis) of a chain-folded apβ-sheet that is consistent with the x-ray data. The γ-turns are necessary to generate the *polar* apβ-sheets.[36] Alanine residues are placed at the apex of each γ-turn. There are two possible sequences for the γ-turns, either GAG or AGA. Since we knew *a priori* that the resolution of the experimental data would not allow us to delineate the fine details of the fold geometry we chose the GAG γ-turn as the basis of our model. It should be noted that the folds on the right-hand edge of the sheet are conformationally different from those on the left. A more detailed perspective view of one of the γ-turns is shown in Figure 2.6. The sheets are stacked by making a rotation, π,

about the *a*-axis; thus, in the chain-folded lamellar crystal both surfaces are equally populated with the two types of fold conformation. With regard to the stacking of the polar apβ-sheets, there are two possibilities if like surfaces are to be in contact, either a rotation, π, about the *a*-axis, or a rotation, π, about the *c*-axis. The former structure was favored since it results in a chain folded lamellar crystal with both surfaces equally populated with the two types of fold conformations.

Various structures for poly(AG) were generated by computer and the stereochemical feasibility of each was examined using modeling procedures. SXDPs were generated for comparison with the observed x-ray data. We discovered that all structures that incorporate regular inter-sheet shears of $\pm a/4$ parallel to the *a* axis generate unwanted intensity for the 1*kl* diffraction signals. This can be seen in the SXPD shown in Figure 2.3c. The only way to remove this intensity is by incorporating random $\pm a/4$ shears in the *ac* plane. In addition there are unwanted diffraction signals on the equator which are removed by alternating $+c/2$ and $-c/2$ shears in the *ac* plane. We have also found this effect in the structure of poly$(AG)_3$EG.[36] A still better fit can be found if the random shears are only$\approx \pm a/4$. The closest overall fit with the observed x-ray data is illustrated in Figure 2.3d, and the final structure is shown in Figure 2.7.

Fraser *et al.*[55,56] did not raise the issue of chain-folding in the apβ-sheets of poly(AG). In our recent studies of related periodic polypeptides[36,74] crystallized in very similar circumstances, we have found that the chains fold regularly through γ-turns to form crystalline lamellae approximately 3-4 nm thick. Chain folding, of course, is an obvious geometric contender in structures involving antiparallel chains. We suspect that our slightly increased value for the average inter-sheet stacking parameter b/2 is a result of steric interactions at fold surfaces. It was noticed that the *b*-value decreased as the fold period increased in the series poly(AG)$_x$EG[36] as the integer x changed successively from 3 to 6, which would be consistent with our suggestion. Further support was found in the systematic study of the series: poly(AG)$_3$XG, where X varied from serine to tyrosine; a linear relationship between increasing volume and increasing *b*-value was established.[74] Given the low degree of polymerization of the poly(AG) used by Fraser *et al.*;[55,56] it may be that little, if any, chain folding occurred. No low-angle diffraction features were reported.

2.5 Conclusions

Poly(AG) has been prepared by biological synthesis in multigram quantities; 25 g of the recombinant fusion protein was recovered from 35 liters of culture. This required only a simple fed-batch fermentation without elaborate feedback

controls. The observation that there is no decrease in recombinant protein production with increased cell density suggests that limiting yields have not yet been reached. Little or no loss in recombinant protein production with increased cell doubling also indicates good plasmid stability in the host strain.

The x-ray diffraction results show that poly(AG) can crystallize in the form of chain-folded lamellae approximately 3.2 nm thick. The structure consists of polar apβ-sheets folding through γ-turns. The sheets stack in pairs with alanyl faces together and glycyl faces together, respectively, with a stacking periodicity about 4% greater than that reported previously by Fraser *et al.*,[55,56] where chain folding was not evident. To obtain good agreement between the calculated and observed x-ray structure factors, successive sheets must shear randomly ≈ $\pm a/4$ and alternately $+c/2$ and $-c/2$ in the *ac* plane. The calculated diffraction data are presented in the form of look alike patterns which are a convenient and, we judge, a stringent test for the proposed structure.

Table 2.1 Minimal Medium Composition for High Cell Density Fermentation

component	initial concn.
KH_2PO_4	13.3 g/L
$(NH_4)HPO_4$	4.0 g/L
citric acid	1.7 g/L
$MgSO_4 \cdot 7H_2O$	1.2 g/L
trace metal solution[a]	10 mL/L
thiamine hydrochloride	4.5 mg/L
glucose.H_2O	27.5 g/L
antifoam	0.1 mL/L
feed solution	
glucose	500 g/L
NH_2OH	25%

[a]Trace metal solution: 6 g/L iron(III) citrate, 1.5 g/L $MnCl_2 \cdot 4H_2O$, 0.8 g/L $Zn(CH_3COO)_2H_2O$, 0.3 g/L H_3BO_3, 0.25 g/L $NaMoO_4 \cdot 2H_2O$, 0.25 g/L $CoCl_2 \cdot 6H_2$), 0.15 g/L $CuCL_2 \cdot 2H_2O$.

Table 2.2 Recombinant Protein ($(AG)_{240}$ Fusion) Recovered from Cultures of Three Different Cell Densities

OD_{600}	wet cell weight (g/L)	recombinant protein/wet cell weight (mg/g)	product yield (g/L)	total product yield (g)
1[a]	3	16	0.048	0.048
10[b]	26	20	0.42	5.2
25[b]	64	15	0.96	25

[a] 1 L overall culture volume
[b] 35 L overall culture volume

Table 2.3 Theoretical and Experimental Amino Acid Analyses for $(AG)_{64}$ and $(AG)_{240}$

	mol % $(AG)_{64}$		mol % $(AG)_{240}$	
amino acid	theor.	exptl.	theor.	exptl.
aspartic acid	0.00	0.62	0.00	0.00
alanine	49.23	52.59	49.79	49.00
glycine	49.23	46.28	49.79	46.54
arginine	0.77	0.51	0.21	0.00
homoserine	0.77	-	0.21	0.00
valine	0.00	0.00	0.00	4.45

Table 2.4 Elemental Analyses of $(AG)_{64}$ Including both Experimental and Theoretical Calculations

element	theor.	theor ± 3%H_2O	exptl.
carbon	46.85	45.45	45.39
hydrogen	6.33	6.48	6.35
nitrogen	21.86	21.20	19.78

Table 2.5 Comparison of Observed Diffraction Signal Spacings (d_0) with Those Calculated (d_c), in Nanometers (Errors ± 0.002 nm), for the Orthorhombic Unit Cell of $(AG)_{64}$, Together with an Estimate of Observed Intensities

S = sharp, M = medium, W = weak

(I_0)

$(AG)_{64}$: a = 0.948 nm, b = 0.922 nm, c = 0.695 nm

hkl	d_0	d_c	I_0
010	0.922	0.922	S
020	0.461	0.461	S
021	0.375	0.384	M
030	0.310	0.307	M
031	0.282	0.281	M
022		0.277	
040	0.231	0.231	W
200	0.474	0.474	M (sharp)
210	0.420	0.422	M
211	0.356	0.360	M (broad)
301	0.282	0.288	M
311		0.275	
400	0.237	0.237	W (sharp)
410	0.230	0.230	W
006	0.116	0.116	W

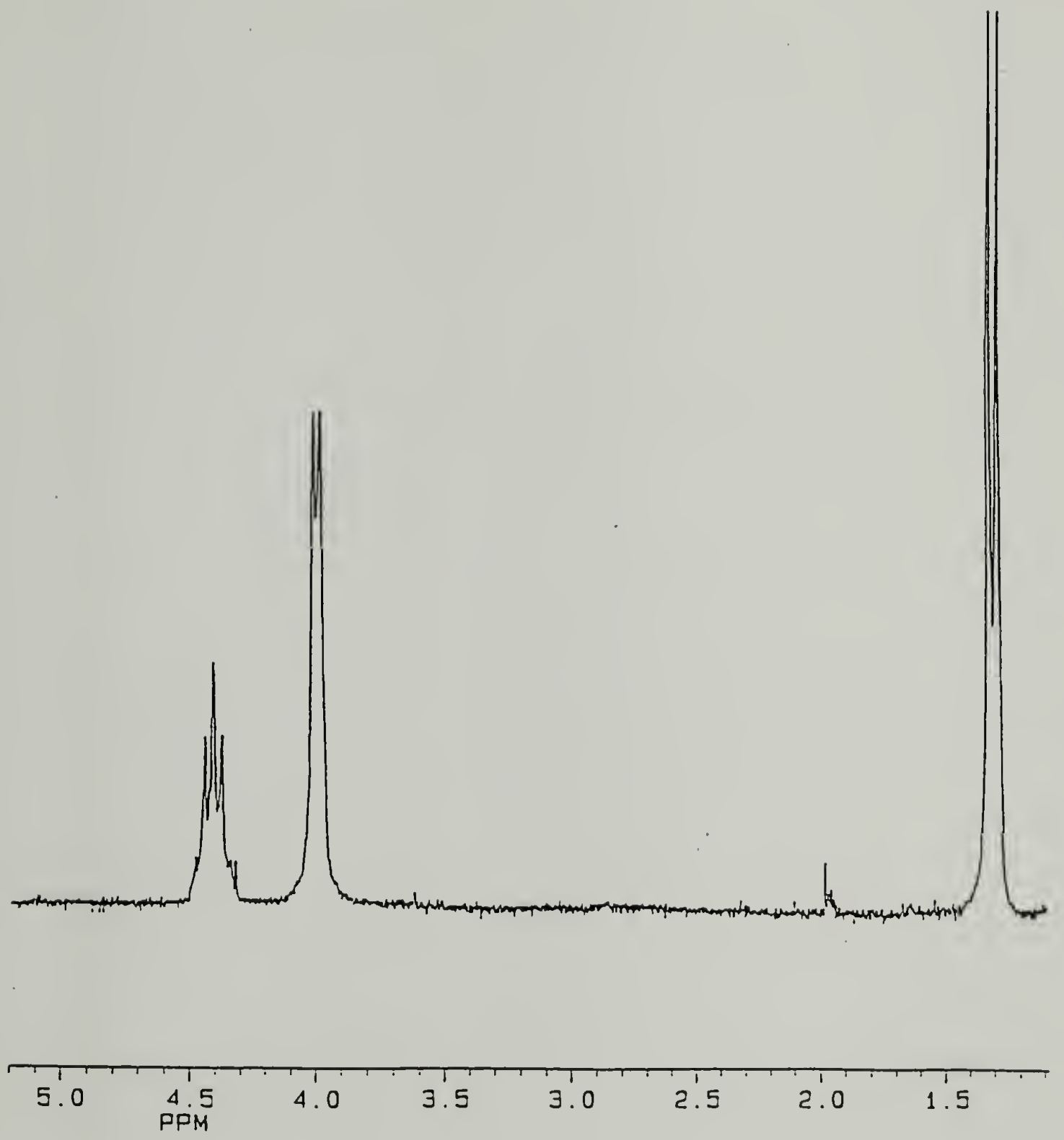

Figure 2.1. ^{1}H NMR spectrum of $(AG)_{64}$ in formyl-d formic acid taken on a Bruker 500 MHZ NMR spectrometer. The alanine α CH signal appears at 4.45 ppm and the CH_3 peak is observed at 1.36 ppm. The glycine α CH_2 peak protons appear at 4.05 ppm.

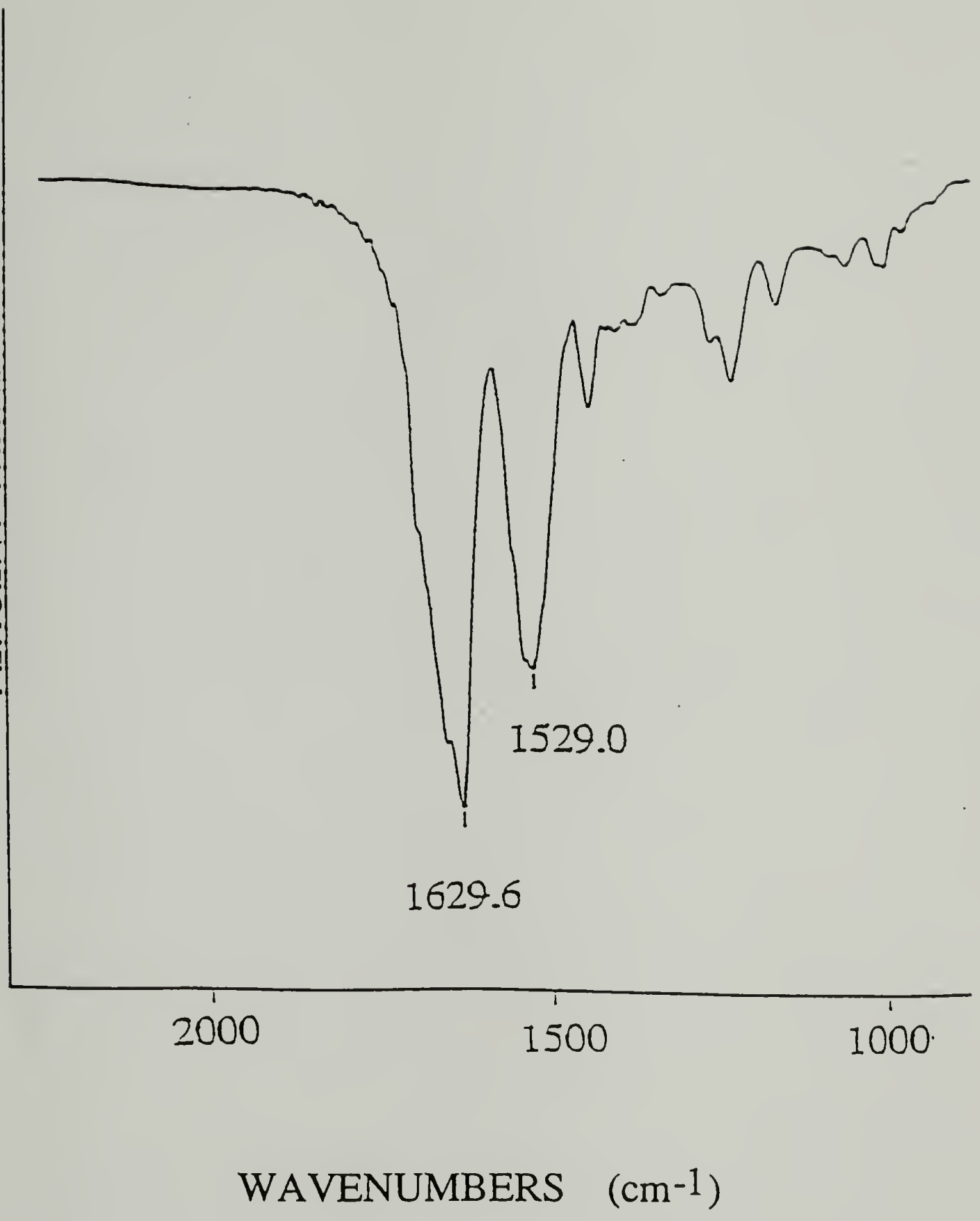

Figure 2.2. FTIR spectrum of silk II form of $(AG)_{64}$. Amide peaks at 1529 and 1629 indicate the β-sheet architecture.

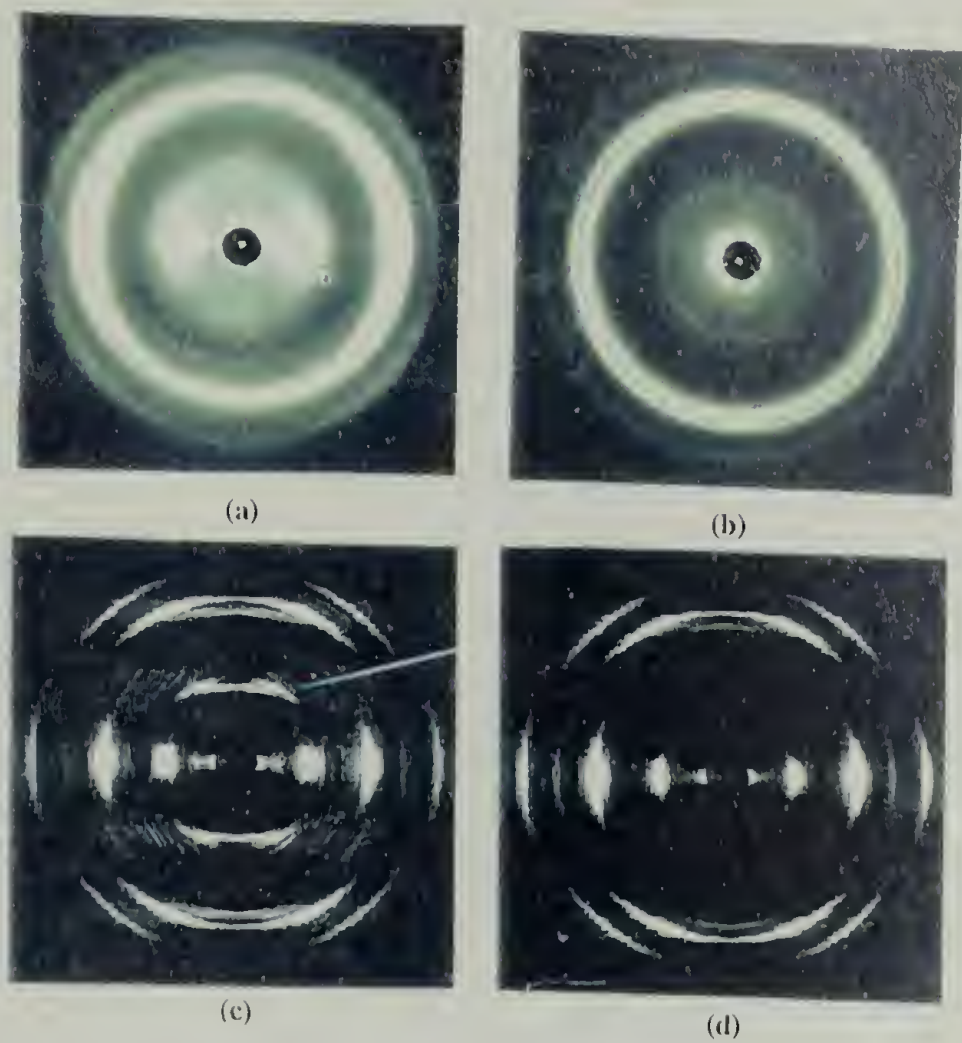

Figure 2.3. X-ray diffraction photographs from poly(AG). (**a**) With the x-ray beam directed parallel to the plane of the compressed mat and with the mat normal horizontal. The diffraction signals on this texture-oriented pattern index on an orthorhombic unit cell with dimensions: *a* (hydrogen bond direction) = 0.948 nm, *b* (inter-apβ-sheet direction) = 0.922 nm, *c* (chain direction) = 0.695 nm. Only *h*00 diffraction signals occur on the meridian (vertical bisector) and 0*kl* on the equator (horizontal bisector). The low angle diffraction signals are indicated by LX. (**b**) With the x-ray beam directed orthogonal to the plane of the compressed mat. In this case the diffraction signals are a set of concentric rings which index on the same orthorhombic unit cell as in (**a**). **c**) SXDP of the poly(AG) model proposed by Fraser *et al.*[56], with alternating ±a/4 shears in the *ac* plane. Notice the unwanted diffraction intensity on the first layer line (*h*=1) as indicated. (**d**) SXDP of the chain-folded model shown in Figure 7 which incorporates random ≈±*a*/4 shears and alternating +c/2 and -c/2 shears in the *ac* plane.

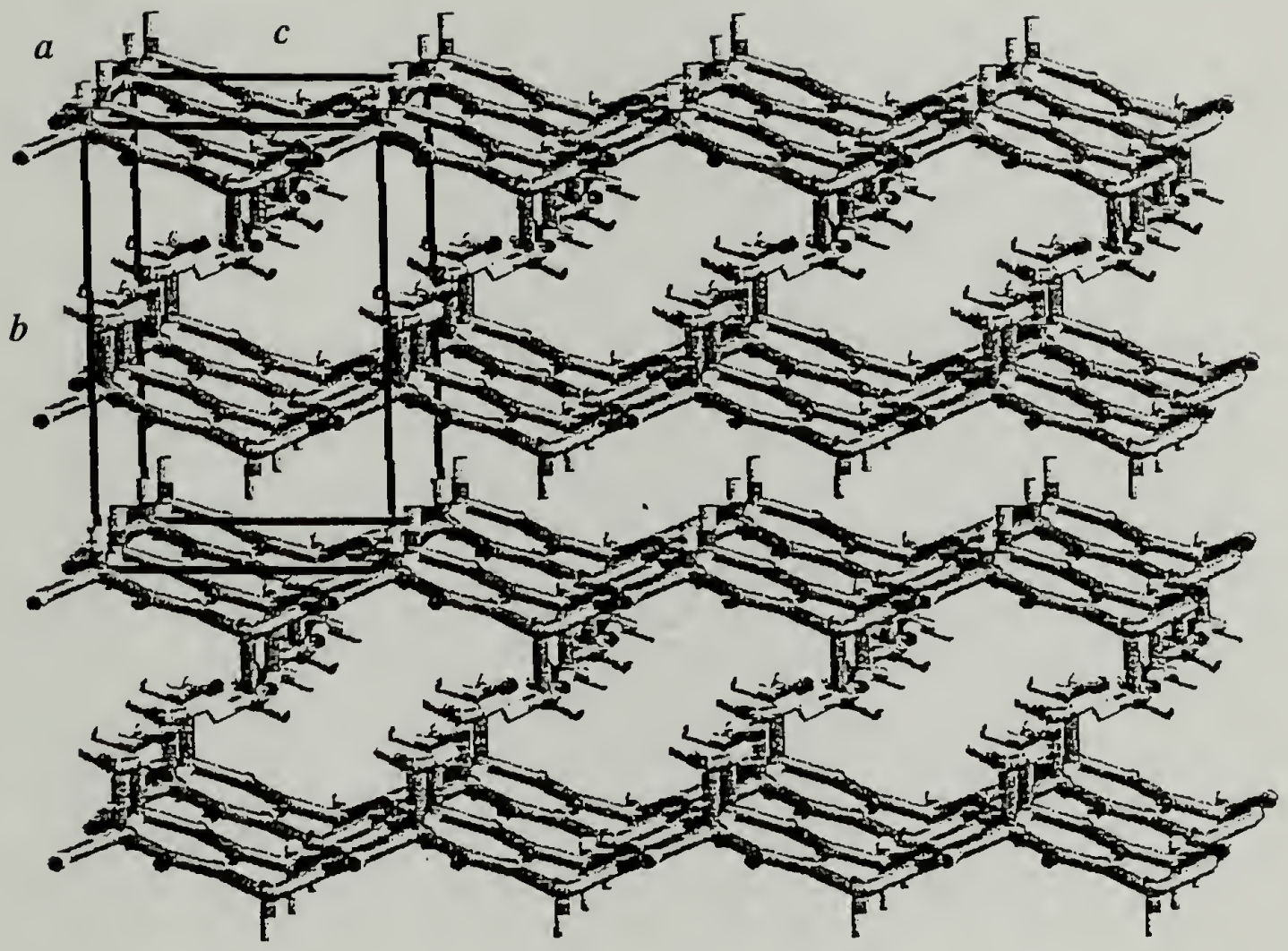

Figure 2.4. Three-dimensional structure generated by a stack of *polar* apβ-sheets of poly(AG). They are arranged so that like surfaces are in contact; thus the hydrophobic methyl groups are layered between a pair of apβ-sheets, followed by a layer of hydrogen atoms. The unit cell is shown; note the sheets are alternately sheared by ±*a*/4 in the *ac* plane. The alternating deviation from the *b*/2 stacking periodicity is evident and is, in part, responsible for the occurrence of the 010 diffraction signal. The *b*-value is 3.8% greater than that reported for oriented films of poly(AG) by Fraser *et al.*[56] We believe this is due to steric interactions at the regular (every eighth amino acid) γ-turns in our structure (see Figure 2.7).

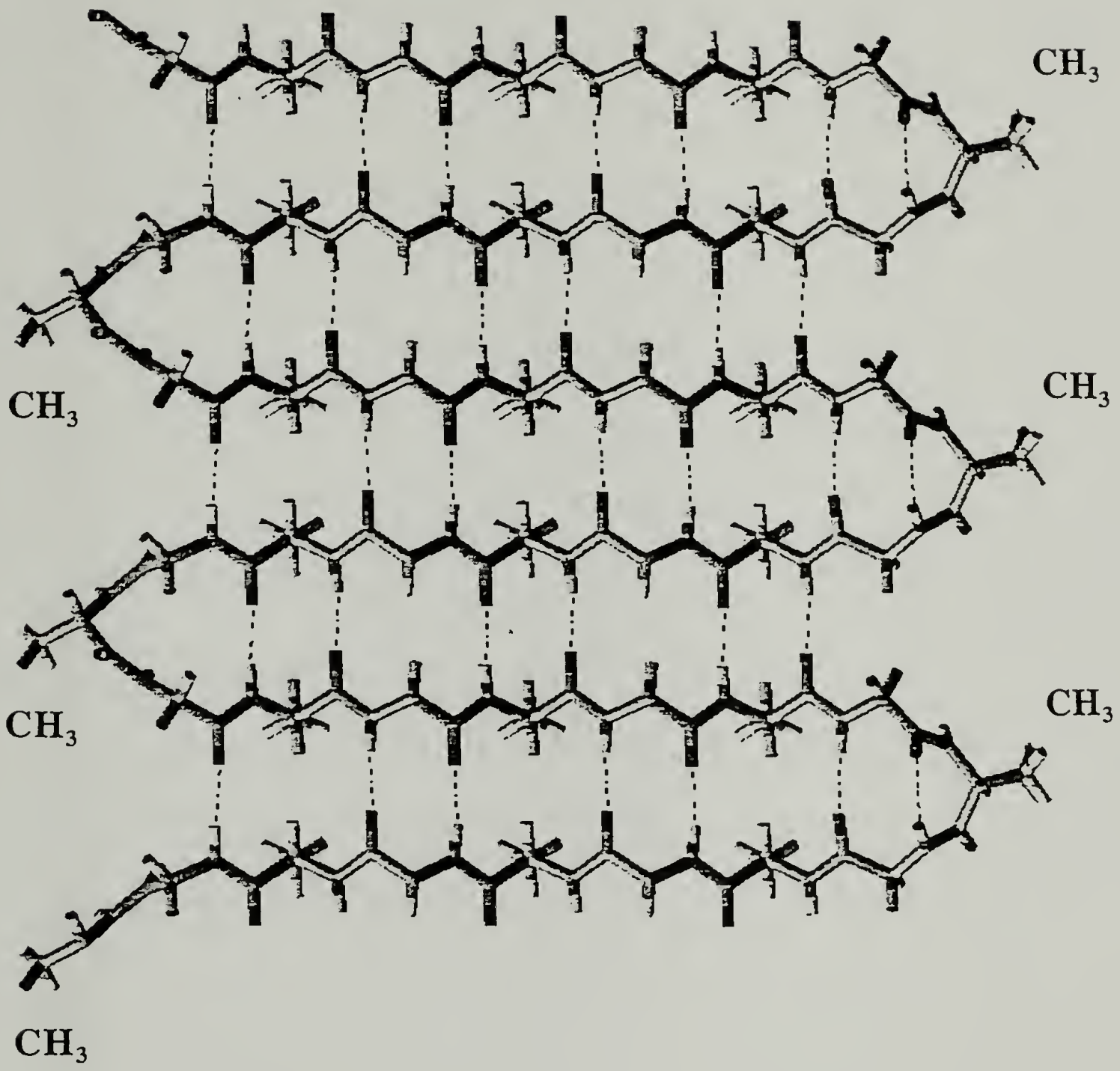

Figure 2.5. View orthogonal (parallel to *b*-axis) to a single apβ-sheet of poly(AG), folding in phase with the octapeptide periodicity and forming γ-turns. The chains (*c*-direction) run horizontally and the linear hydrogen bonds (shown as dashed lines) are directed vertically (*a*-direction). Note that the conformations of the γ-turns are different at the left-hand and right-hand edges (fold surfaces) of the apβ-sheet. The peptides connect through *inward-pointing* bonds on the left and *outward-pointing* bonds on the right.[64]

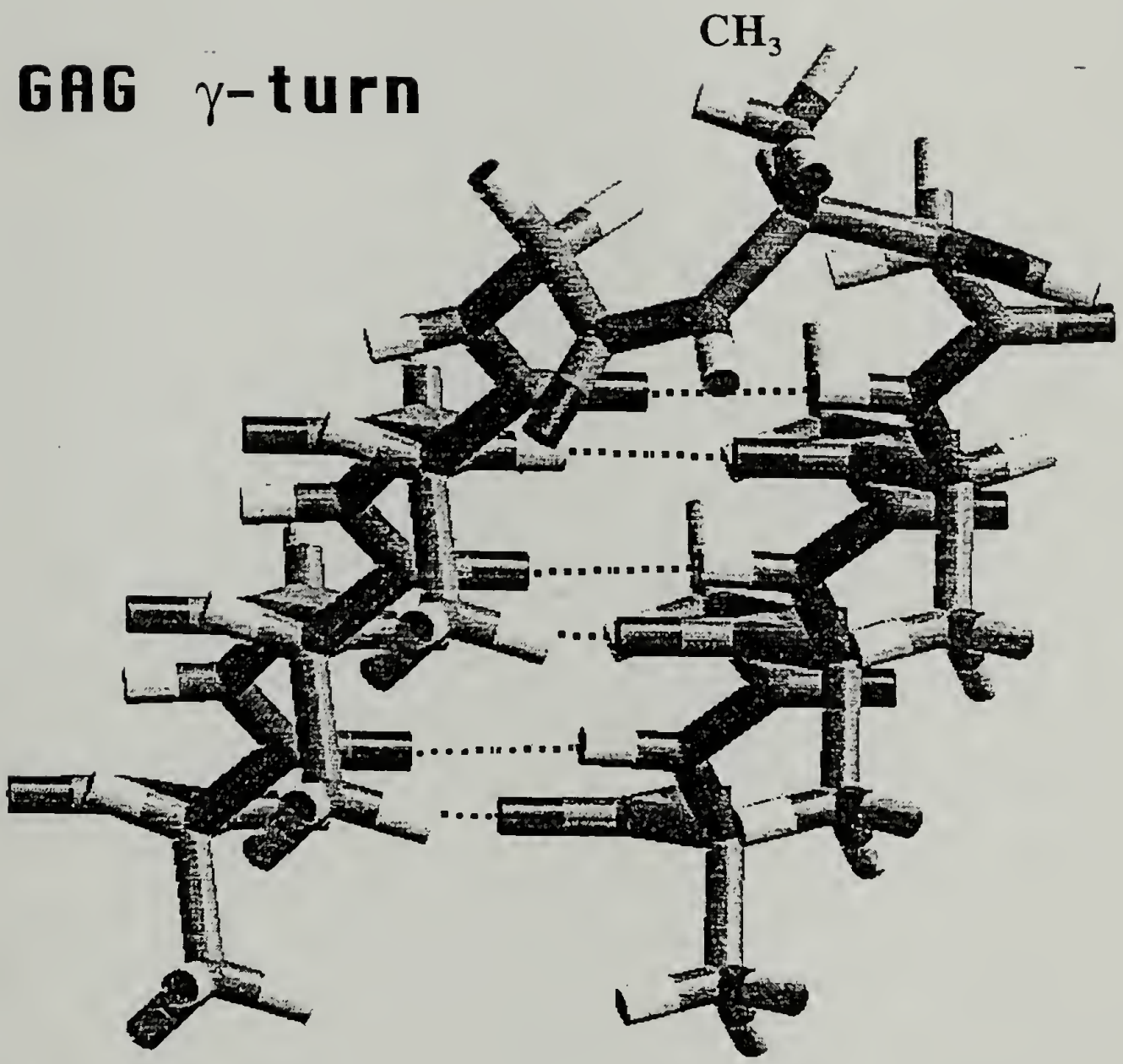

Figure 2.6. Perspective view of a GAG γ-turn (from left-hand side folds of Figure 2.5). The methyl groups of the alanine residues on the underside of the apβ-sheet surface can be clearly seen. The dashed lines represent the hydrogen bonds. Note the CH_3 group at the apex of the γ-turn.

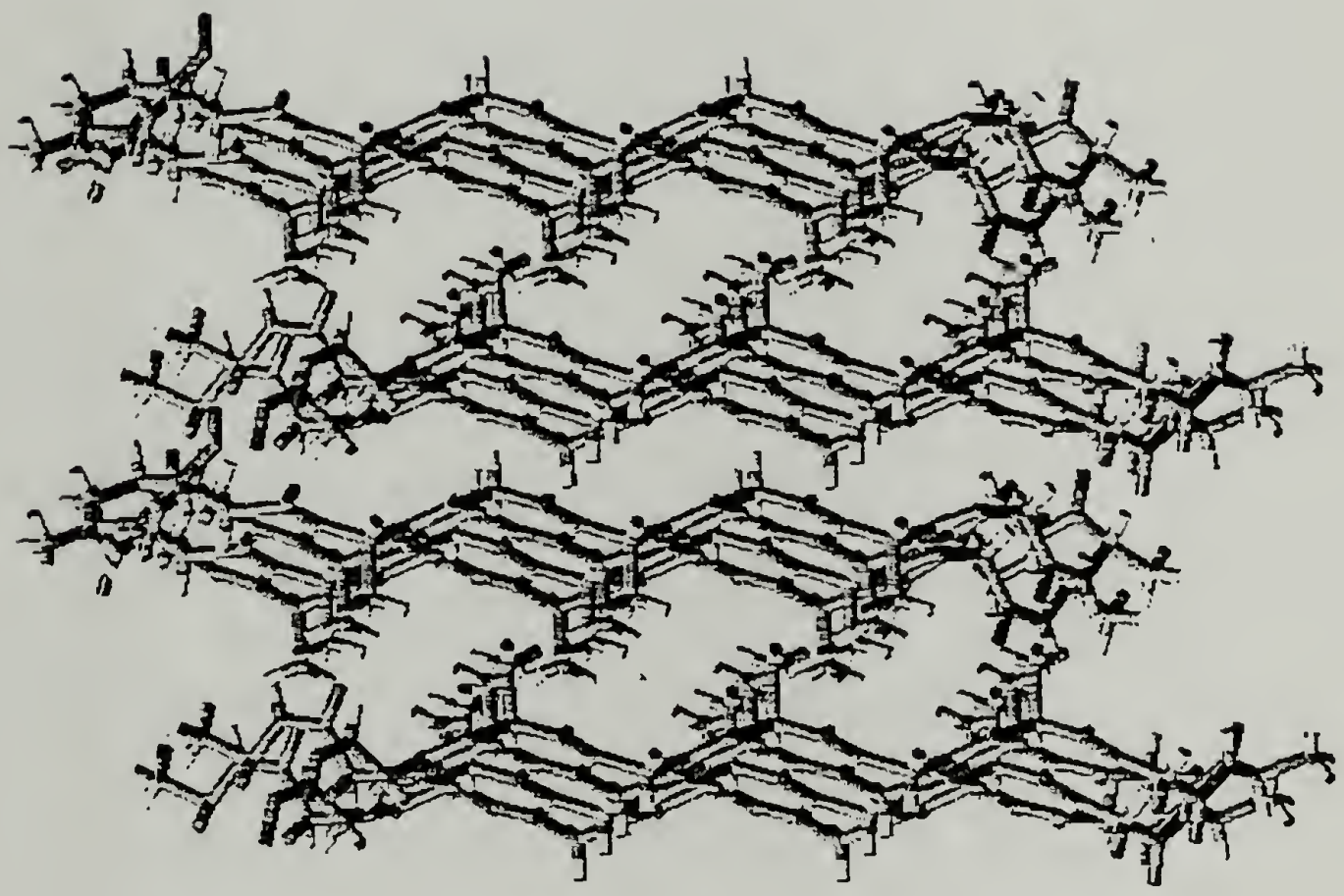

Figure 2.7. A computer-drawn view of refined structure of the chain-folded lamellar structure of poly(AG). The SXDP of this structure is shown in Figure 2.3d and can be compared with the experimental x-ray photograph shown in Figure 2.3a.

CHAPTER 3

DESIGN AND BIOSYNTHESIS OF ELASTIN-LIKE ARTIFICIAL EXTRACELLULAR MATRIX PROTEINS CONTAINING PERIODICALLY SPACED CS5/FIBRONECTIN DOMAINS WHICH BIND HUMAN UMBILICAL VEIN ENDOTHELIAL CELLS

3.1 Abstract

The biosynthesis of artificial extracellular matrix proteins for use in vascular reconstruction has been achieved. These proteins are based on an elastin-like pentapeptide repeat (VPGIG) periodically interspersed with the CS5 region of fibronectin. Both recombinant $(CS5(VPGIG)_{20})_5$ and $(CS5(VPGIG)_{40})_3$ promote adhesion and spreading of human umbilical vein endothelial cells (HUVECs). Although the binding domain (CS5) density is twice as high in $(CS5(VPGIG)_{20})_5$ as in $(CS5(VPGIG)_{40})_3$, the number of HUVECs spread on the former is more than twice that on the latter. This is likely due not only to the domain density, but to its availability based on the conformation of the proteins on the surface. This is the first step in the synthesis of recombinant, artificial extracellular matrix proteins for tissue reconstruction.

3.2 Introduction

Small diameter vascular grafts, < 6mm in diameter, are plagued by failure. Currently the optimal choice for vascular reconstruction is autologous saphenous vein if it

is available and healthy; unfortunately, the patency rate after 5 years is only 70%.[4] Polytetrafluoroethylene (PTFE) and polyethylene terephthalate (PET) are also commonly used for small diameter vascular grafts; however, the patency rate of these materials is lower than that of saphenous vein.[5] Failure most often occurs through thrombosis and occlusion of the graft or through neointimal hyperplasia at the anastomosis of the vascular grafts.[5]

Several techniques have been used to improve the effectiveness of PTFE and PET grafts. Much of the work has been directed toward achieving a confluent layer of endothelial cells on the luminal surface of the graft. Since healthy vessels are lined with a layer of endothelial cells, which provide a naturally nonthrombogenic interface, it is thought that a similar layer on a synthetic surface will also provide a naturally nonthrombogenic surface.[75] Taking this idea one step further, it is believed that a combination of the biological nature of saphenous vein (which is mechanically more similar to the artery that is to be replaced than are the noncompliant synthetic materials) along with the naturally confluent, luminal lining of endothelial cells make saphenous vein superior to PTFE and PET as a small diameter arterial replacement.[75]

We have designed artificial extracellular matrix proteins[76] exhibiting two main features. They provide structural support while providing sites for cell adhesion. These proteins are elastomeric in nature due to blocks of

(VPGIG) (the one letter amino acid code is used here and will be used throughout). (VPGIG) is known to have a modulus on the order of 1 x 10^6 dynes/cm^2 (depending on crosslink density and water uptake)[9] which is similar to that of native elastin, an extracellular matrix (ECM) protein. The materials also bind endothelial cells due to the presence of the CS5 region of fibronectin (FN).[46] These artificial extracelluar matrix proteins should provide a scaffolding for endothelial cells, which can attach and proliferate, while the cells remodel the ECM to create a natural environment. The artificial ECM should also maintain structural support until the seeded cells can create a native extracellular matrix.

Two techniques are currently available to achieve a confluent monolayer of endothelial cells on vascular grafts. Endothelial cells can be induced to grow into the graft by transinterstitial capillary ingrowth. This has been shown to be an effective means of endothelializing expanded PTFE (with a 60 μm internodal distance) in primates[77] and in canines[22], but has not been shown to be an effective method in humans. The lack of capillary ingrowth in humans may have to do with the thin, external, nonporous PTFE wrapping found on PTFE grafts used for human vascular bypass surgery.[77]

A second technique used to create a monolayer of endothelial cells on the luminal surface is to preseed the grafts with endothelial cells. This can be done by

harvesting autologous endothelial cells and seeding synthetic grafts immediately prior to implantation;[75,78] or, autologous cells can be harvested, cultured and then seeded onto the graft prior to implantation. [24,79] Recent data from several laboratories has suggested that the patency rate on these preseeded, synthetic vascular grafts is equivalent to that of saphenous vein.[24,79]

The improvement in patency, in humans, of preseeded, synthetic vascular grafts over those grafts which are implanted denuded of endothelial cells suggests that seeding of vascular grafts is indeed a method that, when employed with new materials, may result in improved vascular reconstruction. We will herein describe the design, synthesis and preliminary characterization of novel artificial extracellular matrix proteins that are expected to provide not only structural support, but to bind endothelial cells as well.

Structural support is provided by the pentapeptide repeat (VPGIG), a variant of the pentapeptide repeat (VPGVG), which has been found to repeat up to 11 times consecutively in native elastin.[41] Polymers composed of these repeats exhibit an inverse temperature transition,[80] with a change in temperature causing an entropic expansion or contraction of the material.[41] Using chemical synthetic techniques Nicol *et al.* incorporated RGDS peptides into the backbone of polymers based on the (VPGVG) peptide. The proteins were found to bind human foreskin fibroblasts and

bovine aortic endothelial cells.[48] In addition, proteins based solely on (VPGVG) were found to be nonadhesive toward these cell types.

The cell binding domain used here is the CS5 region of fibronectin found in the alternatively spliced type III connecting segment of fibronectin. It is a 20 amino acid long peptide found to promote cell binding.[11] Humphries *et al.* found that melanoma cells adhere to the CS5 region through the $\alpha_4\beta_1$ integrin receptor; more specifically, the receptors bound to REDV, the minimal sequence necessary for recognition by $\alpha_4\beta_1$, contained in the CS5 region.[11,42-44] Massia and Hubbell demonstrated that human umbilical vein endothelial cells (HUVECs) bind to the REDV peptide through the $\alpha_4\beta_1$ integrin receptor.[46] In further studies the authors found that the orientation of REDV was quite important for HUVEC adhesion. GREDVY peptide attached to a glass surface through the amine terminus promoted HUVEC binding while peptide bound to the surface through the carboxyl terminus was not adherent to HUVECs.[29] It was also shown that GREDVY-grafted surfaces were adherent toward HUVECs, but not toward smooth muscle cells (SMC), fibroblasts or platelets.[29,45]

Due to the apparent specificity of REDV for endothelial cells over other cell types regularly found in the vasculature, it was chosen for the cell adhesion domain. The entire CS5 region of fibronectin was chosen because it was anticipated that the naturally occurring amino acids surrounding the REDV domain would help to present the

sequence in such a way that it would be recognized by the $\alpha_4\beta_1$ integrin receptor. Nicol *et al.* found that chemical synthetic incorporation of short REDV sequences into a backbone made primarily of (VPGVG) repeats did not promote adhesion to the REDV sequences by the $\alpha_4\beta_1$ receptor in HUVECs.[47]

Recombinant protein molecules containing either a 20:1 or a 40:1 ratio of (VPGIG):CS5 have been synthesized. More specifically, MG(CS5$(VPGIG)_{20})_5$LE and MG(CS5$(VPGIG)_{40})_3$LE have been synthesized with the elastic portion spanning CS5 regions containing twice as many (VPGIG) repeats in the latter as in the former. Preliminary results show that HUVECs do bind to these materials. We find a 5-fold increase in the number of HUVECs bound to the $(CS5(VPGIG_{20}))_5$ protein as compared to the $(CS5(VPGIG)_{40})_3$ protein. It is believed that this adhesion is through the $\alpha_4\beta_1$ receptor as anticipated. This achievement is the first step in the design of precise materials for which biological recognition elements are engineered in or out depending on the specific intended use of the material.

3.3 Experimental Section

3.3.1 Materials

T4 DNA ligase, T4 polynucleotide kinase, calf intestinal phosphatase, and all restriction enzymes were purchased from New England Biolabs. Ribonuclease A,

Deoxyribonuclease I, ampicillin, kanamycin and chloramphenicol were purchased from Sigma Chemical Co. *Escherichia coli* strain DH5αF' was purchased from Bethesda Research Laboratories. Plasmid pUC18 and the XTT cell counting kit were purchased from Boeringer Mannheim. The expression plasmid pET-28a and *E. coli* strain BL21(DE3)pLysS[66] were obtained from Novagen. The HUVEC lines and complete medium were purchased from Clonetics. Falcon and Corning tissue culture dishes were purchased from Fisher Scientific. Versine EDTA solution for cell detachment and M199 serum free medium were purchased from Gibco.

3.3.2 General Methods

Bacterial growth in rich medium, DNA manipulations and transformations were performed as described in Sambrook, Frisch and Maniatis[67]. Polymerase chain reactions (PCR) were run in a Techne cyclogene thermocycler. ^{1}H NMR spectra were run on a Bruker AMX 500 MHZ spectrometer. Cell density measurements were done in plastic cuvettes with a path length of 1 cm at λ=600 nm on a Hitachi U2000 spectrophotometer. HUVEC culturing was done according to Clonetics protocol with the exception that cell detachment was performed nonenzymatically using 0.02% EDTA (w/v). Briefly, HUVECs were grown in polystyrene tissue culture flasks with Clonetics EBM complete medium. Cells were grown to 90% confluence prior to passaging. Cells were passaged 1

to 6 (i.e., 1/6 of the harvested cells were replated). All manipulations were performed in a laminar flow hood. Cell cultures were incubated in 5% CO_2 incubators at 37 °C. Cell counting was performed according to the Boeringer Mannheim XTT cell counting kit instructions; absorption was measured in disposable cuvettes with a path length of 1 cm at λ = 480 nm on a Hitachi U2000 spectrophotometer. Briefly, 0.4 ml of EBM complete medium was added to each well (containing HUVECs) of a 24 well plate; 0.2 ml of the XTT reagent was then added to each well. Cells were incubated with the reagent in the CO_2 incubator for 20 hr prior to reading the absorbance of the medium. Hydrolysis for amino acid analysis was done using propionic acid and 6.0 M hydrochloric acid followed by derivatization with phenyl isothiocyanate (PITC); amino acid content was analyzed using a Waters Picotag System.

3.3.3 Preparation of Synthetic DNA

Oligonucleotides (**1-3**) were synthesized on a 1 μmol scale on a Biosearch Model 8700 DNA synthesizer using phosphoramidite chemistry.[68] Crude oligonucleotides were purified by denaturing polyacrylamide gel electrophoresis and eluted using the "crush and soak" method.[67] Purified oligonucleotides were annealed at 80 °C and allowed to cool to room temperature over several hours. The annealed duplexes: CS5 (**1**), 28ap (**2**), and $(VPGIG)_5$ (**3**) were

phosphorylated with T4 polynucleotide kinase, ethanol precipitated and dried *in vacuo*.

(1)

```
Eco RI(Z) Sal I
|           |  G  E  E  I  Q  I  G  H  I  P  R  E  D  V  D Y  H  L
AATTCTAAGTCGACGGTGAAGAGATCCAGATCGGCCACATCCCGCGTGAAGACGTTGACTACCACCTG
    GATTCAGCTGCCACTTCTCTAGGTCTAGCCGGTGTAGGGCGCACTTCTGCAACTGATGGTGGAC

        Ban I  Xho I Bam HI
 Y  P    |      |     |
TACCCGGGGGTGCCGCTCGAGG
ATGGGCCCCCACGGCGAGCTCCCTAG
```

(2)

```
Nco I   Xho I Z  Z   Sal I
|         |             |
CCATGGGCCTCGAGTAATAAAG
    CCGGAGCTCATTATT TCAGCT
```

(3)

```
Eco RI Z Ban I
|        G|V  P  G  I  G  V  P  G  I  G  V  P  G  I  G  V  P  G  I
AATTCTAAGGGGTGCCGGGTATCGGCGTTCCGGGCATCGGTGTACCGGGCATCGGTGTTCCGGGCATC
    GATTCCCCACGGCCCATAGCCGCAAGGCCCGTAGCCACATGGCCCGTAGCCACAAGGCCCGTAG

                  Ban I  Bam HI
 G  V  P  G  I  G|V  P  |
GGTGTTCCGGGTATCGGGGTGCCGG
CCACAAGGCCCATAGCCCCACGGCCCTAG
```

3.3.4 Cloning and Amplification of Synthetic DNA

Purified CS5 DNA was ligated into Eco RI/Bam HI digested pUC18 and used to transform *E. coli* strain DH5αF'.

Cells were grown at 37 °C overnight on 2xYT solid medium containing 200 μg/ml ampicillin, 25 μg/ml β-isopropylthiogalactoside (IPTG) and 40 μg/ml of the chromogenic substrate 5-bromo-4-chloro-3-indolyl-β-D-galactopyranoside (X-Gal) for blue-white screening. Plasmid DNA from white transformants was sequenced using Sequenase 2.0 (Amersham Life Sciences) to verify the identity of the insert. After isolation of the recombinant plasmid from a 1 liter 2xYT culture, the CS5 DNA was excised by digestion with Eco RI and Bam HI and the fragments were separated by nondenaturing polyacrylamide gel electrophoresis. DNA monomer was eluted from the polyacrylamide gel by the "crush and soak" method.[67]

Similarly purified $(VPGIG)_5$ DNA was ligated into Eco RI/Bam HI digested pUC18 and used to transform *E. coli* strain DH5αF'. Cells were grown at 37 °C overnight on 2xYT solid medium containing 200 μg/ml ampicillin, 25 μg/ml β-isopropylthiogalactoside (IPTG) and 40 μg/ml of the chromogenic substrate 5-bromo-4-chloro-3-indolyl-β-D-galactopyranoside (X-Gal) for blue-white screening. Plasmid DNA from white transformants was sequenced using Sequenase 2.0 (Amersham Life Sciences) to verify the identity of the insert. After isolation of the recombinant plasmid from a 1 liter 2xYT culture, the $(VPGIG)_5$ DNA was digested with Ban I and the fragments were separated by nondenaturing polyacrylamide gel electrophoresis. DNA monomer was eluted

from the polyacrylamide slice, using the "crush and soak" method.[67]

Purified 28ap was ligated into Nco I/Xho I digested pET-28a and used to transform *E. coli* strain DH5αF'. Cells were grown overnight on 2xYT solid medium containing 34 μg/ml kanamycin. Plasmid DNA from single colonies was sequenced using Sequenase 2.0 (Amersham Life Sciences) to verify the identity of the insert. The recombinant plasmid was designated pET-28ap.

3.3.5 Cloning of CS5 in Transfer Vector

Purified CS5 monomer was ligated into Bam HI/Eco RI digested pEC2 plasmid DNA (shown in appendix A). The resulting plasmid (designated pEC2-CS5) was used to transform *E. coli* strain DH5αF'. Cells were grown overnight on 2xYT solid medium containing 34 μg/ml kanamycin. Plasmid DNA from single colonies was verified for CS5 insert by Bam HI/Eco RI digestion followed by 1% agarose gel electrophoresis and visualization of the DNA with ethidium bromide (EtBr). The expected band was observed at 100 bp.

3.3.6 Polymerization of the $(VPGIG)_5$ Monomer and Cloning of $(VPGIG)_5$ Multimers

Purified monomeric $(VPGIG)_5$ DNA was self-ligated with T4 DNA ligase to form a population of multimers. Multimers were ligated into Ban I digested, dephosphorylated pEC2-CS5. The recombinant plasmids were used to transform *E. coli*

strain DH5αF'. Transformants were screened by PCR[81] with cycling times and temperatures as follows: 96 °C, 1 min; 45 °C, 2 min; 72°C, 2 min with 35 cycles. Vent polymerase was used with Pst I site primers for pBR322 (New England Biolabs). Clones encoding 4 and 8 repeats of the $(VPGIG)_5$ monomer were chosen and the recombinant plasmids were designated pEC2-CS5$(VPGIG)_{20}$ and pEC_2-CS5$(VPGIG)_{40}$ respectively.

3.3.7 Construction of Bacterial Expression Vector

Recombinant pEC2-CS5$(VPGIG)_{20}$ or pEC2-CS5$(VPGIG)_{40}$ was digested with Xho I/Sal I to release the CS5$(VPGIG)_x$ cassette. The cassettes were separated by 1% agarose gel electrophoresis and recovered by extraction with Qiaex II DNA extraction kit (Qiagen). The recovered DNA was ligated into Xho I digested, dephosphorylated pET-28ap and used to transform *E. coli* strain DH5αF'. Transformants were screened for the presence and orientation of each multimer by Pflm I/Xho I digestion. Digested DNA was visualized with EtBr following 1% agarose gel electrophoresis. Bands comprising 430 base pairs plus the length of the insert indicate DNA insertion in the correct orientation. This process was performed repeatedly to obtain recombinant plasmids, designated pET-28ap-$(CS5(VPGIG)_{20})_5$ or pET-28ap-$(CS5(VPGIG)_{40})_3$, which were used to transform the expression host, *E. coli* strain BL21(DE3)pLysS.

3.3.8 Protein Expression, Batch Phase, Rich Medium

Single colonies of BL21(DE3)pLysS containing recombinant pET-28ap-$(CS5(VPGIG)_{20})_5$ or pET-28ap-$(CS5(VPGIG)_{40})_3$ were used to inoculate 10 ml of 2xYT medium containing chloramphenicol (34 μg/ml) and kanamycin (34 μg/ml). The cultures were grown to saturation and used to inoculate 1 L volumes of 2xYT medium containing chloramphenicol (34 μg/ml) and kanamycin (34 μg/ml). The cultures were grown to OD_{600} = 1 at 37 °C and protein expression was induced by the addition of IPTG to a final concentration of 1.0 mM. Cells were harvested after 3 hours by centrifugation (5,000 x g, 15 min at 4 °C). The cell pellets were resuspended in 15 mL of TEN (50mM Tris-Cl (pH 8.0), 1 mM EDTA, 100 mM NaCl) and stored at -20 °C.

3.3.9 Purification of $(CS5(VPGIG)_{20})_5$

Frozen cells were thawed and phenylmethyl sulfonyl fluoride (PMSF) (1 mM), $MgCl_2$ (5 mM), RNAse (20 μg/ml) and DNAse (20 μg/ml) were added to the suspension. The resulting solution was incubated at 37 °C for 30 min and the soluble portion was recovered by centrifugation (10,000 x g, 4 °C, 30 min). The supernatant was acidified to pH 5.0 by addition of 0.1 N HCl and left at room temperature for 1 hr. The suspension was centrifuged at 10,000 x g for 20 minutes at room temperature to recover the precipitate. The pellet was resuspended in 5 ml 1 M urea and incubated at room temperature for 1 hr, then centrifuged at 10,000 x g for 20

min to recover the soluble portion. The supernatant was dialyzed (25,000 molecular weight cut off (MWCO) dialysis tubing, Spectrapore) against H_2O at 4 °C for 2 days with H_2O changes. The dialysate was centrifuged to remove impurities and the supernatant was lyophilized to recover the recombinant $(CS5(VPGIG)_{20})_5$.

3.3.10 Purification of $(CS5(VPGIG)_{40})_3$

Frozen cells were thawed and phenylmethyl sulfonyl fluoride (PMSF) (1 mM), $MgCl_2$ (5 mM), RNAse (20 μg/ml) and DNAse (20 μg/ml) were added to the suspension. The solution was incubated at 37 °C for 30 min and the insoluble portion was recovered by centrifugation (10,000 x g, 4 °C, 30 min). The pellet was resuspended in 15 ml 1 M urea and incubated at room temperature for 1 hr, then centrifuged at 10,000 x g for 20 min to recover the soluble portion. The supernatant was dialyzed (25,000 MWCO dialysis tubing, Spectrapore) against H_2O at 4 °C for 3 days with H_2O changes. The dialysate was then centrifuged to remove impurities and the supernatant was lyophilized to recover the recombinant $(CS5(VPGIG)_{40})_3$.

3.3.11 Film Casting

Glass coverslips (12 mm) were coated with $(CS5(VPGIG)_{20})_5$ or $(CS5(VPGIG)_{40})_3$ from solutions in formamide or water by addition of 40 μl of a 1 mg/ml solution to the top surface of the coverslip followed by spreading of the

solution with the tip of a pipet. Fibronectin films were cast from 100 μg/ml solutions in distilled H_2O(dH_2O); 20 μl of solution was applied to a glass coverslip and spread with the tip of a pipet. All coverslips were then dried at 55 °C in a vacuum oven. Coverslips were incubated in 0.5 ml sterile H_2O at 37 °C for 2 hours to remove excess protein and again dried in vacuo at 55 °C for 2 hours.

3.3.12 Cell Culturing

Pooled primary HUVECs were cultured and maintained in Clonetics EBM complete medium in 10 cm Falcon tissue culture polystyrene petri dishes. HUVECs from passages 2-10, in our hands, were used for all cell adhesion studies. Cells were washed with 5 ml phosphate buffered saline (PBS) once and then harvested using Versine, a 0.02% EDTA solution in PBS. Harvested cells were resuspended in serum free M199 medium, counted using a hemocytometer and diluted to a density of 1×10^4 cells/ml. HUVECs were transferred to 24 well dishes, 1×10^4 cells/well, containing protein coated glass coverslips. Cells were maintained at 37 °C and 5% CO_2 for 4 hours and counted using XTT following the Boeringer Mannheim XTT kit protocol. Briefly, glass coverslips containing attached cells were removed from the culture well, washed three times with phosphate buffered saline + $CaCl_2$ (0.2 g/L) and $MgCl_2$ (0.2 g/L) (PBS+) and placed in new 24 well plates. Endothelial cell medium, phenol red free, (0.4 ml, Clonetics) and 0.2 ml of cell counting reagent were

added to each well. Cells were returned to the CO_2 incubator for 20 hr. The absorbance of the supernatant was then read at 460 nm.

3.3.13 Cell Counting Calibration

Calibration curves were made during each cell culturing experiment. HUVECs were cultured at the following concentrations (2 wells each) in serum free medium: 10,000; 7,500; 5,000; 2,500; 1000; 750; 500; and 250 cells/well. Cultured cells were maintained in an incubator, 37 °C and 5% CO_2, for 4 hours. After 4 hours the medium was removed; the HUVECs were washed with 0.5 ml PBS and 0.4 ml of medium containing serum, and 0.2 ml of cell counting reagent was added to each well. The calibration wells were maintained and evaluated as described above.

3.3.14 Cell Adhesion after Removal with Trypsin

Removal of HUVECs from polystyrene dishes was performed as recommended by Clonetics.

3.4 Results and Discussion

3.4.1 Gene Construction

The strategy used in our laboratory to prepare artificial proteins has been described previously.[32] In this work, DNAs encoding two chain-length variants of $CS5(VPGIG)_x$ which contain 5' Sal I cohesive ends and 3' Xho

I cohesive ends were ligated into the Xho I site of the expression plasmid pET-28ap. The cohesive ends generated by Xho I and Sal I digestion are the same, and hence can be ligated; however, the flanking base pairs are different, so once the ends are ligated the Sal I and Xho I sites are destroyed. This process maintains an Xho I site at the 3' end of the gene for addition of DNA cassettes, while eliminating other restriction sites in the gene so that it will not be cut into pieces upon enzymatic digestion with Xho I. This strategy allows for ease in construction of longer genes. The resulting recombinant plasmids encode either $(CS5(VPGIG)_{20})_5$ or $(CS5(VPGIG)_{40})_3$ (**4**) and (**5**) respectively.

$MG(LDGEEIQIGHIPREDVDYHLYP(GVPGI)_{20})_5LE$ (**4**)

$MG(LDGEEIQIGHIPREDVDYHLYP(GVPGI)_{40})_3LE$ (**5**)

These genes are constructed in such a way that upon translation into protein only minimal amino acid fusions are added to the ends of the protein of interest. A methionine residue must always be added as it indicates the translational start; in addition a glycine residue is added to the start as a result of the use of the Nco I site in cloning. Two amino acids are also added to the amino terminus due to cloning into the Xho I site. These additions result in minimal amino acid fusions.

3.4.2 Protein Expression

The host used for protein expression was *E. coli* strain BL21(DE3)pLysS.[66] In this strain, a gene encoding T7 RNA polymerase is incorporated into the bacterial chromosome under *lacUV5* control, and protein production is induced by the addition of IPTG. The pLysS plasmid provides low levels of T7 lysozyme, which inhibits T7 RNA polymerase and suppresses the basal level of protein expression.

Protein expression in rich medium was performed as described in the Experimental Section. Aliquots of cultures representing approximately equal numbers of cells (as determined by the optical density at 600 nm - OD_{600}) were removed periodically after induction of protein synthesis (t= 0 - 180 minutes). Samples were loaded on a 10% polyacrylamide gel and separated by electrophoresis. Protein bands were stained with Coomassie Brilliant Blue R-250. The recombinant protein does not stain well; however it forms a pale blue band which, owing to over-expression and consequent distortion of the adjacent electric field, appears to compress lower molecular weight protein bands, as can be seen near 65,000 da $(CS5(VPGIG)_{40})_3$ (Figure 3.1). Figure 3.1 is a 10% polyacrylamide gel containing whole cell lysate samples of BL21(DE3)pLysS pET-28ap-$(CS5(VPGIG)_{40})_3$. Lane 1 contains molecular weight standards while lanes 2 through 5 contain whole cell lysate from cultures at t = 0, t = 1 hr, t = 2 hr and t = 3 hr respectively. A pale blue band corresponding to $(CS5(VPGIG)_{40})_3$ (molecular weight

59,765 da) can be seen to grow in over the observed observation period.

3.4.3 Protein Purification and Analysis

For cultures grown to OD_{600} = 0.8, 60 mg/L of $(CS5(VPGIG)_{40})_3$ and 40 mg/L of $(CS5(VPGIG)_{20})_5$ (molecular weight 56,984 da) can be recovered through a simple procedure involving selective precipitation of contaminating proteins below the lower critical solution temperature of the target protein.

The ^{1}H and ^{13}C NMR spectra of $(CS5(VPGIG)_{40})_3$ and $(CS5(VPGIG)_{20})_5$ in formic acid (Figures 3.2 & 3.3) indicate the presence of the (VPGIG) repeat. As the CS5 regions of the molecules represent only a few percent of the entire protein, they are not easily detected by 1D NMR; and therefore the peaks corresponding to those amino acids are not seen in Figures 3.2a and 3.3a. Splitting of the β, γ and δ Pro $C\underline{H}_2$ can clearly be seen near 3.8-4.0 and 2.0-2.5 ppm due to cis trans isomerization.[8] Only one Gly $C\underline{H}_2$ is resolved at 2.5 ppm in the proton spectrum; however, both glycine residues in the pentapeptide repeat are resolved in the carbon spectrum and are seen as two distinct peaks at 45-46 ppm (Fig. 3.2b & 3.3b). These spectra compare quite nicely with spectra obtained by McPherson *et al.* of recombinant $(VPGVG)_{x,}$ save that of isoleucine peaks replacing the peaks due to the 4th valine residue as a result of substitution of Ile for Val in the pentapeptide.[8]

Table 3.1 shows amino acid analysis results for $(CS5(VPGIG)_{40})_3$ and $(CS5(VPGIG)_{20})_5$. Both analyses are in agreement with the expected protein compositions within the uncertainty of the measurement. Experimental values indicate that both the amino acids of the CS5 region and the amino acids of the (VPGIG) region are present in the correct ratios as are as expected from NMR spectra. The absence of unassigned peaks in the NMR spectra, combined with the amino acid analysis, are consistent with sample purity.

3.4.4 HUVEC Adhesion and Spreading

Table 3.2 contains cell counting data obtained from culturing 10^4 HUVECs per well in 24 well culture dishes (as described above). Each well contained a glass coverslip coated with protein. As shown, $(CS5(VPGIG)_{20})_5$ and fibronectin (FN) coated coverslips bind nearly all of the cells plated into the well. The value for $(CS5(VPGIG)_{20})_5$ cast from H_20 is higher than the number of cells plated into each well; 11,760 cells were counted while only 10,000 were plated. This can be explained by a small amount of cell growth during the 20 hour incubation time with complete medium and XTT cell counting reagent. Significantly fewer cells are seen to attach to $(CS5(VPGIG)_{40})_3$ cast from water and from formamide. There are relatively few cells attached to the glass surface.

Figures 3.4a-e show HUVECs on the surfaces after 4 hours, prior to rinsing with PBS. Greater numbers of HUVECs

are seen on the $(CS5(VPGIG)_{20})_5$ surfaces cast from formamide (Figure 3.4b) and from water (Figure 3.4c) as compared to the other surfaces. The majority of the cells are spread or spreading as judged from their nonrefractile nature. Fewer cells are retained on the $(CS5(VPGIG)_{40})_3$ surfaces cast from formamide (Figure 3.4d) and water (Figure 3.4e) but, again, the majority of the HUVECs are spread or spreading. Although a similar number of HUVECs appear on the glass surface (Figure 3.4a) and on the $(CS5(VPGIG)_{40})_3$ surfaces, the majority of the cells on the glass surface are not adherent as judged from the highly refractile images of the cells. The artificial extracellular proteins promote cell attachment and spreading.

Urry and colleagues chemically synthesized poly{20(GVGVP),(GREDVP)}.[47] These proteins are random block copolymers where the ratio of (GVGVP) to (GREDVP) is 20 to 1. They found no adhesion of HUVECs or of A375 melanoma cells, which are known to express $\alpha_4\beta_1$,[42] to these materials. This result may be due to the short (GREDVP) peptide not achieving the proper conformation for binding to $\alpha_4\beta_1$.

Hubbell and colleagues have observed HUVEC spreading on glycophase glass which has been modified through N-terminal grafting of GREDVY peptides to the surface at a concentration of approximately 10 pmol/cm^2.[45] They report the percentage of attached cells that are spread, but do not report the number of cells that are attached. They also fail to report their criteria for attachment or how to

define attached vs nonattached.[45] These uncertainties make accurate comparison of results difficult; however, as determined from protein stability results reported in chapter 4, 19 ± 2 pmol/cm^2 of $(CS5(VPGIG)_{20})_5$ is present on the glass coverslips. Assuming that HUVECs have access to the top 10 Å of the recombinant protein film, there is 10 ± 2 pmol/cm^2 of CS5 ligand available for adhesion (comparable to that achieved by Hubbell *et al.*).[45] The attachment and spreading of HUVECs to $(CS5(VPGIG)_{40})_3$ and $(CS5(VPGIG)_{20})_5$ are consistent with the results of Hubbell *et al.* and attributable to adhesion of the HUVECs to the CS5 region.

There are significant differences in the number of cells attached to surfaces cast from $(CS5(VPGIG)_{20})_5$ and surfaces cast from $(CS5(VPGIG)_{40})_3$. Although the receptor density in the former is only twice the density of the latter, more than twice as many cells attach and spread on $(CS5(VPGIG)_{20})_5$ (≈10,000) as on $(CS5(VPGIG)_{40})_3$ (≈2000) (Table 3.2). This is likely due not only to the density of the receptor in the protein itself, but to the accessibility of the receptor once the protein has adhered to a surface. While the two artificial proteins are quite similar in primary structure, it is probable that upon adhesion to glass surfaces their secondary and tertiary structures become quite different; thus the CS5 domain in $(CS5(VPGIG)_{40})_3$ may not be as accessible to the HUVECs as it is in the $(CS5(VPGIG)_{20})_5$ protein, due to conformational differences.

Figure 3.5a-f show HUVECs that were harvested using trypsin (Figure 3.5a, 3.5c, 3.5e) and HUVECs that were harvested using EDTA (Figure 3.5b, 3.5d, 3.5f) spreading on glass, $(CS5(VPGIG)_{20})_5$, or $(CS5(VPGIG)_{40})_3$ surfaces after 1 hour in serum free medium. It is evident in all cases that HUVECs removed from polystyrene culture dishes using trypsin do not spread as well as HUVECs removed with EDTA. The difference in spreading of nonenzymatically vs enzymatically harvested cells on $(CS5(VPGIG)_{20})_5$ cast from formamide is striking (Figures 3.5c, d, e and f). If the adhesion to $(CS5(VPGIG)_{20})_5$ is mediated by the $\alpha_4\beta_1$ integrin receptor, as expected, then this difference in adhesion can be explained. Masumoto and Hemler found that trypsin cleaves the extracellular domain of the α_4 integrin subunit.[82] Cleavage of the α_4 subunit by trypsin would inhibit binding by $\alpha_4\beta_1$ to CS5.

3.5 Conclusions

The biosynthesis and purification of $(CS5(VPGIG)_{20})_5$ and $(CS5(VPGIG)_{40})_3$ have been successfully achieved as indicated by polyacrylamide gel electrophoresis, ^1H and ^{13}C NMR spectroscopy and amino acid analysis. The proteins induce the adhesion and spreading of HUVECs. It is likely that the adhesion is through $\alpha_4\beta_1$ integrin recognition of the CS5 block of the proteins.

It is possible to synthesize artificial extracellular matrix proteins using recombinant DNA techniques. These

proteins can be designed in such a way that they provide support for the growing cells and provide biological signals specific for these cells. We have demonstrated that we can design and synthesize elastin-like materials which contain binding sites for HUVECs. The number of binding sites is readily varied to control the initial density of the seeded cells. This approach may be important in the reconstruction of tissues and organs.

The technique described herein is not limited to building in a single biological signal. It is equally possible to choose specifically several signals and build these simultaneously into one or, should this approach prove more desirable, into a selected number of different artificial extracellular matrix proteins. The current work is a first step in the biosynthesis of biological scaffolding for the reconstruction of blood vessels.

Table 3.1 Amino Acid Analyses of $(CS5(VPGIG)_{20})_5$ and $(CS5(VPGIG)_{40})_5$

	$(CS5(VPGIG)_{20})_5$		$(CS5(VPGIG)_{40})_3$	
amino acids	theor.	expl.	theor.	expl.
ASP + ASN	2.44	2.22	1.34	2.31
GLU+GLN	3.42	3.03	1.94	3.25
SER	------	0.37	------	0.64
GLY	34.36	34.01	36.87	33.93
HIS	1.63	1.19	0.9	0.95
ARG	0.81	0.89	0.45	0.82
THR	------	0.35	------	0.005
ALA	------	0.72	------	1.11
PRO	16.29	17.27	18.8	16.92
TYR	1.63	1.34	0.9	1.09
VAL	17.1	17.73	18.36	17.61
MET	0.16	0.16	0.15	0.21
CYS	------	------	------	------
ILE	18.73	18.06	19.25	17.77
LEU	1.79	1.92	1.04	1.79
PHE	------	0.21	------	0.30
LYS	------	0.44	------	0.62

Table 3.2 Number of HUVECs on Surfaces after 4 Hours in Serum Free Medium

Protein / Cast From	Number of Cells on Surface
Glass	2,880 ± 1670
$(CS5(VPGIG)_{20})_5$ / Formamide	9,170 ± 1800
$(CS5(VPGIG)_{20})_5$ / Water	11,700 ± 760
$(CS5(VPGIG)_{40})_3$ / Formamide	1,150 ± 360
$(CS5(VPGIG)_{40})_3$ / Water	2,590 ± 570
Fibronectin	10,140 ± 290

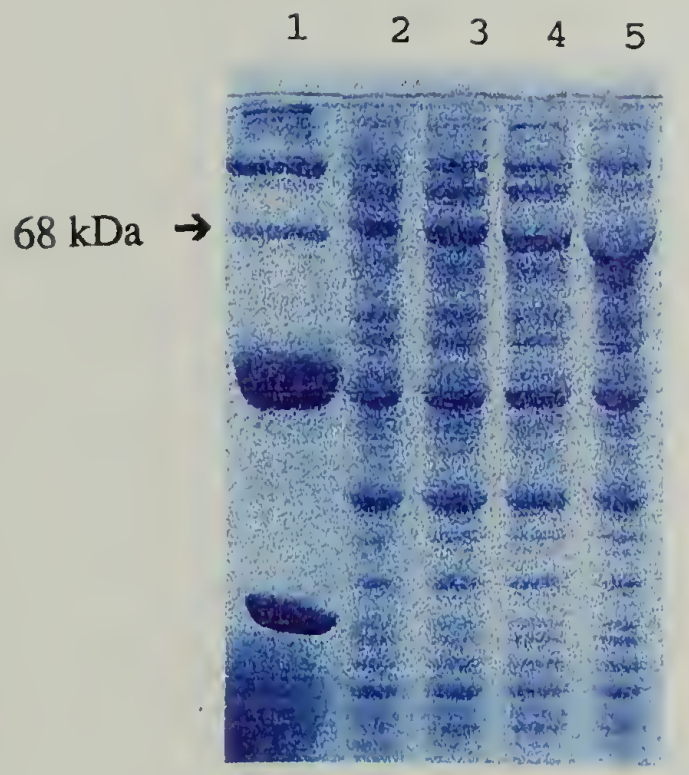

Figure 3.1 A 10% SDS-PAGE of $(CS5(VPGIG)_{40})_3$ whole cell lysate is shown. Lane 1 contains molecular weight marker, bands from top to bottom: 200, 97.4, 68, 43, 29, 18.4, & 14.3 kDa. Lanes 2-5 contain whole cell lysate of t = 0, t = 1, t = 2, & t = 3 hrs respectively. The recombinant protein can be seen as a pale blue band growing into lanes 3-5 at 68 kDa.

2a

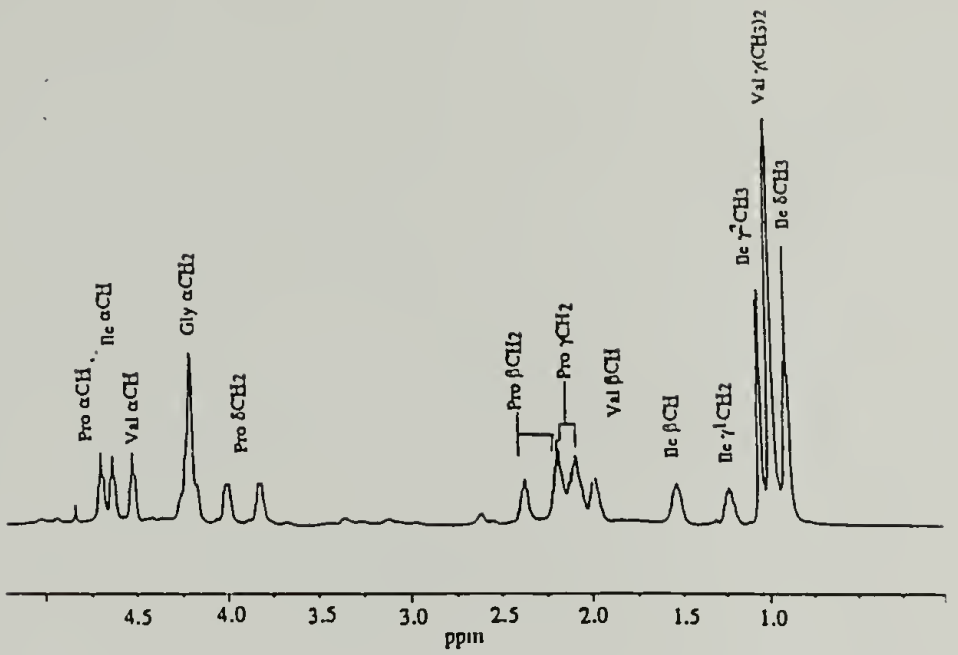

2b

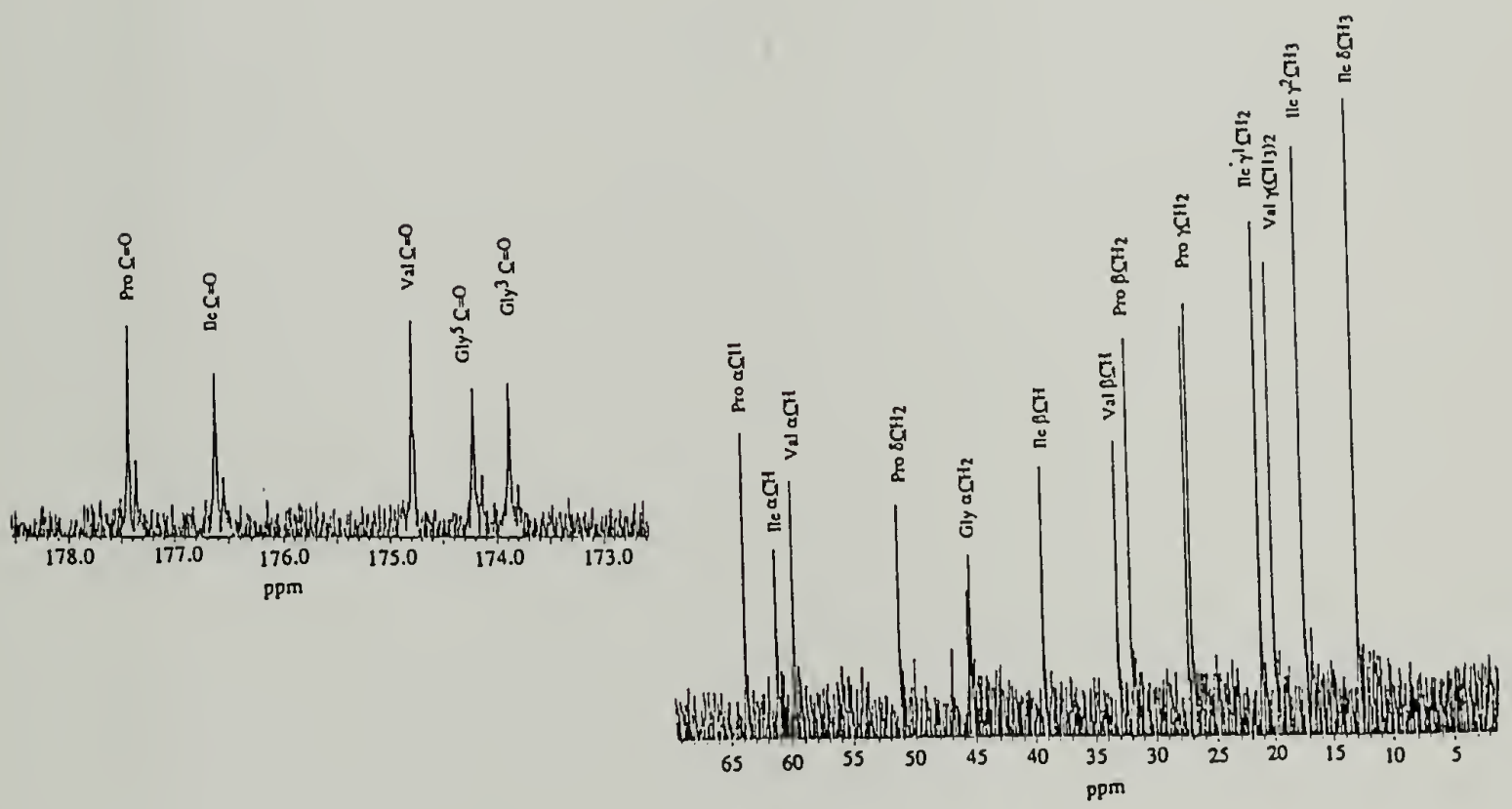

Figure 3.2. NMR spectra of purified $(CS5(VPGIG)_{40})_3$ in formyl-d formic acid. 3.2a shows the 500 MHz proton NMR spectrum; all peaks are identified as shown. Identification of all peaks is consistent with assignments made by McPherson *et al.*[8] with the exception of the isoleucine chemical shifts which were assigned independently. 3.2b shows the carbon-13 spectrum. Only the resonances from the major amino acid components (VPGIG) can be seen.

3a

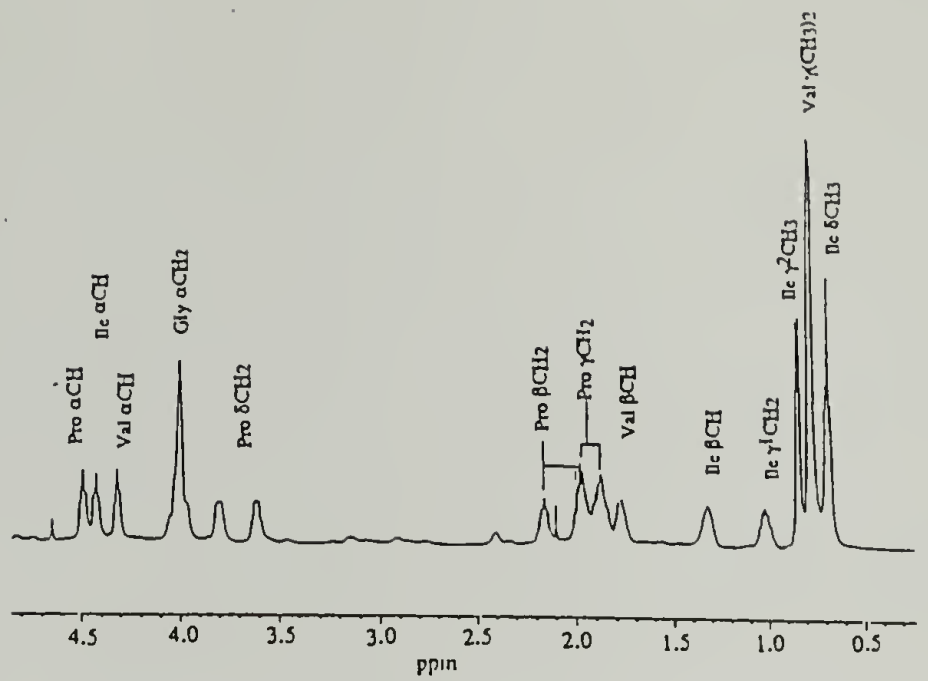

3b

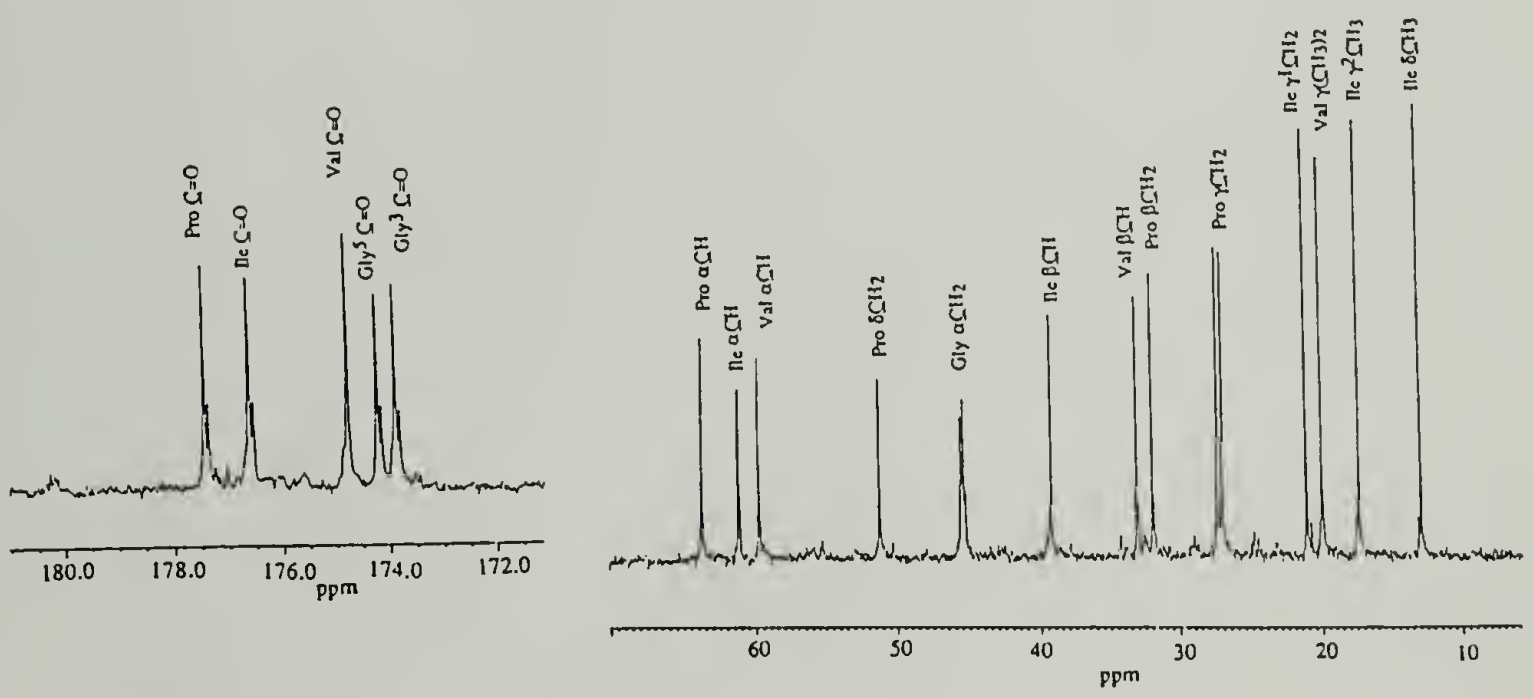

Figure 3.3. NMR spectra of purified $(CS5(VPGIG)_{20})_5$ in formyl-d formic acid. 3.3a shows the 500 MHz proton NMR spectrum; identification of all peaks is consistent with assignments made by McPherson *et al.*[8] with the exception of the isoleucine chemical shifts which were assigned independently. 3.3b shows the carbon-13 spectrum. Only the resonances from the major amino acid components (VPGIG) can be seen.

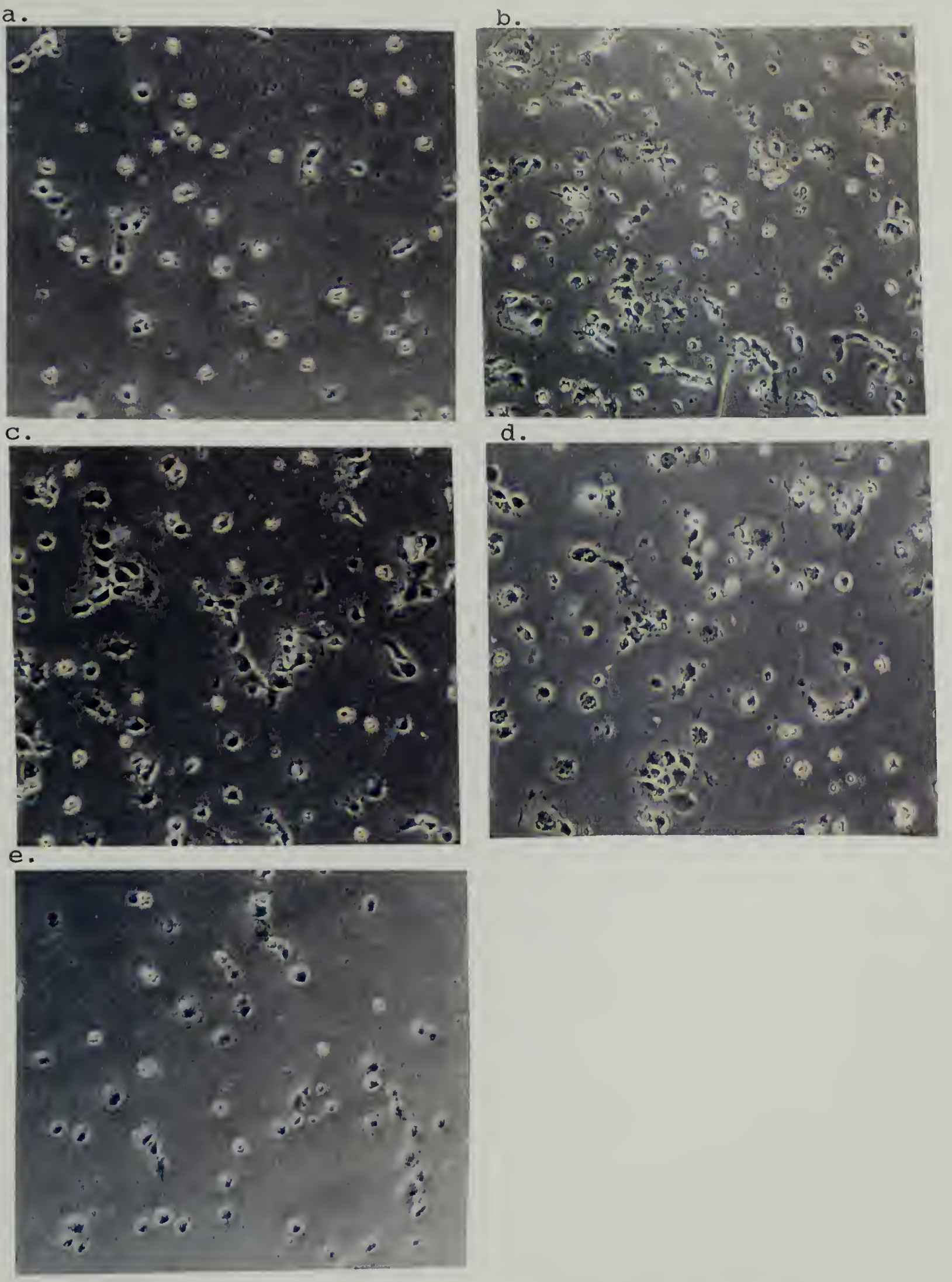

Figure 3.4. Phase contrast images of HUVECs spreading on a) glass, b) $(CS5(VPGIG)_{20})_5$ cast from formamide, c) $(CS5(VPGIG)_{20})_5$ cast from water, d) $(CS5(VPGIG)_{40})_3$ cast from formamide, and e) $(CS5(VPGIG)_{40})_5$ cast from water.

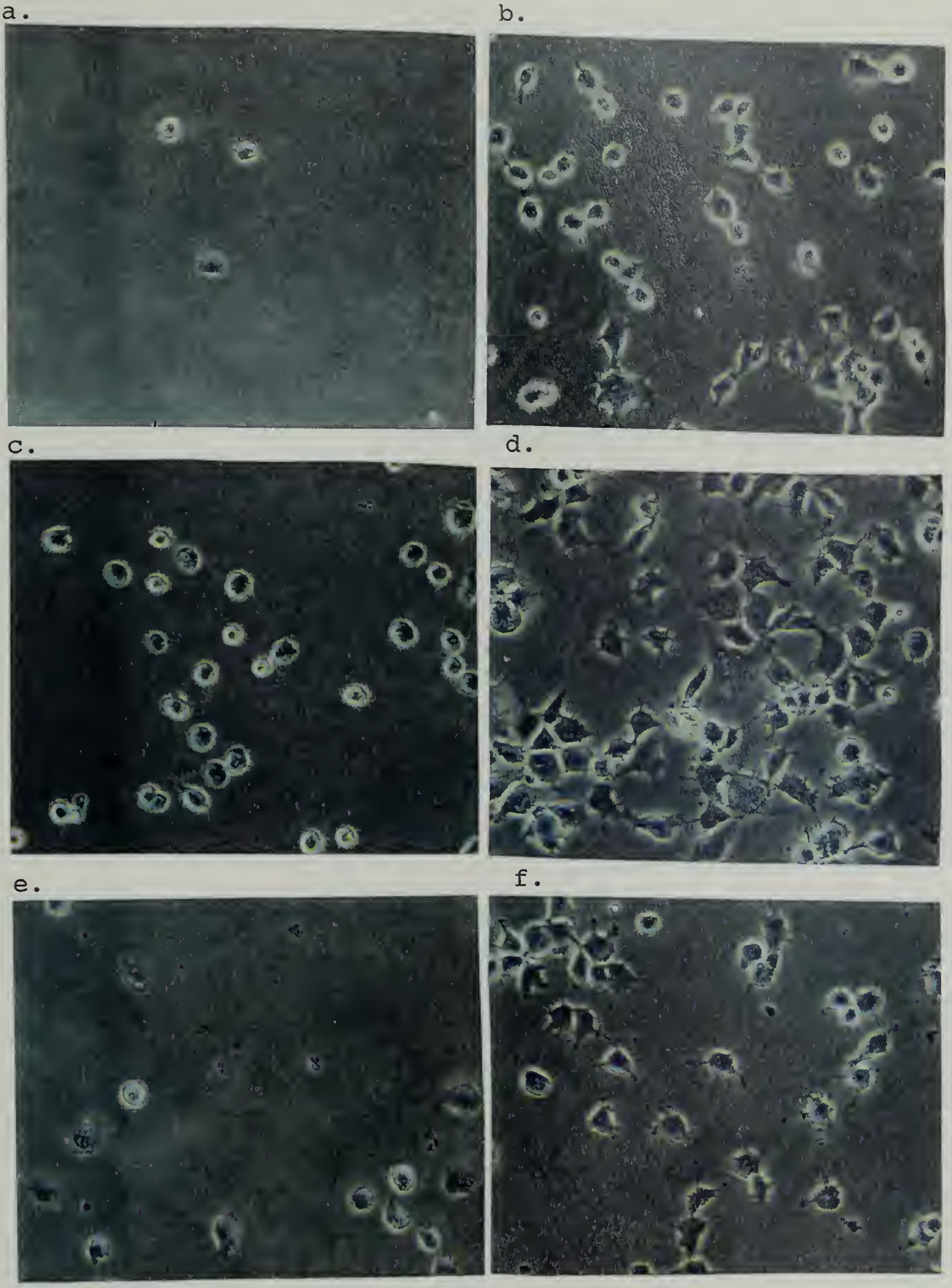

Figure 3.5. Phase contrast images of HUVECs harvested with Trypsin (5a, 5c, 5e) or EDTA (5b, 5d, 5f). Images show spreading on: a&b) glass, c&d) $(CS5(VPGIG)_{20})_5$ cast from formamide, e&f) $(CS5(VPGIG)_{40})_3$ cast from formamide.

CHAPTER 4

RECOMBINANT ARTIFICIAL EXTRACELLULAR MATRIX PROTEINS: CHARACTERIZATION AND CELL - BINDING BEHAVIOR

4.1 Abstract

Recombinant artificial extracellular matrix proteins have been evaluated as materials for use in the design of new vascular prostheses. Two proteins $(CS5(VPGIG)_{40})_3$ and $(CS5(VPGIG)_{20})_5$ which contain the CS5 region of fibronectin, known to bind to the $\alpha_4\beta_1$ integrin receptor,[11] and an elastin like pentapeptide (VPGIG),[12] have been cast into films upon which human umbilical vein endothelial cells (HUVECs) were cultured. These proteins promote the adhesion and spreading of HUVECs. The number of cells adherent to the surface is dependent on the density of the CS5 domain with $(CS5(VPGIG)_{20})_5$ exhibiting 5 times the number of adhered cells as $(CS5(VPGIG)_{40})_3$. The extent of individual cell spreading is seen to be similar on both materials. Adhesion of HUVECs to these materials supports the formation of actin filaments as shown by fluorescent staining of the actin. The existence of the LCST in both materials suggests that they retain the properties of the elastin-like backbone despite the periodic insertion of CS5.

4.2 Introduction

It has been well documented that cells respond to the surface with which they are in contact. These surfaces may

be biological in nature and thus contain biospecific moieties that signal the cells to respond in a defined manner, or they may be synthetic materials that, due to their chemical or physical properties, signal the cells in a nonspecific fashion. Grande *et al*. demonstrated that chondrocytes cultured *in vitro* on polyglycolic acid produce proteoglycans, while chondrocytes cultured on type I collagen produce primarily collagen.[49] Peluso *et al*. found that poly(hydroxyethyl methacrylate) P(HEMA) supported minimal fibroblast attachment and spreading, while an interpenetrating polymer network containing 10 wt % polycaprolactone and 90 % P(HEMA) induced cell spreading and stimulated a 4-5 fold increase in collagen production by the fibroblasts.[83] By functionalizing polyethylene with COOH, CH_2OH, $CONH_2$, and CH_2NH_2 groups (using corona discharge treatment), Lee *et al*. found that they could change the ability of Chinese hamster ovary cells to adhere, spread and grow on the surfaces; the positively charged CH_2NH_2 surface was found to maximize these behaviors.[84] By altering the surface charge of poly(vinylidene fluoride)(PVDF), Bouaziz *et al*. demonstrated that the secretion of prostacyclin and thromboxane by endothelial cells cultured on these surfaces varied; PVDF with a piezoelectric coefficient of $25pCN^{-1}$ showed the highest prostacyclin : Thromboxane A2 ratios.[85]

Controlling the behavior of the cells on surfaces offers the best possibility for the reconstruction of tissues and organs. Artificial extracellular matrix

proteins can be designed with built-in control of both the mechanical and biological properties of the resulting material. Recombinant DNA technology provides a powerful technique with which these novel artificial extracellular matrix materials can be synthesized. We have previously reported the synthesis of two such proteins: $(CS5(VPGIG)_{20})_5$ and $(CS5(VPGIG)_{40})_3$, in which the CS5 designates the CS5 region of fibronectin.[11] The REDV sequence, contained within the CS5 peptide, was shown to be the minimal sequence necessary to bind to the $\alpha_4\beta_1$ integrin.[44] Massia *et al.* found that the $\alpha_4\beta_1$ integrin is present in human umbilical vein endothelial cells (HUVECs) and that this HUVEC receptor adheres to both soluble and surface-grafted GREDVY peptide.[46] The authors also reported that the peptide does not promote the adhesion and spreading of fibroblasts, smooth muscle cells (SMC) or platelets when bound to glycophase glass.[29,45]

In our biosynthetic constructs the $(VPGIG)_x$ block provides the mechanical support. The $(VPGIG)_x$ structural block is based on the pentapeptide (VPGVG) which, when polymerized has been shown by Urry to have mechanical properties similar to those of native elastin.[86] These proteins are elastomeric in nature due to blocks of (VPGVG) known to have a modulus on the order of 1×10^6 dynes/cm^2 (depending on crosslink density and water uptake)[9] similar to native elastin, an extracellular matrix (ECM) protein. These new artificial extracellular matrix proteins are

expected to provide structural support while promoting the adhesion and spreading of HUVECs through the $\alpha_4\beta_1$ integrin receptor. It is also anticipated that they will selectively bind HUVECs and not fibroblasts, platelets and SMC due to the specificity of the REDV peptide.[29,45] In addition, a similar polymer, $(VPGVG)_x$, was found by Nicol *et al.* not to support the adhesion of ligamentum nuchae fibroblasts, human malignant melanoma cells and HUVECs.[47,48]

As reported in the previous chapter, HUVECs adhere to $(CS5(VPGIG)_{40})_3$ and $(CS5(VPGIG)_{20})_5$. This adhesion is thought to be moderated by the REDV sequence contained in the CS5 block of the proteins. These novel materials also promote the spreading of HUVECs and support cell growth and monolayer formation.

It has been reported that similar proteins based on $(VPGVG)_x$, when crosslinked using gamma-irradiation, exhibit elastomeric properties.[12,86] By analogy, the present artificial extracellular matrix proteins are expected to be elastomeric in nature. HUVEC adhesion and elasticity are favorable qualities for vascular prostheses. These grafts would be expected to provide elastic recoil during diastole, match the compliance of native artery, and promote the formation of a confluent endothelium. These proteins are the first step in the design of vascular grafts that will promote cell adhesion and growth as well as provide mechanical support which is similar to that found in native arteries. Furthermore, such materials are expected to

degrade into nontoxic biological molecules which can then be utilized by the body in protein production while the cells are remodeling their own extracellular matrix. Finally, materials based on the pentapeptide (VPGVG), poly(VPGVG)$_x$ as well as crosslinked poly(VPGVG) (20 mrad γ-irradiation) have been subjected to extensive biomaterials testing, including determination of mutagenicity (Ames test), toxicity (mice and rabbits), antigenicity (Guinea pigs), pyrogenicity (rabbits) and thrombogenicity (dogs) and have performed well in each of these tests.[87]

4.3 Experimental Section

4.3.1 Materials

HUVEC and human aortic SMC lines as well as medium were purchased from Clonetics. M199 serum free medium and Versine were purchased from Gibco. The XTT cell counting kit was purchased from Boeringer Mannheim. Falcon 10 cm and Corning 24 well tissue culture dishes and 12 mm glass cover slips were purchased from Fisher Scientific. Mouse monoclonal anti human α_4 (P4G9) was purchased from Life Technologies. Mouse anti human α_4 monoclonal B-5G10 was a kind gift from Martin Hemler at the Dana Farber Cancer Institute. Oregon Green™ 488 phalloidin was purchased from Molecular Probes. Vecta Shield mounting fluid was obtained from Vector Research Laboratories. The GREDVDY peptide was obtained from Research Genetics, Inc. Ultima Gold

scintillation counting fluid was purchased from Packard Instrument Company.

4.3.2 General Methods

HUVECs were maintained in EBM complete medium (Clonetics) and SMC in SmGM Bullet kit {containing basal medium, 10 μg/L Epidermal Growth Factor, 2 μg/L Fibroblast Growth Factor, 0.39 mg/L Dextramethasone, 50 mg/ml Gentamicin, 50 mg/ml Amphotericin-B, and 10 % Fetal Bovine serum (Clonetics)} in a humidified, 5% CO_2 incubator at 37 °C as specified by Clonetics' protocol (described briefly in chapter 3) with the exception that cell detachment was performed nonenzymatically. Cloud point curves were obtained in distilled water in quartz cuvettes with a pathlength of 1 mm at λ = 300 nm on a Jasco Model J-715 spectropolarimeter equipped with a Peltier type temperature control system; Jasco J-700 for Windows software was used for data analysis. Scintillation counting was performed using a Beckman Instruments, Inc. LS 1800 scintillation counter. Confocal images were obtained with a BioRad MRC 1000 confocal microscope.

4.3.3 Protein Expression, Batch Phase, M9AA Medium

Single colonies of *E. coli* strain BL21(DE3)pLysS transformed with recombinant pET-28ap-$(CS5(VPGIG)_{20})_5$ or pET-28ap-$(CS5(VPGIG)_{40})_3$ (cf. previous chapter) were used to inoculate 5 ml of M9AA medium containing chloramphenicol

(34 μg/ml) and kanamycin (34 μg/ml). The cultures were grown to saturation and used to inoculate 0.5 L volumes of M9AA medium containing chloramphenicol (34 μg/ml) and kanamycin (34 μg/ml). The cultures were grown to OD_{600} = 0.8 at 37 °C and protein expression was induced by the addition of IPTG to a final concentration of 1.0 mM; 2 ml 1 μCi/μl (0.13-0.27 mmol) ^{3}H glycine was added for radiolabeling of the artificial protein. Cells were harvested after 3 hours by centrifugation (5,000 x g, 15 min at 4 °C). The cell pellets were resuspended in 7 mL of TEN (50mM Tris-Cl (pH 8.0), 1 mM EDTA, 100 mM NaCl) and stored at -20 °C.

4.3.4 Protein Purification $(CS5(VPGIG)_{40})_3$ and $(CS5(VPGIG)_{20})_5$

Frozen cells were thawed and phenylmethyl sulfonyl fluoride (PMSF) (1 mM), $MgCl_2$ (5 mM), RNAse (20 μg/ml) and DNAse (20 μg/ml) were added. The solutions were incubated at 37 °C for 30 min and the insoluble portion was recovered by centrifugation (10,000 x g, 4 °C, 30 min). The pellet was resuspended in 7.5 ml 1 M urea ($(CS5(VPGIG)_{20})_5$ is found in the insoluble fraction when grown in minimal medium), incubated at room temperature for 1 hr, then centrifuged at 10,000 rpm for 20 min to recover the soluble portion. The supernatant was dialyzed (25,000 molecular weight cutoff, MWCO, dialysis tubing, Spectrapore) against 4° C H_2O for 3 days with H_2O changes. The dialysate was then centrifuged to remove impurities and the supernatant was lyophilized to recover the recombinant $(CS5(VPGIG)_{40})_3$ or $(CS5(VPGIG)_{20})_5$.

4.3.5 Cloud Point Measurements

The lower critical solution temperature (LCST), or cloud point, was determined as a function of concentration for both $(CS5(VPGIG)_{20})_5$ and $(CS5(VPGIG)_{40})_3$. For each protein solutions of 4, 8, 12, and 16 mg of the protein in 400 μl of distilled H_2O at 4 °C was prepared. Quartz cuvettes (1 mm) were filled with 300 μl of solution and temperature was scanned from 10 °C to 15 °C at a rate of 6 °C/hr. Percent transmittance was measured at 300 nm.

4.3.6 Film Casting

Glass coverslips (12 mm) (presoaked for 24 hr in concentrated H_2SO_4 and repeatedly rinsed with distilled H_2O) were coated with $(CS5(VPGIG)_{20})_5$ or $(CS5(VPGIG)_{40})_3$ from solutions in formamide or water by addition of 40 μl of a 1 mg/ml solution to the top surface of the coverslip followed by spreading of the solution with the tip of a pipet. Fibronectin films were cast from 100 μg/ml solutions in distilled H_2O; 20 μl of solution was applied to a glass cover slip and spread with the tip of a pipet. The coverslips were then dried overnight at 55 °C *in vacuo*. Coverslips were incubated in 0.5 ml sterile H_2O at 37 °C for 2 hours to remove excess protein and again dried in vacuo at 55 °C for 2 hours.

4.3.7 Stability of Protein Coatings

Tritiated $(CS5(VPGIG)_{20})_5$ and $(CS5(VPGIG)_{40})_3$ were cast on glass surfaces as described previously. Phosphate buffered saline (PBS, 0.5 ml) was added to 24 well culture dishes containing coverslips coated with tritiated protein. To determine the accumulation of protein in solution over time, 10 μl aliquots of PBS were removed at 30 min intervals and transferred to scintillation vials containing 4 ml of scintillation counting fluid. Each coating was analyzed in triplicate. To determine the amount of protein removed with repetitive washing, 0.5 ml aliquots of PBS were transferred from the wells to scintillation vials at 30 min intervals. Fresh PBS was added to the wells. These steps were repeated over a period of 3 hours and each surface was analyzed in triplicate. After three hours the glass coverslips were removed from the wells, rinsed briefly with PBS and placed in scintillation vials to determine the amount of protein remaining on the surface. Untreated glass surfaces were used in each case as controls.

4.3.8 Cell Culturing and Morphology

Pooled primary HUVECs were cultured and maintained in 10 mm Falcon petri dishes. HUVECs from passages 2-10, in our hands, were used for all cell adhesion studies. Cells were washed with 5 ml phosphate buffered saline (PBS) once and then harvested using Versine, a 0.02% EDTA solution in PBS. Harvested cells were resuspended in M199, serum free

medium, counted using a hemocytometer and diluted to a density of 5 x 10^4 cells/ml. HUVECs were transferred to 24 well dishes, 5 x 10^4 cells/well, containing protein coated glass coverslips. Cells were maintained at 37 °C and 5% CO_2 for 4 hours and fixed using 3.7 % formaldehyde in PBS. Briefly, glass coverslips containing attached cells were removed from the culture well, washed three times with phosphate buffered saline + $CaCl_2$ (0.1 g/l) and $MgCl_2$ (0.1 g/l)(PBS+) and placed in new 24 well plates. Cells were fixed by addition of 0.5 ml 3.7 % formaldehyde in PBS for 1 hr at 4 °C followed by washing with distilled H_2O. Pictures were taken of two different wells for each surface on a phase contrast microscope. Cell morphology was evaluated from the photographs.

4.3.9 Competitive Inhibition

HUVECs were detached from 10 cm Falcon petri dishes and counted as described above. Cells were resuspended in M199 serum free medium at a concentration of 6 X 10^4 cells/ml. GREDVDY (Research Genetics) peptide was added to the cell suspension to achieve the following final concentrations: 0.0, 0.2, 0.4, 0.6, 0.8, and 1.0 mg peptide/ ml suspension. The suspensions were incubated in a 37 °C water bath for 30 min followed by dilution to 1 x 10^4 cells/ml and addition to the tissue culture wells. HUVECs were maintained at 37 °C and 5% CO_2 for 4 hours and observed and photographed under the phase contrast microscope.

4.3.10 Actin Filament Staining

HUVECs were harvested and counted as described previously, diluted to 5 x 10^3 cells/ml in serum free M199 medium, and plated on coverslips coated with $(CS5(VPGIG)_{20})_5$ cast from formamide. Plated cells were incubated at 37 °C and 5% CO_2 for 4 hours, washed with PBS twice and fixed for 5 min with 3.7 % formaldehyde (from paraformaldehyde) in PBS. The cells were again washed twice with PBS and fixed and permeabilized in PBS with 0.5% Triton x-100 and 3.7% formaldehyde for 5 min at 0 °C. Cells were then washed several times with PBS and incubated for 10 min with PBS + 0.2 % BSA. Oregon Green™ conjugated phalloidin (5 μL, Molecular Probes) was then added to each well with 500 μL PBS. Cells were incubated at 37 °C for 30 min and washed well before mounting on microscope slides using Vecta Shield. Cells were visualized with a confocal microscope.

4.4 Results and Discussion

Proteins composed of repeats of the pentapeptide -VPGVG- exhibit a LCST at approximately 25 °C as shown by Urry and Long.[88] Urry *et al*. went on to show that the temperature at which the phase transition occurs can be altered by varying the residue at the fourth position (X) in the -VPGXG- pentapeptide; inclusion of a more hydrophobic residue reduces the LCST while a more hydrophilic residue raises the transition temperature.[80] Figure 4.1 shows the LCST behavior of $(CS5(VPGIG)_{20})_5$ and $(CS5(VPGIG)_{40})_3$ in

40 mg/ml aqueous solutions. Consistent with the predictions of Urry *et al.*, we find that the inclusion of the more hydrophobic isoleucine residue reduces the transition temperatures to 12.1 and 13.4 °C respectively for the two polymers as measured by cloud point analysis on 40 mg/ml solutions as described above. However, Urry *et al.* predict that the transition temperature of the proteins should be reduced to 10 °C.[80] Our slightly greater values may be due to the incorporation of the CS5 domain within the proteins. On the other hand, the LCST of $(CS5(VPGIG)_{40})_3$ is 1.3 °C higher than $(CS5(VPGIG)_{20})_5$ while the former has pentapeptide blocks 200 amino acids long as compared to 100 amino acids in the latter. This argument would indicate that the LCST of the pentapeptide (VPGIG) itself would be greater than 13.4 °C. This contradictioncan only be resolved when the cloud point data of the polypentapeptide becomes available. Retention of the LCST may be consistent with retention of the elastomeric nature of the proteins.[12]

Despite the existence of an LCST below body temperature, small quantities of the material are soluble in aqueous solution at 37 °C; the two phase system is composed of a protein rich phase and a protein poor, but not protein free, phase. To determine if sufficient protein remains on glass surfaces for full coverage after addition of the aqueous cell culturing medium, glass coverslips were coated with tritiated protein and soaked in PBS as described. Figure 4.2 shows the accumulation of $(CS5(VPGIG)_{20})_5$, cast

from formamide, in solution over a 3 hour time period. The majority of the protein is dissolved within the first hour with very little protein being removed thereafter. The other three protein cast films behave in a similar manner (data not shown).

Table 4.1 shows the amount of protein removed over a three hour period for both the case where the coverslips are soaked in 0.5 ml PBS for 3 hours and when the PBS is removed every 30 minutes and replaced with 0.5 ml aliquots of fresh PBS. Also shown is the amount of protein remaining on the glass coverslips at three hours. In all cases 2-3 μg of $(CS5(VPGIG)_{40})_3$ and approximately 1 μg of $(CS5(VPGIG)_{20})_5$ were found on the coverslips after thorough washing. There is a discrepancy of 8-10 μg of protein being cast and protein being detected in all cases. Although experimental error can account for some of this discrepancy, there is still several unaccounted μg. Since much of the protein goes into solution within the first several minutes, there is a protein solution in contact with the polystyrene tissue culture well for 3 hours. Protein is likely to have adhered to the polystyrene well, which has a surface area 3 times that of the coverslip.

Cast films were presoaked for 2 hours to remove the excess protein prior to addition of the cells in serum free medium.

Table 3.2 reports the number of cells adhered to the cast surfaces of the two artificial extracellular matrix

proteins, glass and fibronectin. We found that essentially all cells cast on fibronectin and on $(CS5(VPGIG)_{20})_5$ were adherent, while only about 25% of the cells cast on glass and $(CS(VPGIG)_{40})_3$ were adherent. We attribute the decrease in the number of cells bound to $(CS5(VPGIG)_{40})_3$ as compared to $(CS5(VPGIG)_{20})_5$ to the lower CS5 density in the former, and possibly to a difference in protein conformation upon adsorption to the glass surface which may present the REDV sequence in a less than optimal manner. Table 4.2 tabulates the cell morphologies when attached to these surfaces. Refractile cells are seen to be round and bright under the phase contrast microscope, cells which were round but not highly refractile were classified as round and grey, spreading cells exhibited 1-2 pseudopodia, while spread cells had >2 pseudopodia. Not only did the glass surface support far fewer cells than $(CS5(VPGIG)_{20})_5$, but half of the cells on glass are highly refractile. In contrast, although $(CS5(VPGIG)_{40})_3$ supports approximately the same number of adherent cells as does glass, < 20% of the HUVECs on $(CS5(VPGIG)_{40})_3$ are highly refractile; in this case half the cells are well spread. The morphology of the cells on $(CS5(VPGIG)_{20})_5$ is similar to that on $(CS5(VPGIG)_{40})_3$; however, the number of attached cells is 4 times as great. Although the data are not shown in table 4.2, all cells plated on fibronectin are well spread after 4 hours in serum free medium.

Hubbell and colleagues have observed HUVEC spreading on glycophase glass which has been modified through N-terminal grafting of GREDVY peptides to the surface at a concentration of approximately 10 pmol/cm^2.[45] As determined from protein stability results 19 ± 2 pmol/cm^2 of CS5 are present on the glass coverslips. Assuming that HUVECs have access to the top 10 Å of the recombinant protein film, there is 10 ± 2 pmol/cm^2 of CS5 ligand available for adhesion (compare to 10 pmol/cm^2).[45] They report the percentage of attached cells that are spread to be 89 %. Defining all nonrefractile cells as spread or spreading, we find that ~80 % of attached cells are spread on both $(CS5(VPGIG)_{40})_3$ and $(CS5(VPGIG)_{20})_5$, which is consistent with results obtained by Hubbell and colleagues with similar ligand densities. Although the percent of well spread HUVECs on fibronectin is higher than that on $(CS5(VPGIG)_{20})_5$ cast from either water or formamide, upon addition of complete medium containing 2 % serum all of the HUVECs on the artificial extracellular matrix protein become well spread within an hour. Both the fibronectin surfaces and the $(CS5(VPGIG)_{20})_5$ surfaces go on to become confluent in 36-48 hours.

Figures 3.4a-3.4e show HUVECs on glass (3.4a), $(CS5(VPGIG)_{20})_5$ cast from formamide and water respectively (3.4b, 3.4c) and $(CS5(VPGIG)_{40})_3$ cast from formamide and water (3.4d, 3.4e). The differences in cell numbers and cell morphology can be seen clearly. Figure 4.3a-b shows

confluent monolayers of HUVECs on fibronectin and on $(CS5(VPGIG)_{20})_5$ respectively. In both cases the expected cobblestone morphology is observed.

Preliminary measurements of competitive inhibition of EC attachment by soluble CS5 analogues have also been made. As expected, pre-incubation of HUVECs with the soluble peptide GREDVDY (Research Genetics, Inc.) at concentrations up to 2 mg/ml has no observable effect on attachment to fibronectin. In contrast, attachment to $(CS5(VPGIG)_{20})_5$ is completely inhibited by GREDVDY at concentrations of 0.6-0.8 mg/ml. Although this result is consistent with specific attachment of HUVECs to CS5 via the $\alpha_4\beta_1$ receptor, we have not yet conducted controls with sequence-scrambled analogues of the inhibitory peptide.

Figure 4.4 shows actin filament staining of a HUVEC spread on $(CS5(VPGIG)_{20})_5$ using Oregon Green conjugated phalloidin. Actin filaments (Figure 4.4a) can be seen clearly on the periphery of the cell, in addition, some filaments can be seen (Figure 4.4b) that originate from near the center of the cell and reach out toward the periphery. Upon adhesion and spreading, many cells form actin filaments or stress fibers. These filaments play a role in the anchorage and movement of membrane proteins and in the locomotion of cells.[10] In addition, many integrins, including $\alpha_4\beta_1$,[46] bind both actin filaments and extracellular matrix proteins and thereby serve as a link between the interior and the exterior of the cells.[89,90]

4.5 Conclusions

Both $(CS5(VPGIG)_{20})_5$ and $(CS5(VPGIG)_{40})_3$ support adhesion and spreading of HUVECs. The presence of actin filaments as seen in the Oregon Green™ conjugated phalloidin confocal images of HUVECs spread on $(CS5(VPGIG)_{20})_5$ (Figures 5a & b) is suggestive of a well organized cytoskeleton. Morphological data shown in Table 4.2 suggests that more than 70% of the adherent cells are spread, and the number of cells bound to $(CS5(VPGIG)_{20})_5$ is similar to the number bound on fibronectin (Table 3.2). The morphology of the cells spread on $(CS5(VPGIG)_{40})_3$ is similar to that of cells on $(CS5(VPGIG)_{20})_5$ as shown in Table 4.2. This equivalencce suggests that by changing the density of ligand we can control the number of cells that attach to a material without affecting the extent of individual cell spreading. In addition, as seen in Figure 4.3 b, $(CS5(VPGIG)_{20})_5$ supports HUVEC monolayer formation subsequent to the addition of serum, which is necessary for optimal vascular regeneration.

Competitive inhibition data suggests that the HUVECs are binding to the artificial extracellular matrix proteins through the CS5 region. Preincubation with soluble GREDVDY has no effect on HUVECs' ability to adhere to fibronectin, indicating that the peptide is not inhibiting adhesion to all surfaces. In contrast, as the concentration of GREDVDY peptide with which the HUVECs are incubated increases, the number of cells that adhere to the artificial extracellular

matrix proteins decreases. The soluble peptide inhibits cell adhesion by blocking the $\alpha_4\beta_1$ integrin through binding to the receptor in solution. The receptor is then unable to bind to the CS5 domain of the proteins.[11] This inference also suggests that the pentapeptide repeat does not support cell adhesion, as blocking of adhesion to the REDV sequence contained within the CS5 block inhibits cellular adhesion. This conclusion will only be confirmed when synthesis of the pentapeptide alone is complete and HUVEC adhesion to this material can be tested. Further evidence of adhesion through the CS5 domain is the increase in number of cells adhered to $(CS5(VPGIG)_{20})_5$ as compared to $(CS5(VPGIG)_{40})_3$, the latter having a 50% decrease in ligand density.

These materials also retain some of the characteristics of the elastin portion of the proteins as suggested by the observation of the LCST. Both of the recombinant proteins exhibit an LCST despite the fact that the elastin segments are interrupted by the CS5 region. Despite the occurrence of the LCST near 13 °C for both materials, they are water-soluble in low concentrations at 37 °C; however, complete coverage of the glass coverslips after incubation in aqueous medium for two hours was confirmed by SEM (data shown in Appendix D) and scintillation counting.

We have synthesized artificial extracellular matrix proteins which contain specific cell binding domains as well as structural blocks that are expected to mimic native elastin. Control of the density of adhesion ligand controls

the number of cells adherent to the materials. In addition, preliminary work by Kathy DiZio in our laboratory suggests that there is little or no smooth muscle cell adhesion to $(CS5(VPGIG)_{20})_5$, consistent with the work of Hubbell *et al.*[29] using GREDVY grafted to glass surfaces.

Table 4.1 Determination of Protein Stability on Glass Coverslips

	0.5 ml PBS for 3 hrs		0.5 ml PBS exchanged every 30 min	
polymer/ casting solvent	accumulation in solution μg	remaining on coverslip μg	total solubilized μg	remaining on coverslip μg
$(CS5(VPGIG)_{20})_5$ Formamide	29.2 ± 0.7	2.0 ± 0.6	32.6 ± 2.9	0.6 ± 0.2
$(CS5(VPGIG)_{20})_5$ Water	30.9 ± 1.3	0.8 ± 0.3	30.3 ± 1.9	0.5 ± 0.1
$(CS5(VPGIG)_{40})_3$ Formamide	24.4 ± 4.9	3.2 ± 1.2	23.5 ± 2.5	3.6 ± 0.6
$(CS5(VPGIG)_{40})_3$ Water	26.1 ± 1.4	1.9 ± 0.4	28.5 ± 1.3	1.2 ± 0.5

Table 4.2 HUVEC Morphology on Glass and Protein Cast Surfaces.

Protein/ Cast From	Refractile %	Round/Gray %	Spreading %	Spread %
Glass	49.5 ± 8.6	12.0 ± 0.4	13.4 ± 2.3	25.1 ± 7.8
$(CS5(VPGIG)_{20})_5$ Formamide	15.2 ± 5.9	14.6 ± 3.4	14.4 ± 5.0	55.8 ± 3.9
$(CS5(VPGIG)_{20})_5$ Water	20.9 ± 5.3	11.4 ± 4.9	11.6 ± 1.4	55.8 ± 9.3
$(CS5(VPGIG)_{40})_3$ Formamide	14.1 ± 1.2	15.9 ± 5.9	21.3 ± 2.5	48.7 ± 2.2
$(CS5(VPGIG)_{40})_3$ Water	18.7 ± 7.2	16.3 ± 5.5	7.9 ± 4.0	53.7 ± 6.6

Spreading = 1-2 pseudopod

Spread = > 2 pseudopod

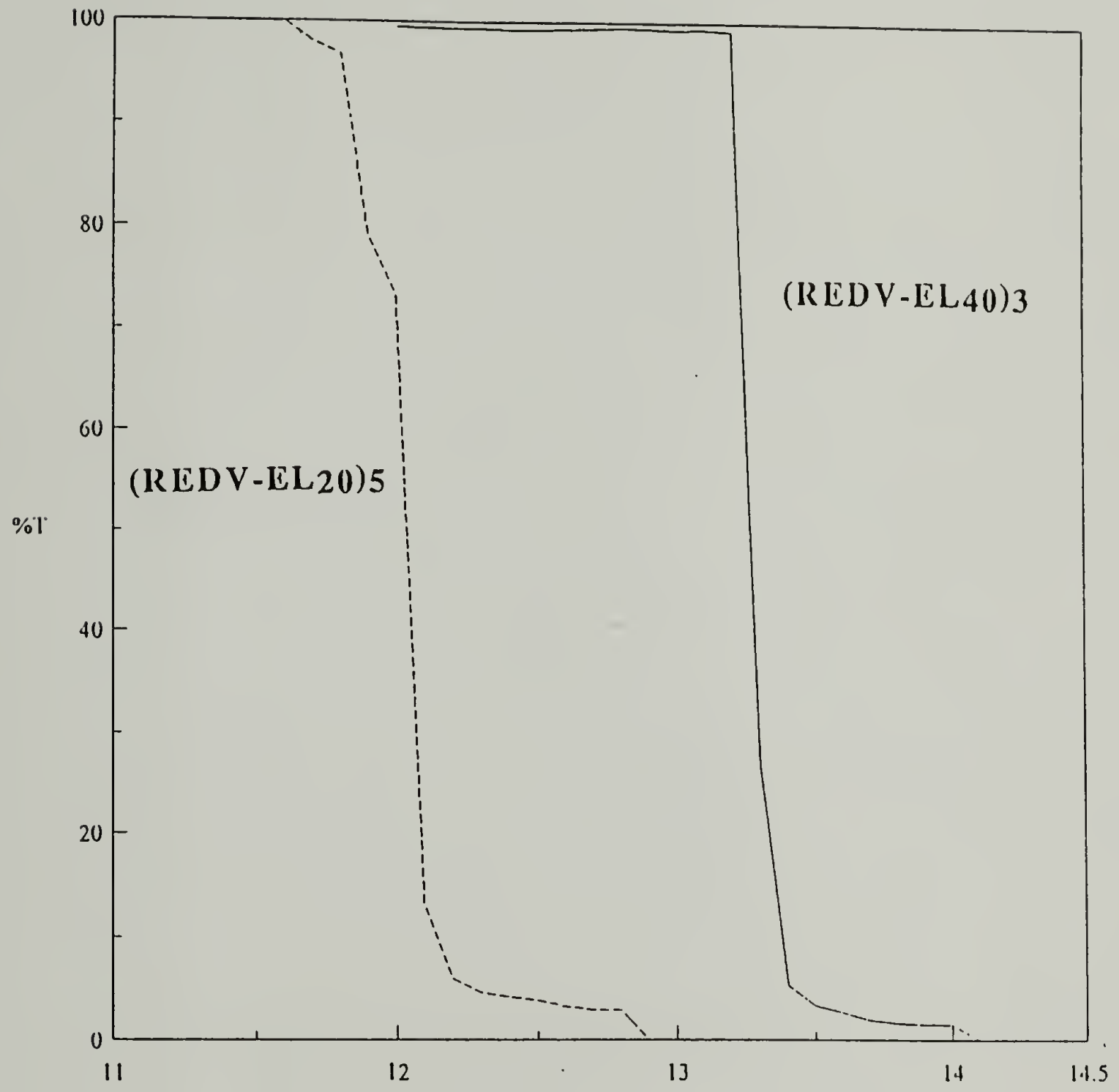

Figure 4.1. LCST data of $(CS5(VPGIG)_{20})_5$ and $(CS5(VPGIG)_{40})_3$ in aqueous solution (40 mg/ml).

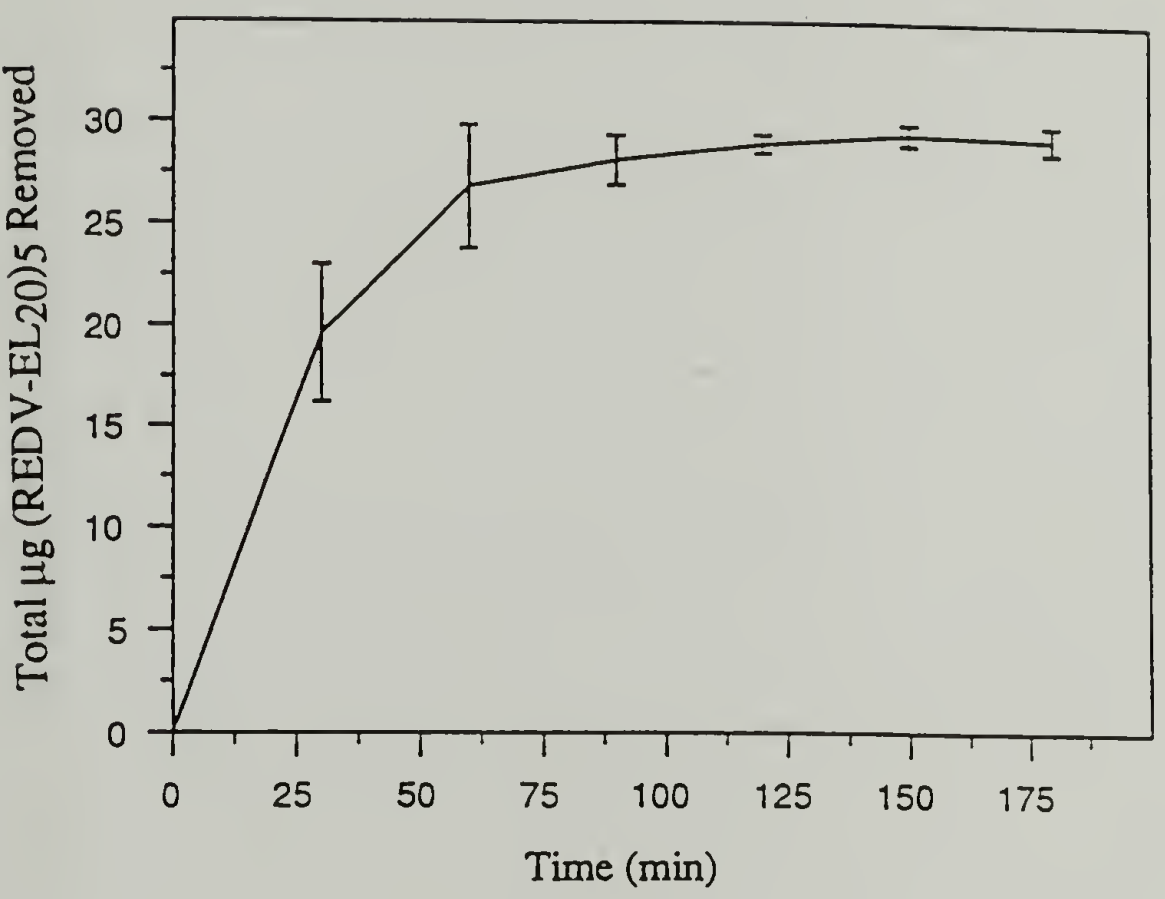

Figure 4.2. Accumulation of ^{3}H - Glycine labeled $(CS5(VPGIG)_{20})_5$ in solution over 3 hours. Films were cast from formamide (total protein cast 40 μg) and soaked in PBS at 37 °C for 3 hrs. The majority of the solubilization occurs within the first hour.

a.

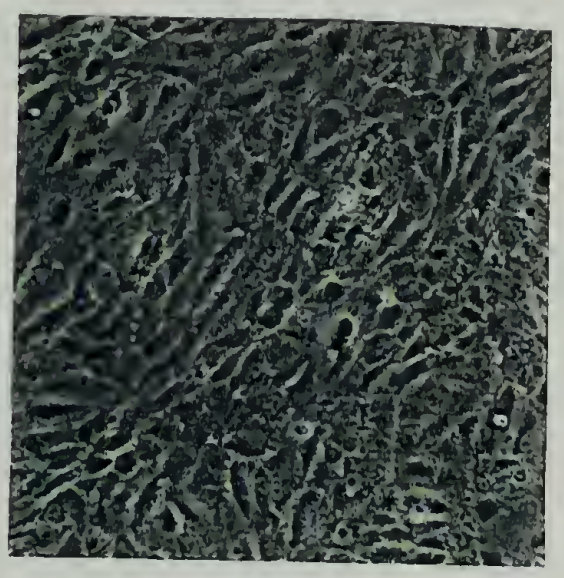

b.

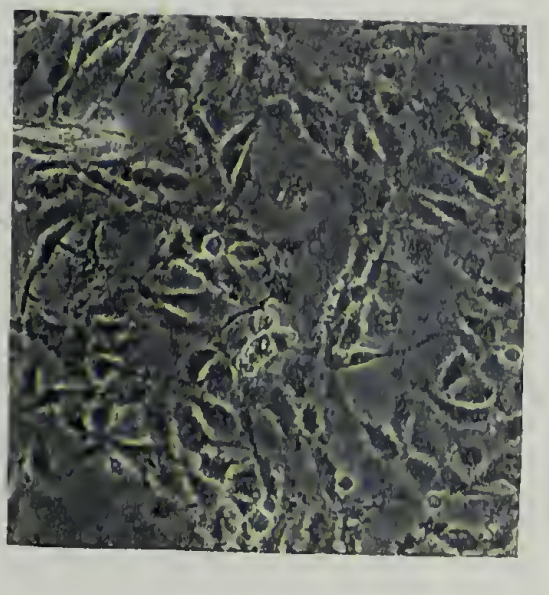

Figure 4.3. Confluent layers of endothelial cells are supported by both fibronectin coated glass surfaces (4.3a) and $(CS5(VPGIG)_{20})_5$ coated glass surfaces (4.3b). In both cases the expected cobblestone morphology is seen.

a.

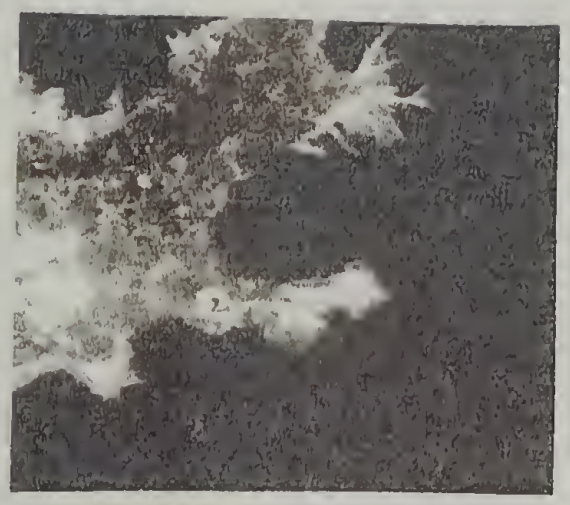

b.

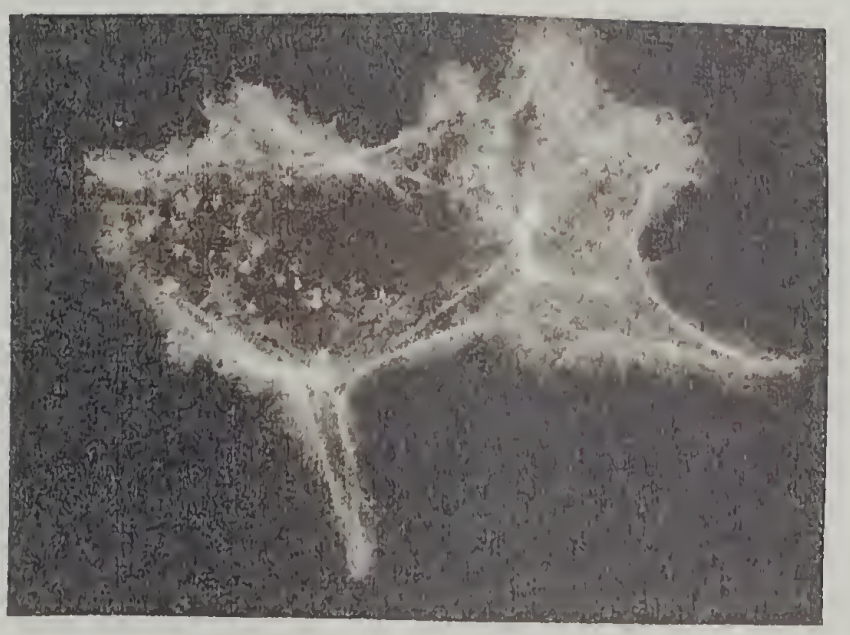

Figure 4.4. HUVECs which are allowed to adhere to $(CS5(VPGIG)_{20})_5$ for 4 hours in serum free medium are spread. Oregon Green™ conjugated phalloidin was used to visualize actin filaments which can be seen at the periphery of the cell (4.4a) and extending from the center of the cell to the periphery(4.4b).

CHAPTER 5

CONCLUSIONS AND FUTURE PERSPECTIVES

Recombinant extracellular matrix proteins have been successfully synthesized as shown by SDS-PAGE, NMR spectroscopy and amino acid analysis. $(CS5(VPGIG)_{20})_5$ and $(CS5(VPGIG)_{40})_3$ were designed with the intent that the pentapeptide repeat $(VPGIG)_{20,40}$ would provide the structural integrity of the material[12,86,88] while the CS5 block would be the ligand for HUVEC binding through the $\alpha_4\beta_1$[29,44-46] integrin receptor.

Both recombinant artificial extracellular matrix proteins support the adhesion of HUVECs. Competitive inhibition studies with soluble GREDVDY suggest that the CS5 region is indeed the ligand for HUVEC adhesion to the artificial extracellular matrix proteins.

Further support for the supposition that HUVECs are binding primarily through the CS5 domain of the polypeptides comes from data showing that significantly fewer HUVECs bind to $(CS5(VPGIG)_{40})_3$ than bind to $(CS5(VPGIG)_{20})_5$. The former contains 50% fewer CS5 blocks per pentapeptide repeat. Thus lower HUVEC adhesion to the former is consistent with binding to the CS5 block. This trend again suggests that the pentapeptide repeat does not promote cell adhesion.

The relationship between the density of the adhesion ligand and the number of HUVECs which bind to the material indicate that it is possible to control the initial cell

seeding density of a material. This control will be important in materials which are used for co-culture. For example, liver is a highly vascular material which contains several different cell types among which are hepatocytes and endothelial cells. Hepatocytes are immediately juxtaposed to the endothelial cells. In this way, no cell is further than two cells away from the bloodstream. There is ready and rapid diffusion of metabolites to all cells. In order to seed both cell types onto a matrix it will be necessary to control the location and number of each type of cell to be seeded. This need is addressed with materials such as these, since we can control precisely the type and density of cell binding domains.

Both control of the binding ligand and control of the structural integrity were designed into the materials. The elastin-based pentapeptide (VPGIG) was incorporated to provide integral structural and elastomeric integrity. Although complete characterization of the mechanical properties has not yet been achieved, we have demonstrated that the materials maintain an LCST, which is inherent to polymers based on multiple repeats of (VPGIG). Urry has suggested that it is the β-turn conformation adopted by the proteins upon phase separation that provides the entropic basis for the elastomeric properties of the proteins.[86] Thus, the observation of the LCST in our materials may suggest retention of the β-turn conformation in the protein

rich phase of the biphasic system and favorable elastic properties.

The surface stability studies show that the materials are not insoluble in aqueous solution at 37 °C despite the sub-ambient LCST. In order to produce an insoluble material it may be necessary to crosslink the protein. Urry *et al.* have crosslinked similar proteins by γ-irradiation[91]; this is not ideal for crosslinking these artificial extracellular matrix proteins because the location of radical formation, and hence of crosslinking, cannot be controlled. Other available options are crosslinking by glutaraldehyde or formaldehyde.[92] The absence of lysine residues preempts the methods. Carbodiimide would cause crosslinking of the glutamic and aspartic acid residues of the binding region with amines.[92] Thus it appears that the traditional crosslinking methods are accordingly less than ideal.

A novel crosslinking option might come from the incorporation of an unnatural alkyne derivative of isoleucine. It has been shown in our laboratory that an isoleucine derivative containing a terminal alkyne can be incorporated into artificial proteins biosynthetically (*vide infra*). This alkyne derivative is apparently bound by the isoleucyl tRNA synthetase and utilized to charge the isoleucyl tRNA. Even low levels of isoleucine replacement by the unatural alkyne derivative would allow sufficient crosslinking of these residues through alkyne chemistry.[93] The crosslink density and the mechanical properties of the

material could then be altered by varying the incorporation of the alkyne derivative.

The incorporation of the alkyne would also allow for crosslinking with other materials. The muscular arteries are generally the arteries of interest for the design of small diameter prostheses, for it is these arteries that fail and are not readily repaired by current methods.[5] As discussed in chapter 1, the arteries are composed of three tunicas. It will be possible to blend the elastin-like proteins with collagen analogues to mimic both the tunica media and the adventitia. Multilayered vascular grafts can be fabricated, with crosslinking between and within the tunicas, to produce vascular prostheses. The fabricated vascular grafts can then be seeded with endothelial cells and smooth muscle cells. These cells would be expected to remodel or rebuild the extracellular matrix to produce a "natural" vessel.

An advantage of artificial extracellular matrix proteins which have been designed through recombinant DNA technology is that the proteins can be designed to contain only specific signals. Fibronectin itself contains fibrin, heparin, collagen, DNA, and cell binding domains.[94] It is not beneficial to have all of these binding domains exposed to the blood stream. Fibrin is involved in clotting and thrombus formation. Readily available binding sites for fibrin may promote the binding of fibrin followed by the formation of thrombi. Recombinant DNA technology allows for the isolation of function by the isolation of domains of a

protein. As we have shown, it is possible to clone the CS5 region of fibronectin thus isolating only the ability to bind to the $\alpha_4\beta_1$ integrin receptor.

As demonstrated by the adhesion of recombinant $(CS5(VPGIG)_{20})_5$ and $(CS5(VPGIG)_{40})_3$ to PTFE (see Appendix E), these novel extracellular matrix materials can be used not only as new graft materials, but to try to improve the characteristics of currently available materials while new materials are being developed. It is also important to note that just as biology is not limited to incorporating one signal into a molecule, we are not limited to one signal per molecule. Through recombinant DNA techniques multiple signals can be built into each molecule, whether they be cell adhesion signals, molecular adhesion signals, or protease degradation sites. Moreover, we are able to design out these same signals and so devise materials for use where the presence of any of these signals would be undesirable. We can make materials that are less prone to degradation by endoproteases. The current materials are the building blocks for artificial extracellular matrices.

APPENDIX A

GENETIC MAPS AND MANIPULATIONS

All DNA was synthesized on a 1 μmol scale on a Biosearch Model 8700 DNA synthesizer using phosphoramidite chemistry.[68] As described in chapter 3, all oligonucleotides were purified, annealed and ligated into pUC18[69], a cloning vector which is depicted in Figure A.1, with the exception of 28ap which was directly ligated into pET-28a (Figure A.2)and pEC2-link which was ligated directly into pEC2. The transfer vector, pEC2 (Figure A.3) was used for inserting $(VPGIG)_x$ into the Ban I site of the CS5 and HBD regions and for amplifying $CS5(VPGIG)_x$ and $HBD(VPGIG)_y$ prior to ligation into pET-28ap, the expression vector.

pET-28ap (Figure A.4) was created by insertion of a new cloning linker between the Nco I and Xho I sites in the polycloning region in pET-28a. As seen in Figure A.5, the new cloning region consists of a start codon encoded in the Nco I site, a cloning site encoding an Xho I restriction site and two stop codons immediately following the cloning site. This allows for the expression of the artificial extracellular matrix proteins without long fusions which would need to be removed after synthesis.

Figures A.5, A.6, A.7, A.8 and A.9 show full restriction maps of the DNA encoding 28ap, CS5, $(VPGIG)_5$, HBD, pEC2-link respectively as synthesized. pEC2-link was

cloned directly into the Eco RI and Eag I sites of pEC2 and sequenced. It was designed to allow cloning of $(VPGIG)_x$ into the Ban I site and then transfer of the DNA into pET-28ap for expression without long fusions.

DNA manipulations are described in more detail in experimental sections pertaining to gene construction and protein expression in Chapter 3 and Appendix B.

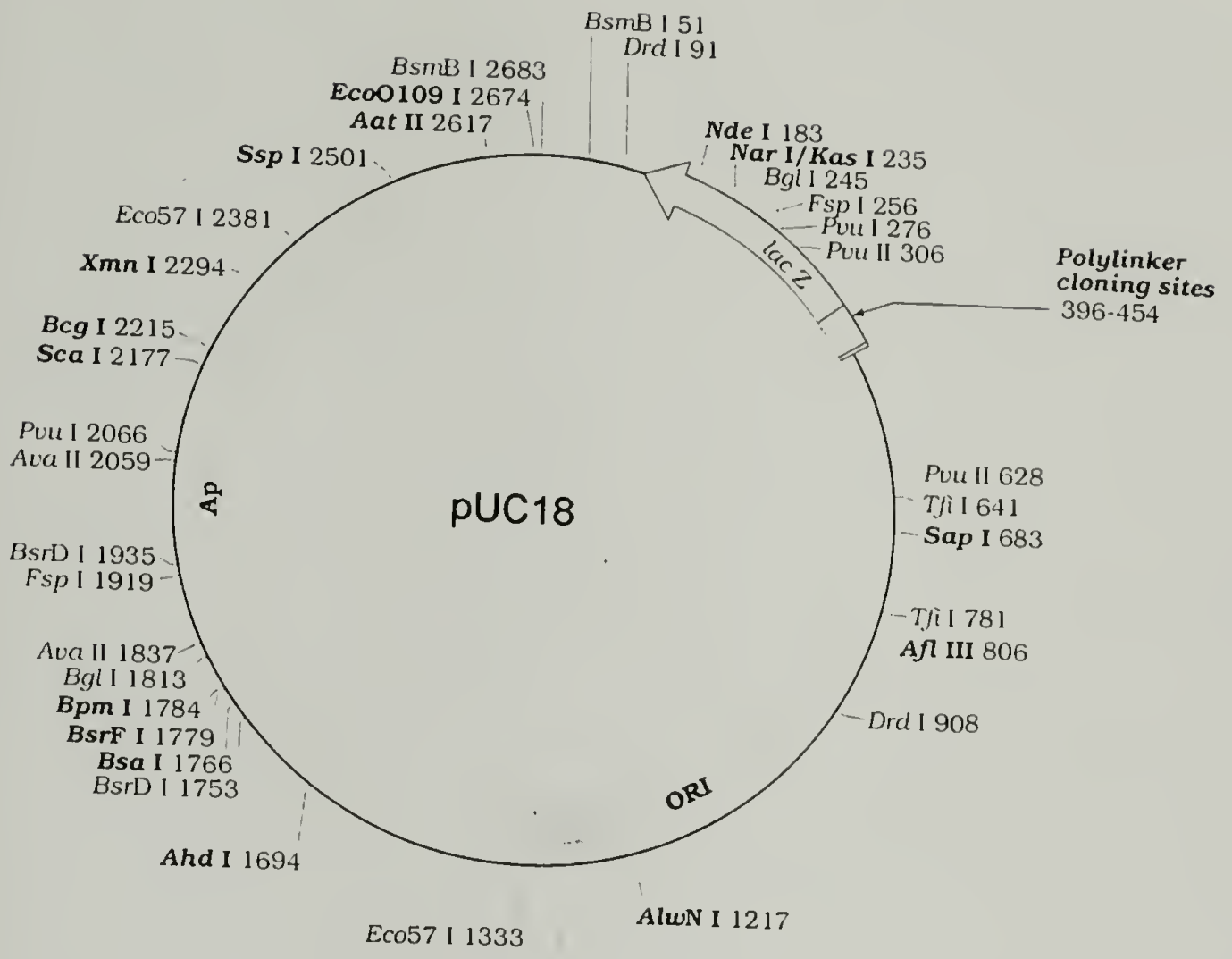

POLYLINKER - ANTISENSE STRAND

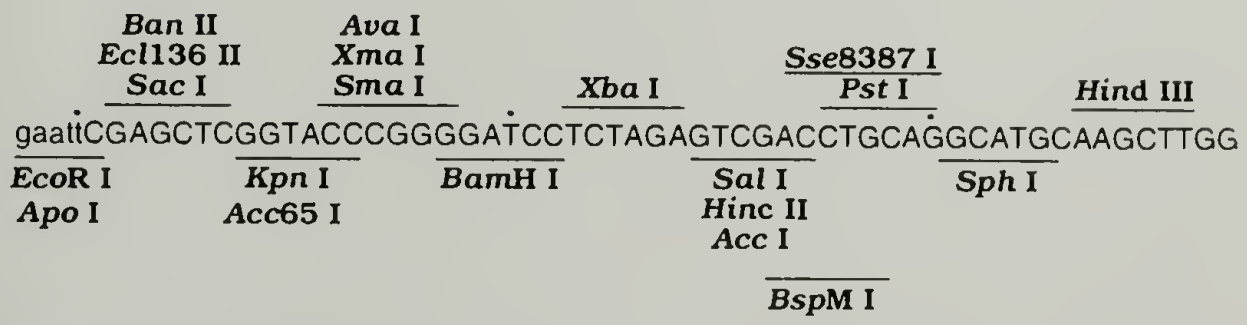

1

LacZ′ Ala Leu Ser Asn Ser Ser Pro Val Arg Pro Asp Glu Leu Thr Ser Arg Cys Ala His Leu Ser Pro Thr Ile Met Thr

Figure A.1 The pUC18 cloning vector. The cloning vector is shown with the DNA sequence of the polycloning region depicted below the plasmid. Synthetic DNA was ligated between the Bam HI and Eco RI site of the cloning region.

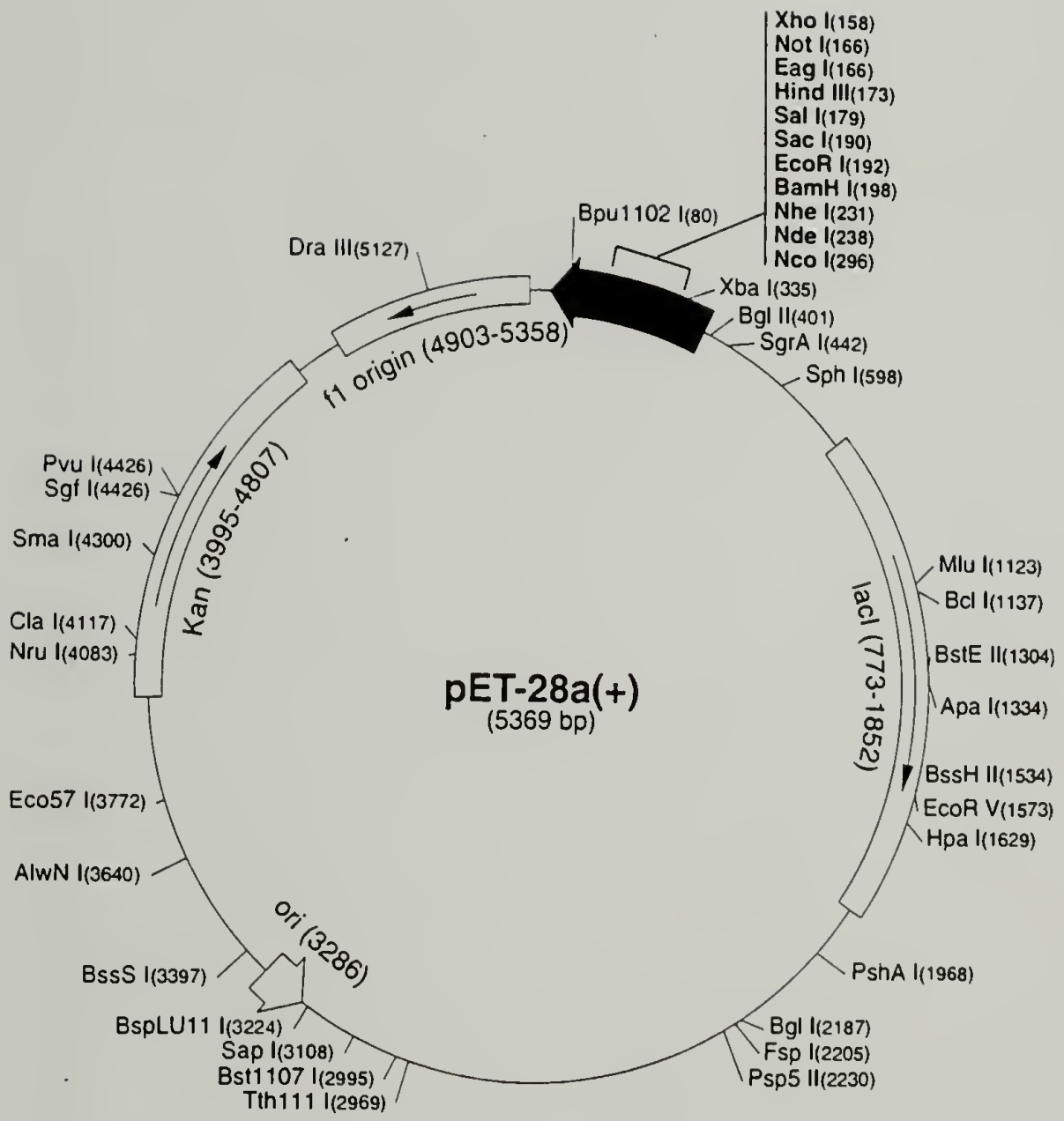

Figure A.2 pET-28a cloning vector. (reprinted with permission from Novagen)

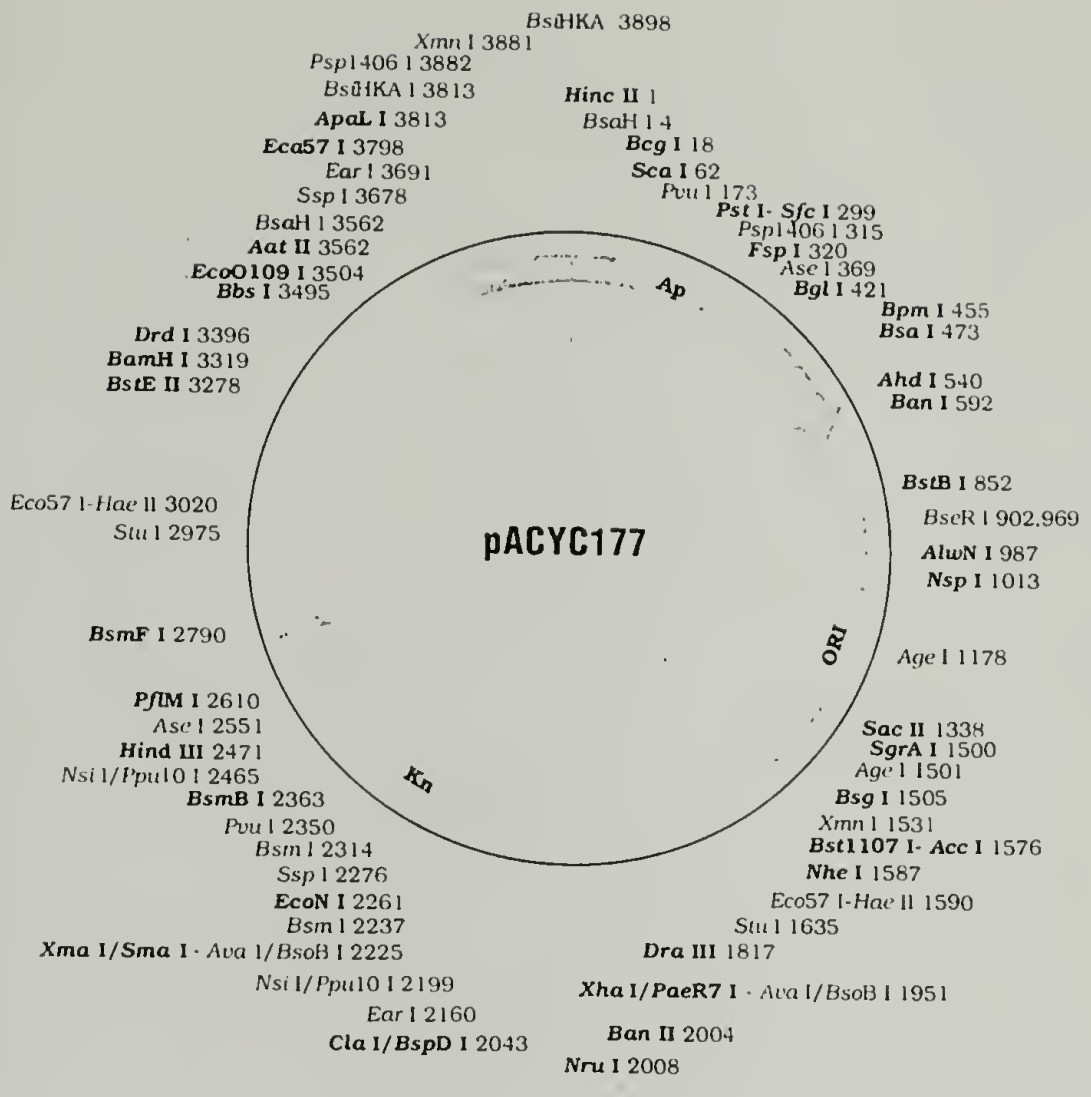

1. Bam HI / Klenow
2. Ban I / Klenow
3. Pst I
2. T4 ligase / polycloning linker

POLYCLONING LINKER

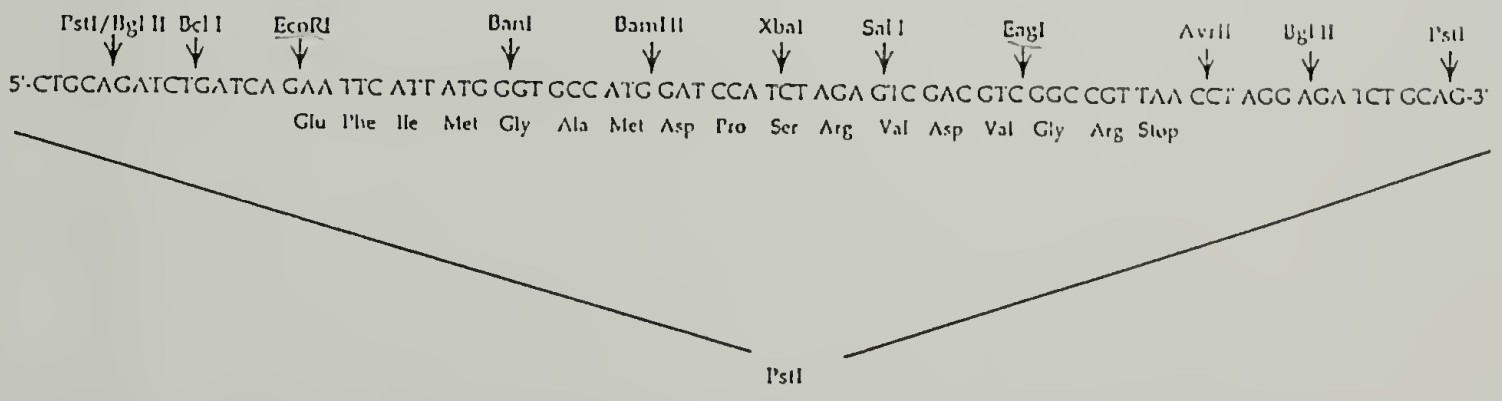

Figure A.3 pEC2, a transfer vector. The transfer vector designed by Eric Cantor is depicted with a blow up of the polycloning region shown below the plasmid.

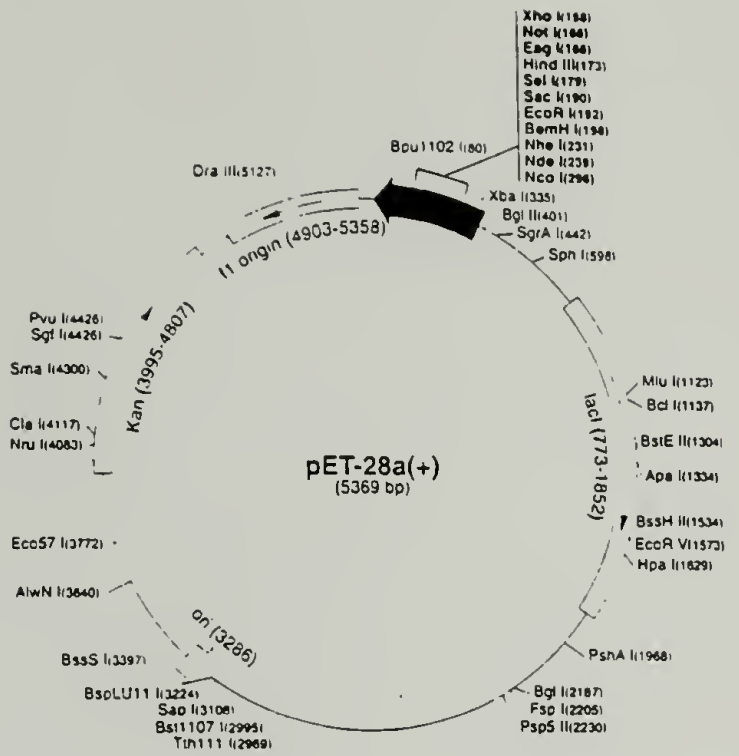

1. Nco I / Xho I
2. T4 ligase / Nco I -Xho I - Stop - Sal I (28ap-linker)

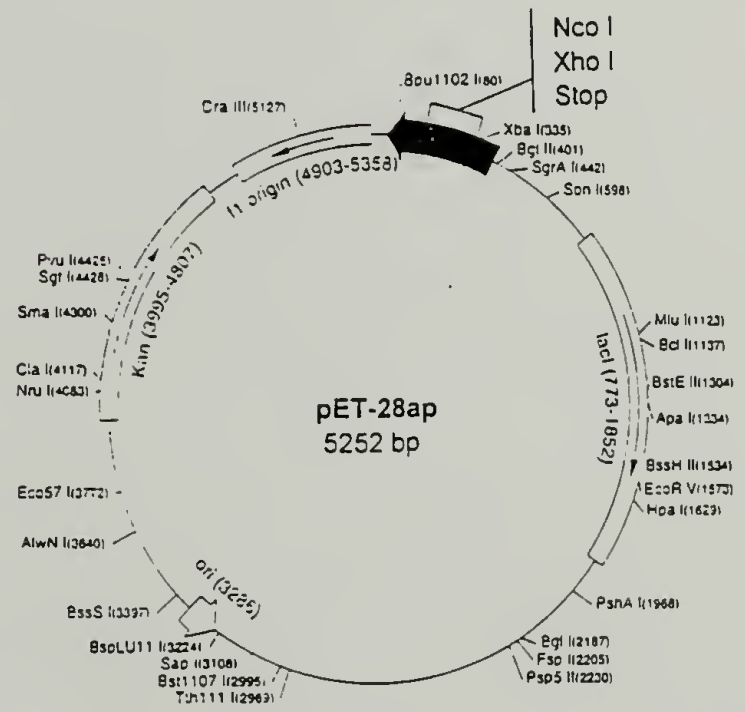

Figure A.4 The expression vector pET-28ap as constructed from pET-28a (reprinted with permission from Novagen). The expression vector with a blow up of the new cloning linker is shown. The new linker allows for cloning into the Xho I site with subsequent expression of the recombinant protein with minimal amino acid fusions corresponding to the start site and the cloning site.

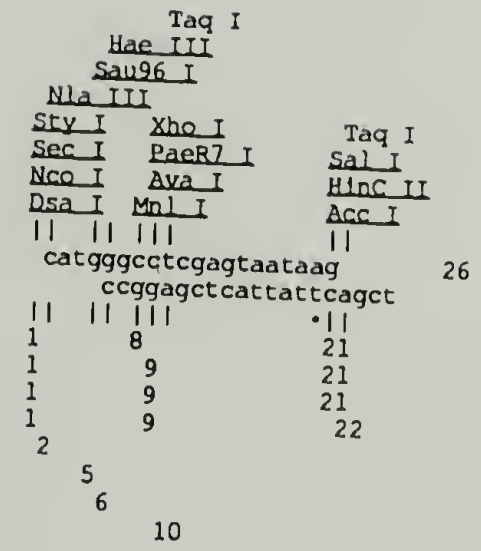

Figure A.5 A full restriction map of 28ap. The restriction map of 28ap as synthesized by solid state synthesis. The Nco I and Sal I sites were used for cloning into the Nco I and Xho I sites of pET-28a.

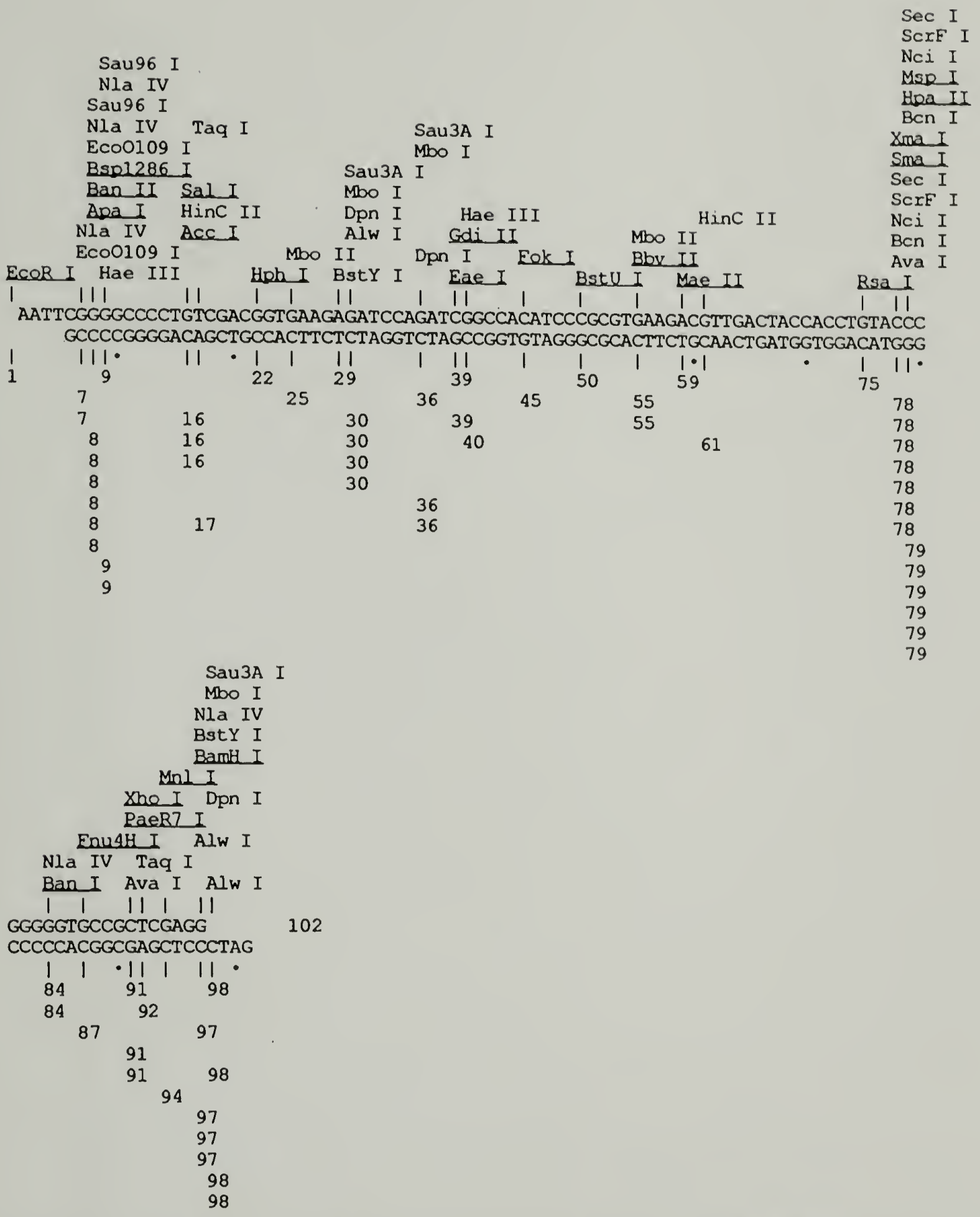

Figure A.6 A full restriction map of CS5. The restriction map of CS5 as synthesized by solid state synthesis. The Eco RI and Bam HI sites were used for cloning into pUC18. The Ban I site was used for insertion of $(VPGIG)_x$ multimers.

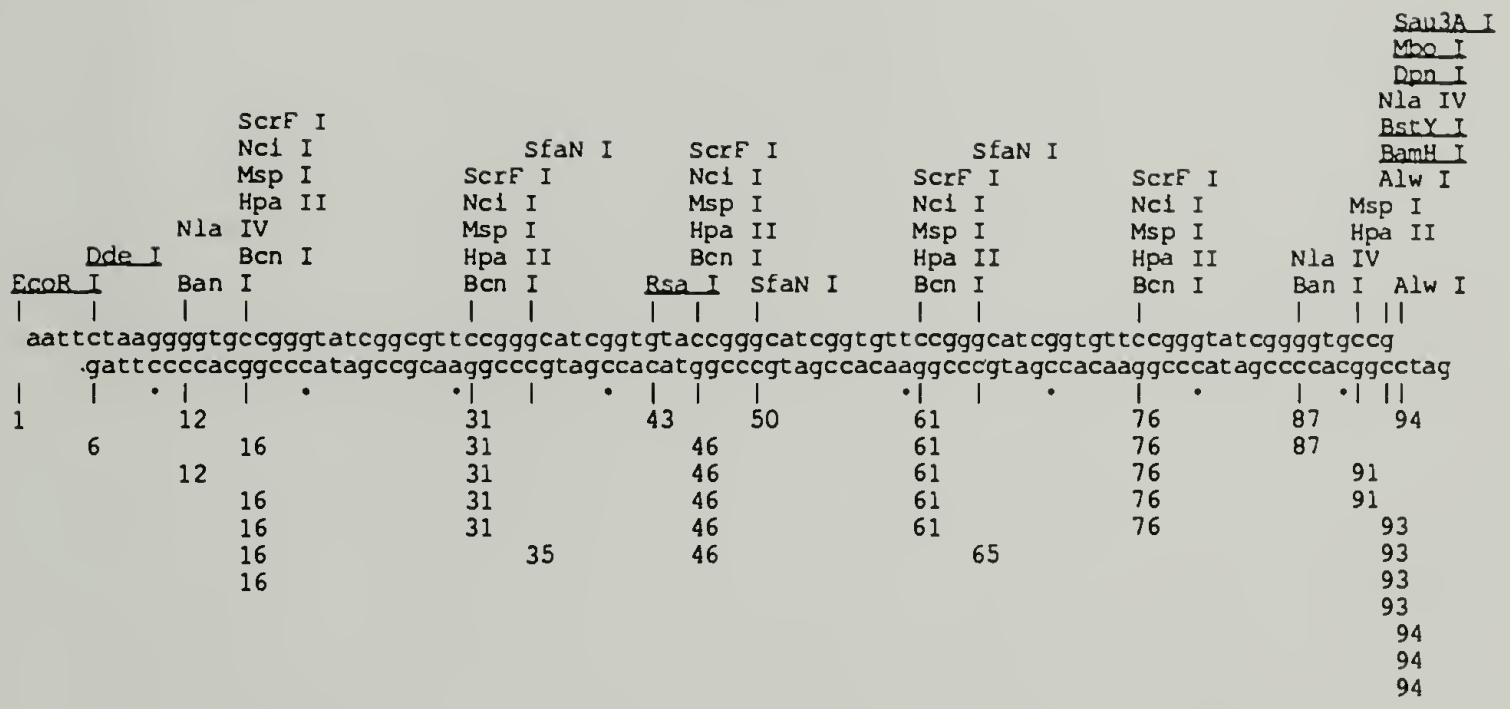

Figure A.7 A full restriction map of $(VPGIG)_5$. The restriction map of $(VPGIG)_5$ as synthesized by solid state synthesis is shown. The Eco RI and Bam HI sites were used for cloning into pUC18.

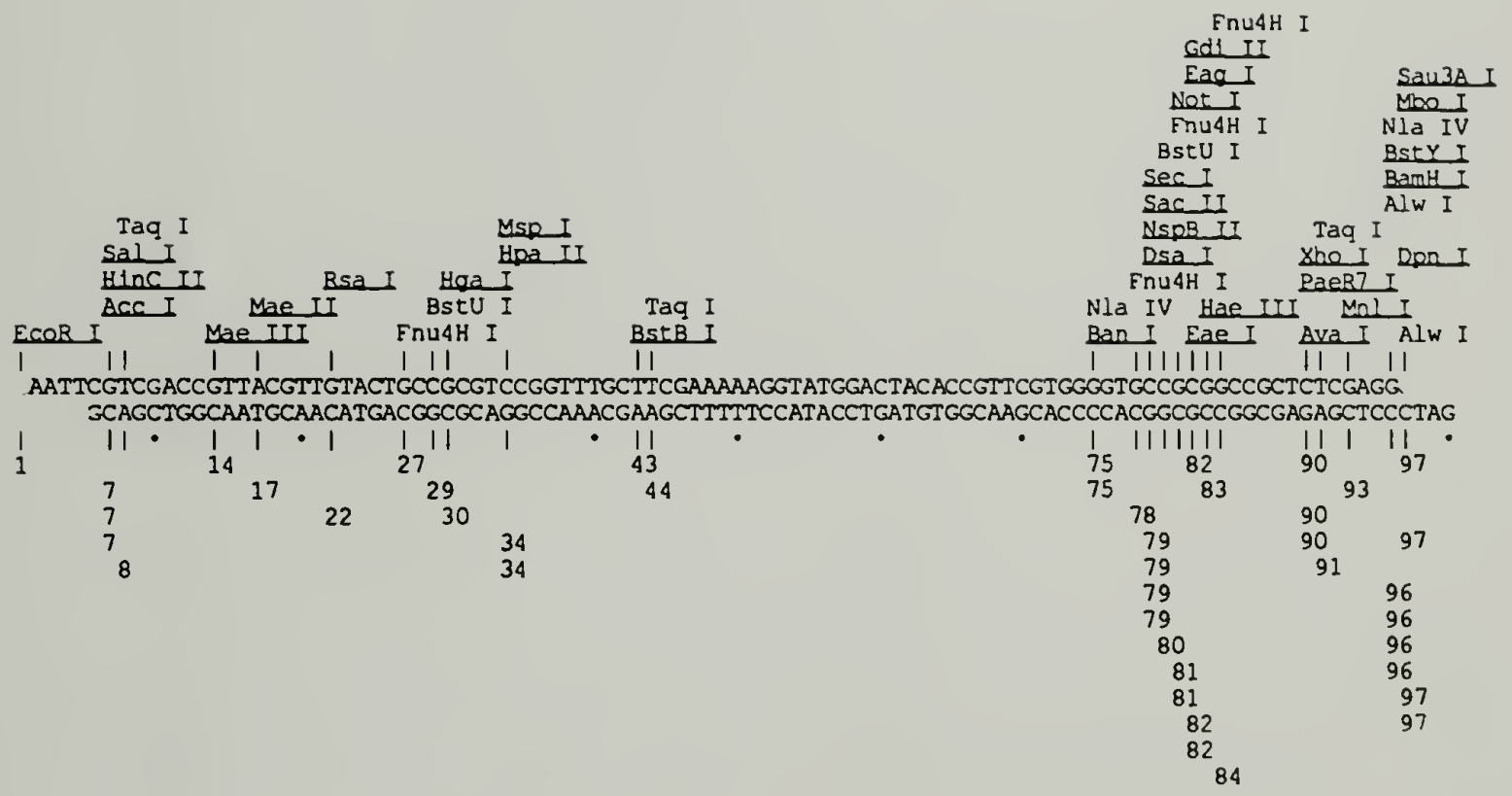

Figure A.8 The restriction map of HBD as synthesized by solid state synthesis. The Eco RI and Bam HI sites were used for cloning into pUC18. The Ban I site was used for insertion of $(VPGIG)_x$ multimers.

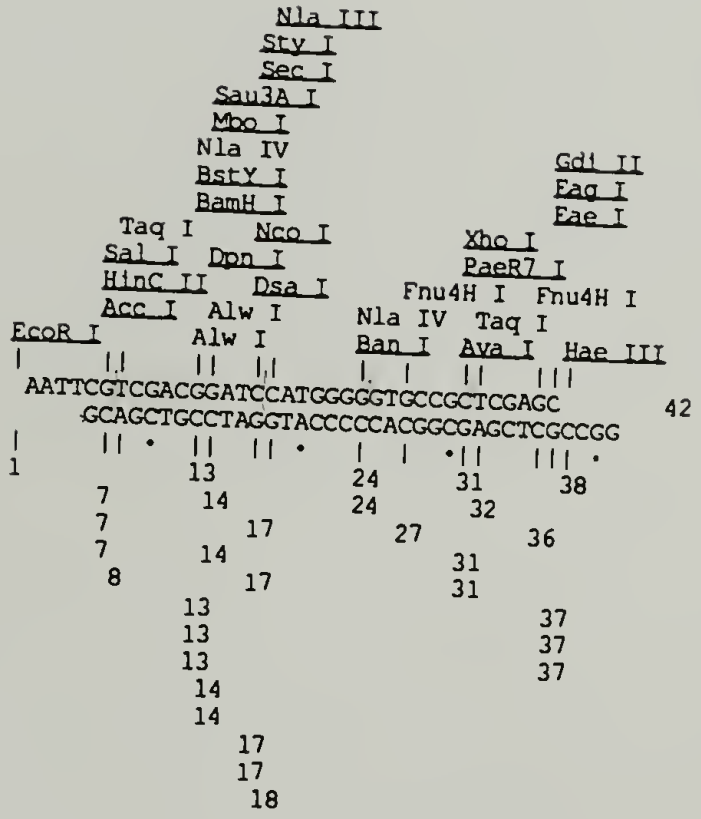

Figure A.9 The restriction map of pEC2-link as synthesized by solid state synthesis. The Eco RI and Sal I sites were used for cloning into pEC2. The Ban I site was used for insertion of $(VPGIG)_x$ multimers.

APPENDIX B

$(HBD(VPGIG)_{20})_4$ DESIGN AND SYNTHESIS

B.1 Introduction

Extracellular matrix proteins contain multiple signals which are encoded in the primary and possibly secondary and tertiary structures of the molecule. Fibronectin contains several integrin binding domains,[11,43,94-96] as well as heparin and collagen binding domains.[94,95] Laminin, a second extracellular matrix protein, also contains integrin and heparin binding domains.[97,98] Furcht and colleagues have found a peptide sequence in porcine laminin (RYVVLPRPVCFEKGMNYTVR) which binds heparan sulfate.[99]

Cells have heparin sulfate proteoglycans on their surfaces that can bind to the heparin binding domain (HBD). It has been demonstrated that a combination of cell binding domains and HBD induces focal adhesion contact formation, a more permanent anchoring where the cytoskeleton fibrils appear to be connected through cell membrane receptors to the extracellular matrix, in fibroblasts[100].

The inclusion of the heparin binding domain may aid in the formation of more permanent adhesions to the artificial extracellular matrix materials. In addition, it has been shown that heparin inhibits the proliferation of smooth muscle cells.[101] It will be possible to bind heparin to the artificial extracellular matrix proteins that include

heparin binding domains to inhibit the proliferation of smooth muscle cells.

B.2 Experimental Methods

B.2.1 Preparation of Synthetic DNA

Oligonucleotides (Figure A.8) were synthesized on a 1 μmol scale on a Biosearch Model 8700 DNA synthesizer using phosphoramidite chemistry[68]. Crude oligonucleotides were purified by denaturing polyacrylamide gel electrophoresis and eluted using the "crush and soak" method[67]. Purified oligonucleotides were annealed at 80 °C and allowed to cool to room temperature over several hours. The annealed HBD duplex (Figure A.8) was phosphorylated with T4 polynucleotide kinase, ethanol precipitated and dried *in vacuo*.

B.2.2 Cloning and Amplification of Synthetic DNA

Purified HBD was ligated into Eco RI/Bam HI digested pUC18 and used to transform *E. coli* strain DH5αF'. Cells were grown at 37 °C overnight on 2xYT solid medium containing 200 μg/ml ampicillin, 25 μg/ml β-isopropylthiogalactoside (IPTG) and 40 μg/ml of the chromogenic substrate 5-bromo-4-chloro-3-indolyl-β-D-galactopyranoside (X-Gal) for blue-white screening. Plasmid DNA from white transformants was sequenced using Sequenase 2.0 (Amersham Life Sciences) to verify the identity of the

insert. After isolation of the recombinant plasmid from a 15 ml 2xYT culture the HBD DNA was digested with Eco RI/Bam HI and the fragments were separated by nondenaturing polyacrylamide gel electrophoresis. The DNA monomer was eluted from the polyacrylamide slice using the "crush and soak" method[67].

B.2.3 Cloning of HBD in Transfer Vector

Purified HBD monomer was ligated into Bam HI/Eco RI digested pEC2 plasmid DNA (the resultant plasmid was designated pEC2-HBD), and used to transform *E. coli* strain DH5αF'. Cells were grown overnight on 2xYT solid medium containing 34 μg/ml kanamycin. Plasmid DNA from single colonies was verified for HBD insert by Bam HI/Eco RI digestion followed by 1 % agarose gel electrophoresis and staining with ethidiumbromide (EtBr); bands of 101 bp indicate proper ligation.

B.2.4 Polymerization of the $(VPGIG)_5$ Monomer and Cloning of $(VPGIG)_5$ Multimers

Purified monomeric $(VPGIG)_5$ DNA was self-ligated with T4 DNA ligase to form a population of multimers. Multimers were ligated into Ban I digested, dephosphorylated pEC2-HBD. The recombinant plasmids were used to transform *E. coli* strain DH5αF'. Transformants were screened by PCR[81] with cycling times and temperatures as follows: 96 °C, 1 min; 45 °C, 2 min; 72°C, 2 min with 35 cycles. Vent polymerase was

used with Pst I site primers for pBR322 (New England Biolabs). Amplified DNA was visualized with EtBr following separation by 1% agarose gel electrophoresis. A clone encoding 4 repeats of the $(VPGIG)_5$ monomer was chosen. The recombinant plasmid was designated pEC2-HBD$(VPGIG)_{20}$.

B.2.5 Construction of Bacterial Expression Vector

Recombinant pEC2-HBD$(VPGIG)_{20}$ was digested with Xho I/Sal I to release the HBD-$(VPGIG)_{20}$ DNA cassette. The cassette was separated by 1% agarose gel electrophoresis and recovered by extraction with Qiaex II DNA extraction kit (Qiagen). The recovered DNA was ligated into Xho I digested, dephosphorylated pET-28ap (the resulting plasmid was designated pET-28ap$(HBD(VPGIG)_{20})_x$ where x designates the number of cassettes which have been ligated), and used to transform *E. coli* strain DH5αF'. Transformants were screened for the presence and orientation of each multimer by Pflm I/Xho I digestion. This process was performed repeatedly (Figure B.1) to obtain a recombinant plasmid, designated pET-28ap$(HBD(VPGIG)_{20})_4$, which was used to transform the expression host, *E. coli* strain BL21(DE3)pLysS.

B.2.6 Protein Expression, Batch Phase, Rich Medium

Single colonies of BL21(DE3)pLysS containing recombinant pET-28ap$(HBD(VPGIG)_{20})_4$ were used to inoculate 5 ml of 2xYT medium containing chloramphenicol (34 μg/ml) and

kanamycin (34 μg/ml). The cultures were grown to saturation and a 50 μl aliquot was used to inoculate fresh 5 ml volumes of 2xYT medium containing chloramphenicol (34 μg/ml) and kanamycin (34 μg/ml). The cultures were grown to OD_{600} = 1 at 37 °C and protein expression was induced by the addition of IPTG to a final concentration of 1.0 mM. Samples were taken at t = 0, 1, 2 hr, centrifuged at 14,000 x g and resuspended in distilled H_2O at a concentration of 0.2 OD_{600} units per 10 μl for analysis by SDS-PAGE.

B.3 Results and Discussion

Samples were loaded onto a 10% polyacrylamide gel and separated by electrophoresis under denaturing conditions. Protein bands were stained with Coomassie Brilliant Blue R-250. Figure B.2 is a 10% polyacrylamide gel containing whole cell lysate samples of BL21(DE3)pLysS pET-28ap-$(HBD(VPGIG)_{20})_4$. Lane 1 contains molecular weight standards while lanes 2-4 contain whole cell lysates from cultures of colony 1 at t = 0, t = 1 hr, t = 2 hr respectively. Lanes 5-7, 8-10, and 11-14 contain whole cell lysate from colonies 2-4 respectively. In no case can a band be seen which corresponds to recombinant protein (expected molecular weight near 46 Kda).

The lack of protein expression may be attributed to the choice of codon usage at the start of the recombinant DNA. The $(CS5(VPGIG)_{20})_5$ construct is very similar to the $(HBD(VPGIG)_{20})_4$ construct. The differences are limited to

the cell binding domains. Since the encoded DNA and mRNA messages begin with the binding domains it is likely that the expression problem lies within HBD. This must be confirmed by sequencing the synthetic gene in the expression vector to be sure that no base pair deletions or additions have occurred during genetic manipulations which may cause lack of expression. If no genetic defects exist copolymers of $(CS5(VPGIG)_xHBD(VPGIG)_y)$ can be constructed. In this case the CS5 domain will be at the start of the gene and may thus allow expression of the HBD.

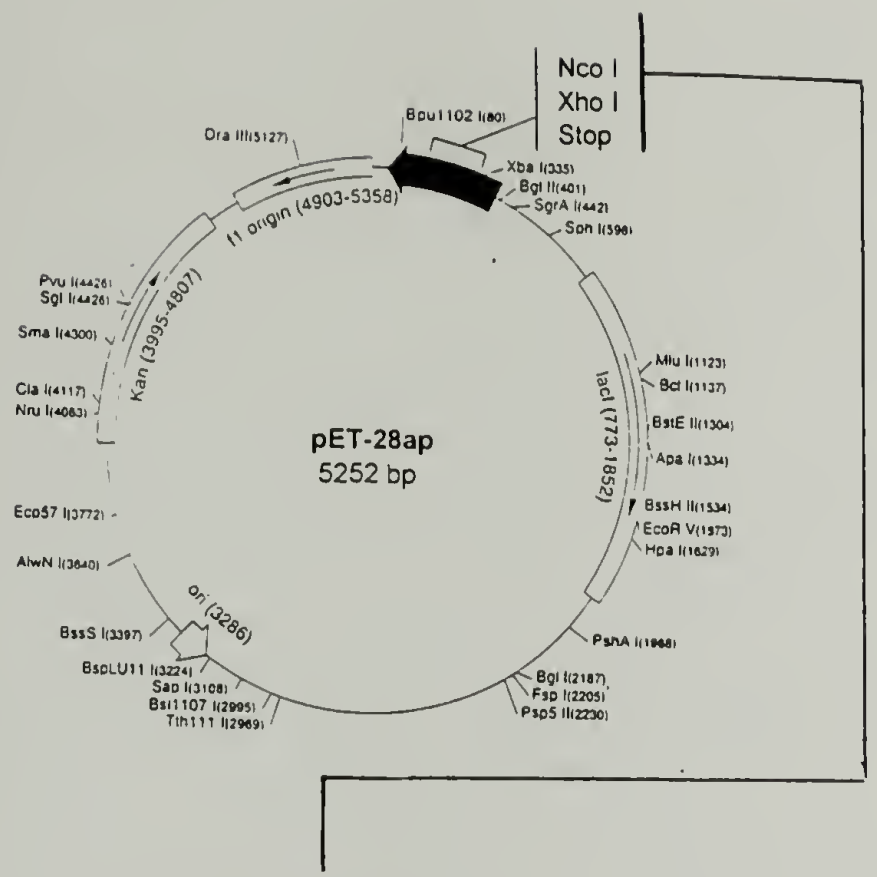

CCATGGGGCCTCGAGTAATAA

Nco I Xho I STOP

1. Xho I
2. T4 ligase/ Sal I - HBD(VPGIG)$_{20}$ - Xho I

CCATGGGGCCTCGAC**HBD(VPGIG)$_{20}$**CTCGAGTAATAA

Nco I Xho I STOP

1. Xho I
2. T4 ligase/ Sal I - HBD(VPGIG)$_{20}$ - Xho I
3. Repeat x-2 times

CCATGGGGCCTCGAC(**HBD(VPGIG)$_{20}$**)$_x$CTCGAGTAATAA

Nco I Xho I STOP

Figure B.1 A schematic of the insertion of HBD(VPGIG)$_{20}$ cassettes into pET-28ap.

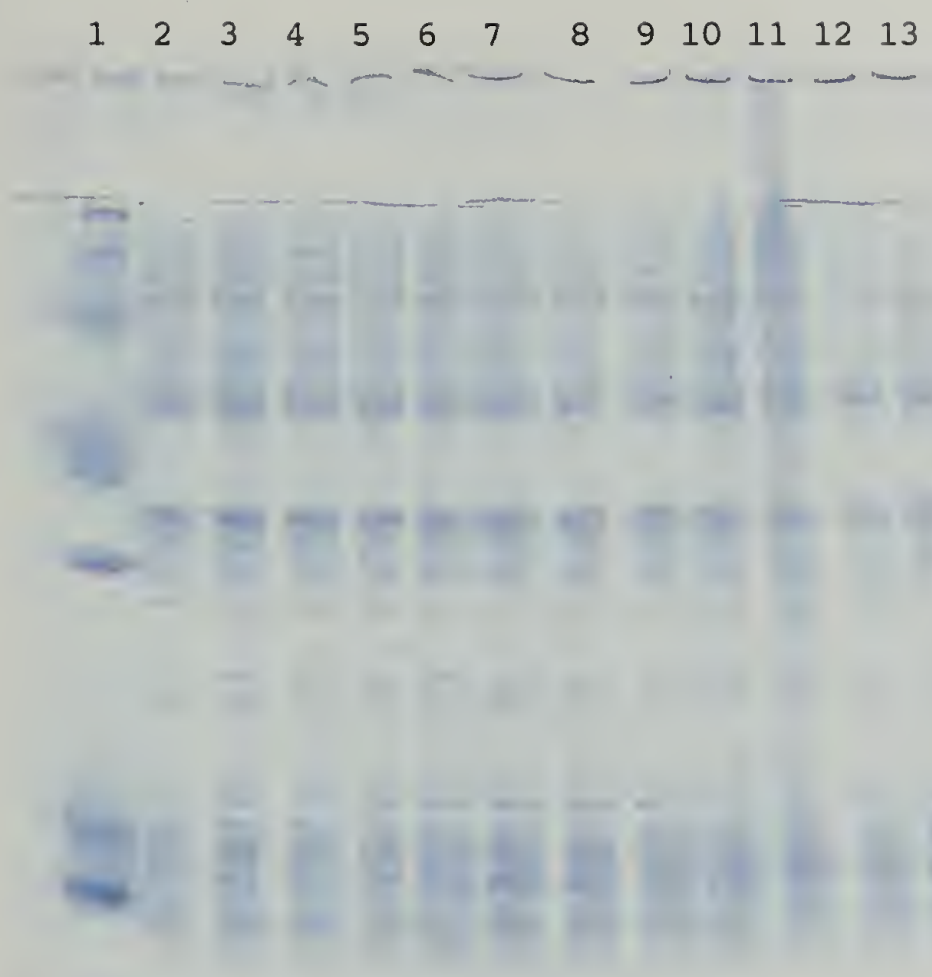

Figure B.2 A 10% SDS-PAGE of an $(HBD(VPGIG)_{20})_4$ expression. Lane 1 contains molecular weight standards while lanes 2-4 contain whole cell lysates from cultures of colony 1 at t = 0, t = 1 hr, t = 2 hr respectively. Lanes 5-7, 8-10, and 11-13 contain whole cell lysates from colonies 2-4 respectively at similar time points.

APPENDIX C

DESIGN AND SYNTHESIS OF $(VPGIG)_X$

C.1 Experimental Methods

C.1.1 Preparation of Synthetic DNA

Oligonucleotides were synthesized on a 1 μmol scale on a Biosearch Model 8700 DNA synthesizer using phosphoramidite chemistry.[68] Oligonucleotides were annealed at 80 °C and allowed to cool to room temperature over several hours. The annealed pEC2-link duplex (Figure A.9) was phosphorylated with T4 polynucleotide kinase, ethanol precipitated and dried *in vacuo*.

C.1.2 Cloning and Amplification of Synthetic DNA

The pEC2-link duplex was ligated into Eco RI/Eag I digested pEC2 and used to transform *E. coli* strain DH5αF'. Cells were grown at 37 °C overnight on 2xYT solid medium containing 25 μg/ml kanamycin. Plasmid DNA from transformants was sequenced using Sequenase 2.0 (Amersham Life Sciences) to verify the identity of the insert.

C.1.3 Cloning and Amplification of $(VPGIG)_5$

Purified $(VPGIG)_5$ DNA was ligated into Eco RI/Bam HI digested pUC18 and used to transform *E. coli* strain DH5αF'. Cells were grown at 37°C overnight on 2xYT solid medium and

sequenced as described in chapter 3. After isolation of the recombinant plasmid from a 1 liter 2xYT culture, the $(VPGIG)_5$ DNA was digested with Ban I and the fragments were separated by nondenaturing polyacrylamide gel electrophoresis. DNA monomer was eluted from the polyacrylamide slice, using the "crush and soak" method.[67]

C.1.4 Polymerization of the $(VPGIG)_5$ Monomer and Cloning of $(VPGIG)_5$ Multimers

Purified monomeric $(VPGIG)_5$ DNA was self-ligated with T4 DNA ligase to form a population of multimers. Multimers were ligated into Ban I digested, dephosphorylated pEC2-link. The recombinant plasmids were used to transform *E. coli* strain DH5αF'. Transformants were screened by PCR with cycling times and temperatures as follows: 96 °C, 1 min; 45 °C, 2 min; 72°C, 2 min with 35 cycles. Vent polymerase was used with Pst I site primers for pBR322 (New England Biolabs). Amplified DNA was visualized with EtBr following separation by 1% agarose gel electrophoresis. A clone encoding 11 repeats of the $(VPGIG)_5$ monomer was chosen. The recombinant plasmid was designated pEC2-link-$(VPGIG)_{55}$.

C.1.5 Construction of Bacterial Expression Vector

Recombinant pEC2-link-$(VPGIG)_{55}$ was digested with Xho I/Sal I to release $(VPGIG)_{55}$. The DNA was separated by 1% agarose gel electrophoresis and recovered by extraction with

Qiaex II DNA extraction kit (Qiagen). The recovered DNA was ligated into Xho I digested, dephosphorylated pET-28ap and used to transform *E. coli* strain DH5αF'; the recombinant plasmid was designated pET-28ap(VPGIG)$_{55}$. Transformants were screened for the presence and orientation of each multimer by Pflm I/Xho I digestion. DNA ligated in the correct orientation was indicated by a DNA band of ~1250 bp as visualized by 1 % agarose gel electrophoresis followed by staining with ethidiumbromide. The expression host BL21(DE3)pLysS was transformed with pET-28ap(VPGIG)$_{55}$.

C.1.6 Protein Expression, Batch Phase, Rich Medium

Single colonies of BL21(DE3)pLysS containing recombinant pET-28ap(VPGIG)$_{55}$ were used to inoculate 5 ml of 2xYT medium containing chloramphenicol (34 μg/ml) and kanamycin (34 μg/ml). The cultures were grown to saturation and 50 μl was used to inoculate fresh 5 ml volumes of 2xYT medium containing chloramphenicol (34 μg/ml) and kanamycin (34 μg/ml). The cultures were grown to OD_{600} = 1 at 37 °C and protein expression was induced by the addition of IPTG to a final concentration of 1.0 mM. Every 60 minutes for 2 hrs 1 ml samples were taken, centrifuged at 14,000 x g and resuspended in distilled H_20 at a concentration of 0.2 OD_{600} units per 10 μl for analysis by SDS-PAGE. However, SDS-PAGE of whole cell lysate followed by staining with Coomassie Briliant blue revealed no bands at 24,483 Da, the expected molecular weight.

C.1.7 Protein Expression, ^{3}H-Glycine, M9AA

A single colony of BL21(DE3)pLysS containing recombinant pET-28ap(VPGIG)$_{55}$ was used to inoculate 5 ml of M9AA containing chloramphenicol (34 μg/ml) and kanamycin (34 μg/ml). The culture was grown to saturation and used to inoculate 25 ml of M9AA medium containing chloramphenicol (34 μg/ml) and kanamycin (34 μg/ml). The culture was grown to OD_{600} = 0.8 at 37 °C and protein expression was induced by addition of IPTG to a final concentration of 1.0 mM; after allowing T7 RNA polymerase to be produced, 34 μg/ml rifampicin was added to inhibit *E. coli* RNA polymerase; 10 minutes later 150 μl of 1 μCi/μl ^{3}H glycine was added for incorporation into the artificial protein. Every 60 minutes for 2 hrs 1 ml samples were taken, centrifuged at 14,000 x g and resuspended in distilled H_2O at a concentration of 0.2 OD_{600} units per 10 μl for analysis by 10 % SDS-PAGE. Following SDS-PAGE, run at 16 mA through the stacking gel and 30 mA through the resolving gel, the gel was stained with Coomassie Brilliant Blue R-250, dried *in vacuo* and Xray film was exposed to the gel for 2 days. The developed film showed a dark band appearing at 23 Kd in the induced samples (data not shown). Still no band could be seen on the Coomassie stained radioactive gel indicating that the recombinant protein does not stain with Coomassie Blue. The lack of staining of the gel makes it difficult to determine the amount of expression prior to purification of the recombinant protein.

APPENDIX D

SEM ANALYSIS OF PROTEIN COATING

Protein coatings were prepared as described in chapter 3. Briefly, 40 μl of 40 mg/ml solutions of protein were spread on 12 mm glass coverslips. The protein coated coverslips were then dried *in vacuo* at 55 °C. Coverslips were imaged at this stage after coating with gold palladium. Protein coated coverslips were incubated at 37 °C with 0.5 ml water to remove excess protein. They were once again dried at 55 °C *in vacuo*. Coverslips were also imaged at this stage.

Imaging and elemental analysis were both performed on a JEOL 6320-FXI field emission microscope. The samples were coated with gold/palladium by sputter coating, then imaged at 10 kV. Samples for elemental analysis were analyzed uncoated at 5 kV.

Figures D.1a & b show x-ray elemental analysis of the glass coverslip (Fig. D.1a) and glass coated with $(CS5(VPGIG)_{20})_5$ (Fig. D.1b) prior to removal of excess protein. A silicon peak is apparent on the uncoated coverslip, but it is not seen on the protein coated coverslip prior to soaking in PBS to remove excess protein. On the protein coated coverslip profile there is also marked suppression of the oxygen peak and loss of the sodium peak while a carbon peak can clearly be seen. The protein

coating was thick enough that detection of the underlying glass was not possible. Once excess protein was removed, the glass signals were visible even with the protein coating, so this method could not be used to determine protein coatings. Determination of coating was then done by scintillation counting as described in chapter 4.

Figures D.2a & b show SEM images obtained from $(CS5(VPGIG)_{20})_5$ coated coverslips before excess protein was removed (Fig D.2a) and after protein removal (Fig D.2b). In both cases the surface looks cracked and textured. Glass alone looks quite smooth with no cracks (data not shown). These images coupled with the scintillation counting data suggest complete coverage of the coverslips prior to cell culturing.

a.

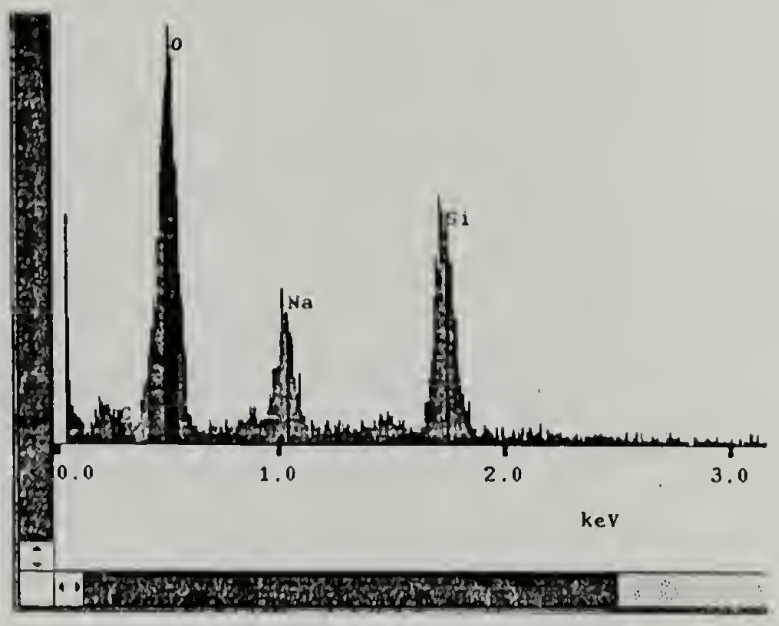

b.

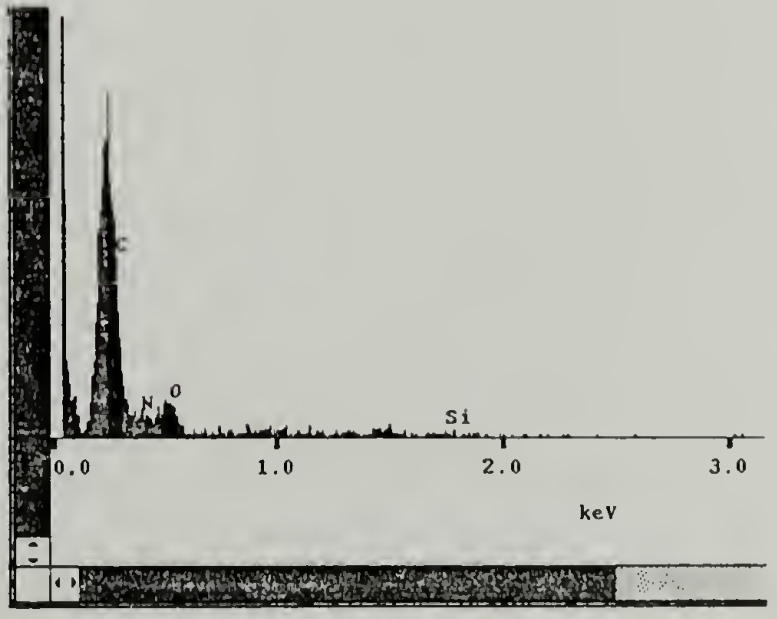

Figure D.1 Elemental analysis of protein coated glass coverslips. A4.1a is a glass coverslip with no coating; prominent Si and Na peaks can be seen and no C peak is seen. A4.1b is a glass coverslip coated with $(CS5(VPGIG)_{20})_5$; the Si and Na peaks have been lost and a C peak can clearly be seen.

a.

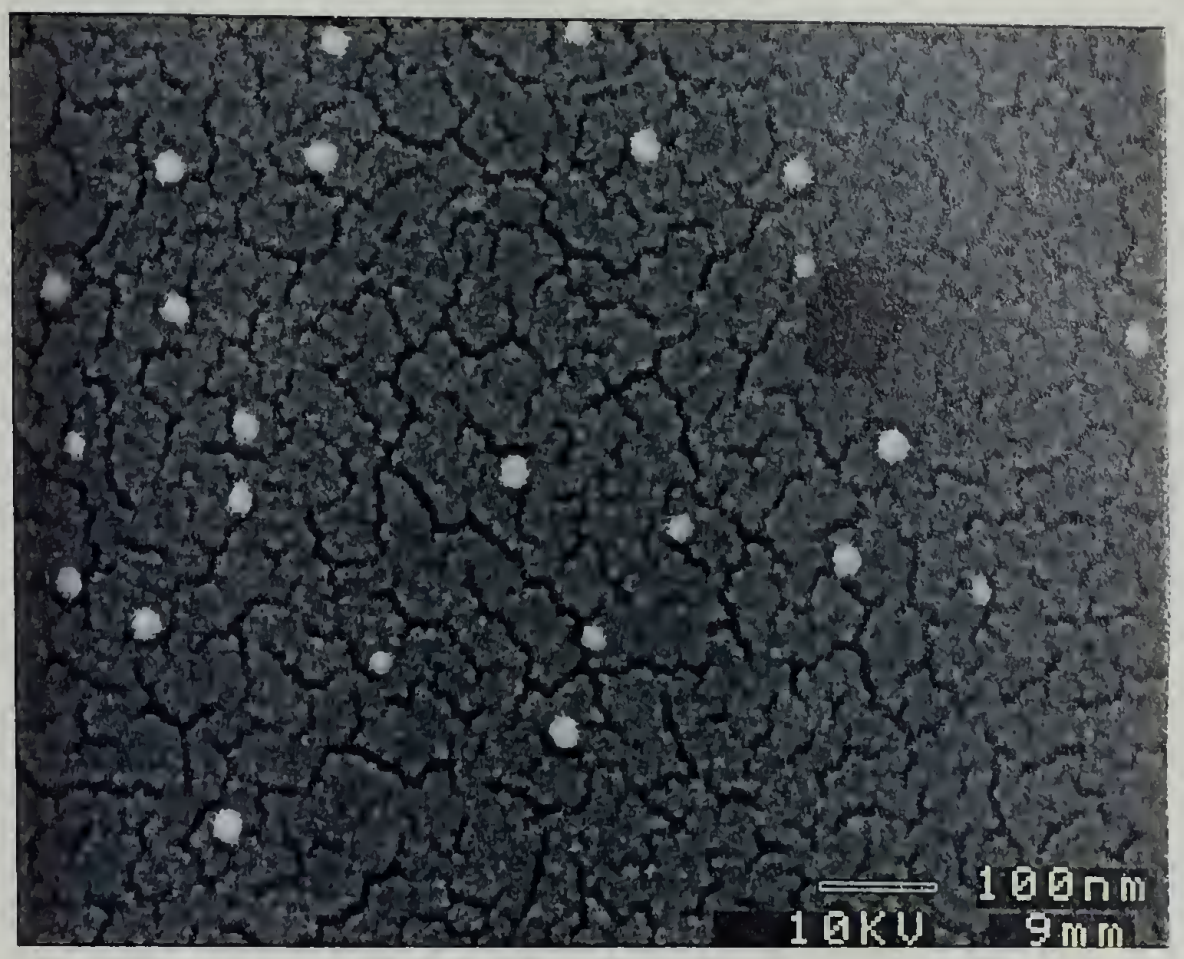

b.

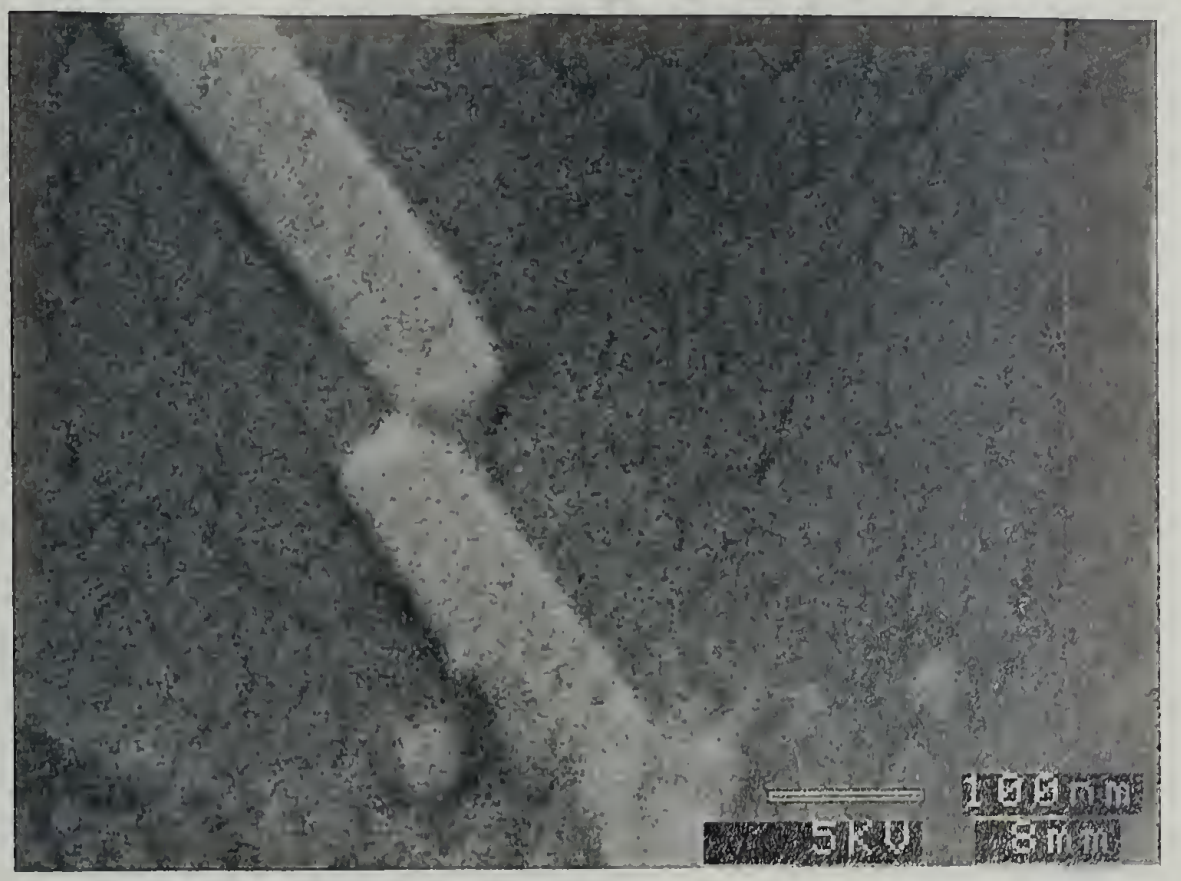

Figure D.2 SEM images of $(CS5(VPGIG)_{20})_5$ coated coverslips. A4.2a shows a protein coated coverslip prior to removal of excess protein, while A4.2b shows a protein coated coverslip after removal of excess protein. Both samples are coated with gold/palladium and imaged at 5 kV.

APPENDIX E

HUVEC CULTURING ON PTFE COATED COVERSLIPS WITH ARTIFICIAL EXTRACELLULAR MATRIX PROTEIN COATINGS

E.1 Materials and Methods

E.1.1 PTFE Coating of Coverslips

Glass coverslips were coated with a thin layer of PTFE.[102] Briefly, a hot plate was heated to 300 °C; a 12 mm glass coverslip was placed on the hot plate and a piece of PTFE was manually drawn across the coverslip 4 times in the same direction. PTFE coating was verified by SEM imaging of gold/palladium coated coverslips. Figure E.1 shows an SEM image; the PTFE is seen in the image as long peaks and valleys.

E.1.2 Protein Coating of Coverslips

Coverslips were placed into the wells of a 24 well culture dish and 0.5 ml of a 40 mg/ml protein solution was added. After incubation at 4 °C overnight, the protein solution was removed and the coverslips were dried at 55 °C *in vacuo* as described in chapter 3.

E.1.3 Determination of Protein Stability

The determination of the stability of the protein on the surface was done using ^{3}H-glycine labeled protein

coupled with scintillation counting as described in chapter 4. The stability was determined only by the method in which 0.5 ml of PBS was added to each well for 3 hours during which time small aliquots were taken at 30 minute intervals to determine the amount of protein solubilized over time. The amount of protein remaining on the coverslips was also determined by scintillation counting as described in chapter 4.

E.1.4 HUVEC Culturing

Cell culturing was done as described in chapter 3. Coverslips coated with PTFE, as well as PTFE adsorbed with $(CS5(VPGIG)_{20})_5$ and $(CS5(VPGIG)_{40})_3$ from solutions of protein in formamide and water, and as suspensions of protein in trifluoroethanol (TFE) were used for cell culturing. HUVECs were suspended in serum free M199 at 10^4 cells/ml and 1 ml of suspension was added to each well. HUVECs were incubated at 37 °C and 5% CO_2 for 4 hours.

E.2 Results and Discussion

Table E.1 shows the amount of protein removed after 3 hr incubation in PBS at 37 °C as well as the amount of protein remaining on the PTFE coated coverslips after the incubation period. Approximately 1 μg of each protein remains on the surface with the exception of $(CS5(VPGIG)_{20})_5$ adsorbed from formamide, where more than 2 μg of protein remained. This correlates to a protein thickness of ≈20 Å.

Only moderate improvement of cell adhesion was seen on the protein coated PTFE surfaces as compared to the PTFE surfaces alone.

A slight increase in the number of cells adhered to artificial extracellular matrix treated coverslips was observed by visualization by phase contrast microscopy. Quantitative evaluation must be done to determine the significance of the increase in cell adhesion.

Table E.1 Stability of Protein Coatings on PTFE Coated Glass

Casting Solvent	$(CS5(VPGIG)_{20})_8$		$(CS5(VPGIG)_{40})_3$	
	Removed	Remaining	Removed	Remaining
Formamide	11.4 ± 3.2	2.4 ± 0.3	14.0 ± 2.9	1.0 ± 0.1
Water	12.6 ± 4.2	1.4 ± 0.1	15.0 ± 1.9	1.5 ± 0.1
TFE	19.0 ± 1.9	0.7 ± 0.1	11.0 ± 2.3	0.8 ± 0.1

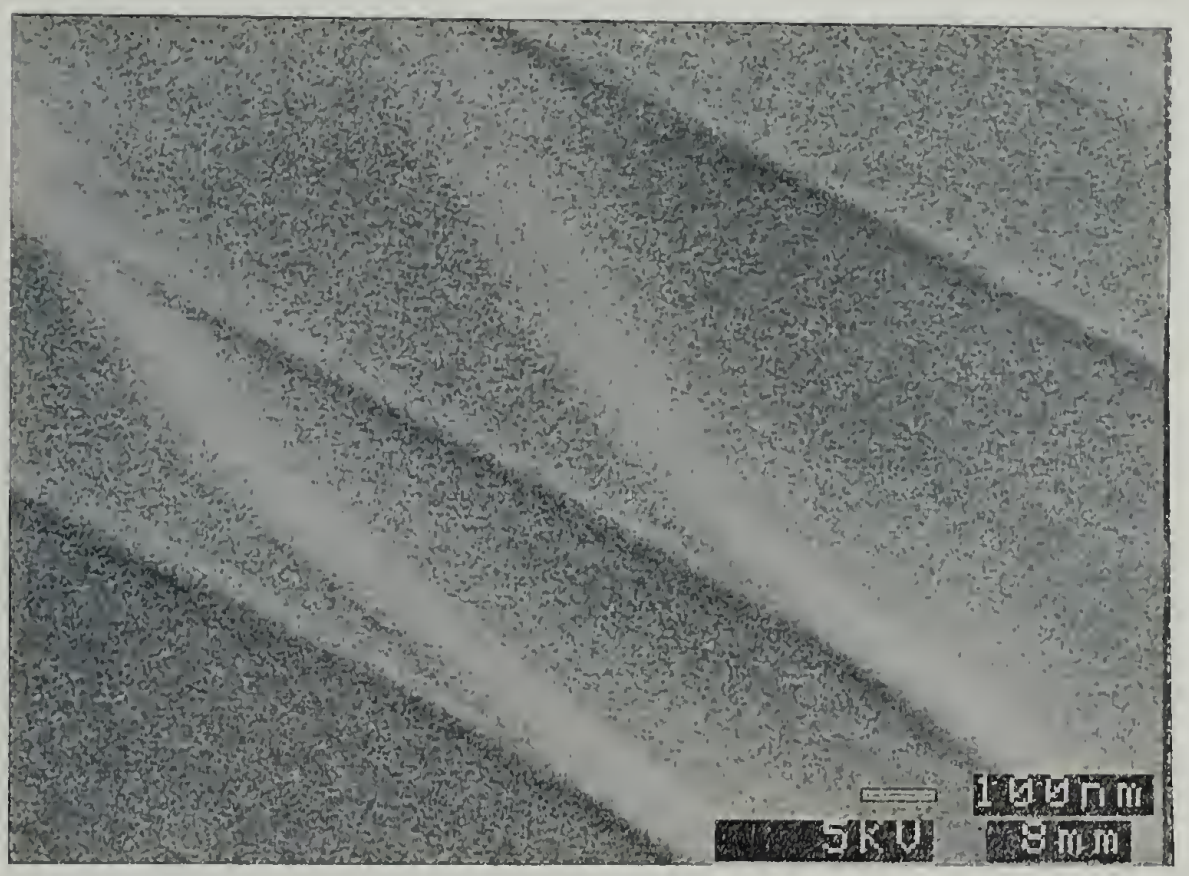

Figure E.1 SEM image of PTFE spread on glass. The PTFE coated coverslip was coated with gold/palladium and imaged at 5 kV. The streaked appearance of the surface is due to the PTFE.

APPENDIX F

2-D NOSY NMR SPECTRUM of POLY(AG)

To determine whether there had been mutation in $(AG)_{240}$ a 2-D NOSY NMR spectrum was taken at 500 MHz. Figure F.1 shows the spectrum obtained. Cross peaks can clearly be seen between putative valine methyl resonance at 1.1 ppm and the Gly C_α peak at 4.3 ppm as well as between the 1.1 ppm peak and the Ala C_β. This information coupled with the amino acid analysis data reported in chapter 2 indicate that there is valine present in the backbone of $(AG)_{240}$.

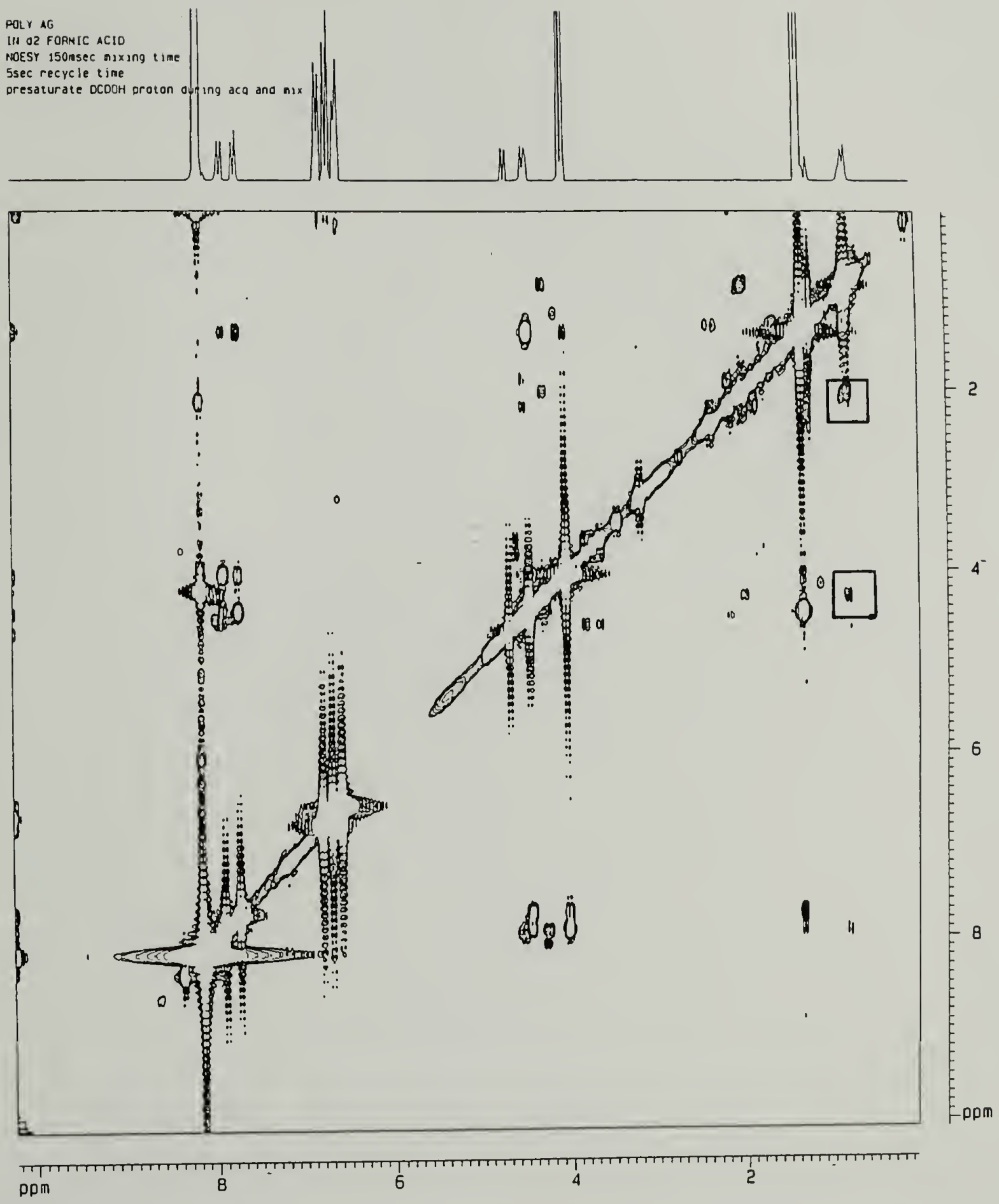

Figure F.1 A 2-D NOSY of $(AG)_{260}$. Cross peaks between the Val signal(1.1 ppm) and the Gly signal (4.3 ppm) can be seen.

REFERENCES

(1) Hubbell, J. A. *Bio/Technology* **1995**, *13*, 565.

(2) Hubbell, J. A.; Langer, R. *Chem Eng N* **1995**, *March 13*, 42.

(3) Langer, R.; Vacanti, J. P. *Science* **1993**, *260*, 920.

(4) Kohler, T. R.; Kirkman, T. R.; Gordan, D.; Clowes, A. W. *Am J Surg* **1990**, *160*, 257.

(5) Greisler, H. P. *New Biologic and Synthetic Vascular Prostheses*; R.G. Landes Company: Austin, 1991.

(6) Pierschbacher, M. D.; Ruoslahti, E. *Nature* **1984**, *309*, 30.

(7) Guda, C.; Zhang, X.; McPherson, D. T.; Xu, J.; Cherry, J. H.; Urry, D. W.; Daniel, H. *Biotech Lett* **1995**, *17*, 745.

(8) McPherson, D. T.; Morrow, C.; Minehan, D. S.; Wu, J.; Hunter, E.; Urry, D. W. *Biotechnol Prog* **1992**, *8*, 347.

(9) Urry, D. W. *J Protein C* **1984**, *3*, 403.

(10) Ross, M. H.; Romrell, L. J.; Kaye, G. I. *Histology A Text and Atlas*; 3 ed.; Williams & Wilkins: Baltimore, 1995.

(11) Humphries, M. J.; Akiyama, S. K.; Komoriya, A.; Olden, K.; Yamada, K. M. *J Cell Biol* **1986**, *103*, 2637.

(12) Urry, D. W.; Hatnes, B.; Zhang, H.; Harris, R. D.; Prasad, K. U. *Proc Natl Acad Sci USA* **1988**, *85*, 3407.

(13) Anderson, J. M. In *Biomaterials Science An Introduction to Materials in Medicine*; Ratner, B. D., Hoffman, A. S., Schoen, F. J., Lemons, J. E., Eds.; Academic Press: New York, 1996; pp 484.

(14) Vroman, L. *Trans Soc Biomater* **1986**, *9*, 59.

(15) Hanson, S. R.; Harker, L. A. In *Biomaterials Science An Introduction to Materials in Medicine*; Ratner, B. D., Hoffman, A. S., Schoen, F. J., E., J., Eds.; Academic Press: New York, 1996; pp 484.

(16) Charo, I. F.; Kieffer, N.; Phillips, D. R. In *Hemostasis and Thrombosis: Basic Priciples and Clinical Practices*; Coleman, R. W., Hirsh, J., Marder, V. J., Salzman, E. W., Eds.; J. B. Lippincott Company: Philadelphia, 1994; pp 489.

(17) Greisler, H. P.; Petsikas, D.; Lam, T. M.; Patel, N.; Ellinger, J.; Cabusao, E.; Tattersall, C. W.; Kim, D. U. *J Biomed Mat Res* **1993**, *27*, 955.

(18) Desai, N. P.; Hubbell, J. A. *J Biomed Mat Res* **1991**, *25*, 829.

(19) Hubbell, J. A. *TRIP* **1994**, *2*, 20.

(20) Mooradian, D. L.; Trescony, P.; Keeney, K.; Furcht, L. T. *J Surg Res* **1992**, *53*, 74.

(21) Kohler, T. R.; Stratton, J. R.; Kirkman, T. R.; Johansen, K. H.; Zierler, B. K.; Clowes, A. W. *Surgery* **1992**, *112*, 901.

(22) Greisler, H. P.; Cziperle, D. J.; Kim, D. U.; Garfield, J. D.; Petsikas, D.; Murchan, P. M.; Applegreen, E. O.; Drohan, W.; Burgess, W. H. *Surgery* **1992**, *112*, 244.

(23) Kirkpatrick, C. J.; Mueller-Schulte, D.; Roye, M.; Hollweg, G.; Gossen, C.; Richter, H.; Mittermayer, C. *Cell Mater* **1991**, *1*, 93.

(24) Zilla, P.; Deutsch, M.; Meinhart, J.; Puschmann, R.; Elbert, T.; Minar, E.; Dudczak, R.; Lugmaier, H.; Schmidt, P.; Noscian, I.; Fischlein, T. *J Vasc Surg* **1994**, *19*, 540.

(25) Pierschbacher, M. D.; Polarek, J. W.; Craig, W. S.; Tschopp, J. F.; Sipes, N. J.; Harper, J. R. *J Cell Bioc* **1994**, *56*, 150.

(26) Hynes, R. O. *Cell* **1992**, *69*, 11.

(27) Walluscheck, K. P.; Steinhoff, G.; Kelm, S.; Haverich, A. *Eur J Endovasc Surg* **1996**, *12*, 321.

(28) Massia, S. P.; Hubbell, J. A. *J Biomed Mat Res* **1991**, *25*, 223.

(29) Hubbell, J. A.; Massia, S. P.; Desai, N. P.; Drumheller, P. D. *Biotechnology* **1991**, *9*, 568.

(30) Luscinskas, F. W.; Lawler, J. *FASEB J* **1994**, *8*, 929.

(31) Creel, H. S.; Fournier, M. J.; Mason, T. L.; Tirrell, D. A. *Macromolecules* **1991**, *24*, 1213.

(32) McGrath, K. P.; Fournier, M. J.; Mason, T. L.; Tirrell, D. A. *J Am Chem Soc* **1992**, *114*, 727.

(33) Parkhe, A.; Fournier, M. J.; Mason, T. L.; Tirrell, D. A. *Macromolecules* **1993**, *26*, 6691.

(34) Deguchi, Y.; Fournier, M. J.; Mason, T. L.; Tirrell, D. A. *J Macromol Sci-Pure Appl Chem* **1994**, *A31*, 1691.

(35) Dougherty, M. J.; Kothakota, S.; Mason, T. L.; Fournier, M. J.; Tirrell, D. A. *Macromolecules* **1993**, *26*, 1779.

(36) Krejchi, M. T.; Atkins, E. D. T.; Waddon, A. J.; Fournier, M. J.; Mason, T. L.; Tirrell, D. A. *Science* **1994**, *265*, 1427.

(37) Yoshikawa, E.; Fournier, M. J.; Mason, T. L.; Tirrell, D. A. *Macromolecules* **1994**, *27*, 5471.

(38) Panitch, A.; Matsuki, K.; Cantor, E. J.; Cooper, S. J.; Atkins, E. D. T.; Fournier, M. J.; Mason, T. L.; Tirrell, D. A. *Macromolecules* **1997**, *30*, 42.

(39) Massia, S. P.; Hubbell, J. A. *J Cell Biol* **1991**, *114*, 1089.

(40) Huttenlocher, A.; Sandborg, R. R.; Horwitz, A. F. *Curr Op Cell Biol* **1995**, *7*, 697.

(41) Urry, D. W. *Angew Chem Int Ed Engl* **1993**, *32*, 819.

(42) Humphries, M. J.; Komoriya, A.; Akiyama, S. K.; Olden, K.; Yamada, K. M. *J Biol Chem* **1987**, *262*, 6886.

(43) Komoriya, A.; Green, L. J.; Mervic, M.; Yamada, S. S.; Yamada, K. M.; Humphries, M. J. *J Biol Chem* **1991**, *266*, 15075.

(44) Mould, A. P.; Komoriya, A.; Yamada, K. M.; Humphries, M. J. *J Biol Chem* **1991**, *266*, 3579.

(45) Hubbell, J. A.; Massia, S. P.; Drummheller *Ann N Y Acad Sci* **1992**, 253.

(46) Massia, S. P.; Hubbell, J. A. *J Biol Chem* **1991**, *267*, 14019.

(47) Nicol, A.; Gowda, D. C.; Parker, T. M.; Urry, D. W. *Cell Adhesive Properties of Bioelastic Materials Containing Cell Attachment Sequences*; Gebelein, C., Carraher, C., Eds.; Plenum Press: New York, 1994; pp 95.

(48) Nicol, A.; Gowda, D. C.; Urry, D. W. *J Biomed Mat Res* **1992**, *26*, 393.

(49) Grande, D. A.; Halberstadt, C.; Naughton, G.; Schwartz, R.; Manji, R. *J Biomed Mat Res* **1997**, *34*, 211.

(50) Riesenburg, D.; Schultz, V.; Knorre, W. A.; Pohl, W. A.; Korz, H.-D.; Sanders, E. A.; Rob, A.; Deckwer, W.-D. J Biotech. **1991**, *20*, 17.

(51) Bailey, F. J.; Blackenship, J.; Condra, R. Z.; Ellis, R. W. J. **1987**, *2*, 47.

(52) Bauer, K. A.; Ben-Bassat, A.; Dawson, M.; Puente, V. T. D. L.; Neway, J. O. *Appl Environ Mocrobiol* **1990**, *56*, 1296.

(53) Capello, J.; Crissman, J.; Dorman, M.; Mikolajcazak, M.; Textor, G.; Marquet, M.; Ferrari, F. *Biotechnol Prog* **1990**, *6*, 198.

(54) Capello, J.; Crissman, J.; Dorman, M.; Mikolajcazak, M.; Textor, G.; Marquet, M.; Ferrari, F. *Mater Res Soc Symp Proc* **1990**, *174*, 267.

(55) Fraser, R. D. B.; MacRae, T. P.; Stewart, F. H. C.; Suzuki, E. *J Mol Biol* **1965**, *11*, 706.

(56) Fraser, R. D. B.; MacRae, T. P.; Stewart, F. H. C. J Mol Biol. **1966**, *19*, 580.

(57) Lotz, B.; Keith, H. D. *J Mol Biol* **1971**, *61*, 201.

(58) Keller, A. *Philos Mag* **1957**, *2*, 1171.

(59) Keller, A. *Rep Prog Phys* **1968**, *31*, 624.

(60) Geil, P. H. ; Interscience: New York, 1963.

(61) Fisher, E. *Z Naturforsh* **1957**, *12*, 753.

(62) Geddes, A. J.; Parker, K. D.; Atkins, E. D. T.; Beighton, E. *J Mol Biol* **1968**, *32*, 343.

(63) Bellinger, M. A.; Waddon, A. J.; Atkins, E. D. T.; MacKnight, W. J. *Macromolecules* **1994**, *27*, 2130.

(64) Atkins, E. D. T.; Hill, M. J.; Hong, S. K.; Keller, A.; Organ, S. J. *Macromolecules* **1992**, *25*, 917.

(65) Yee, L.; Blanch, H. W. *Biotechnol BioEng* **1993**, *41*, 781.

(66) Studier, F. W.; Rosenberg, A. H.; Dunn, A. H.; Dubendorff, J. W. *Meth Enzymol* **1991**, *185*, 60.

(67) Sambrook, J.; Frisch, E. F.; Maniatis, T. *Molecular Cloning*; 2 ed.; Cold Spring Harbor Laboratory Press: Cold Spring Harbor, 1989.

(68) McBride, L. J.; Caruthers, M. H. *Tetrahedron Lett* **1983**, *24*, 245.

(69) Yannish-Perron, C.; Vierira, J.; Messing, J. **1985**, *33*, 103.

(70) Ferrari, F. A.; Richardson, C.; Chambers, J.; Causey, S. C.; Pollock, T. J. In *U. S. Patent no. 53543038*; Protein Polymer Technologies: USA, 1993.

(71) Smith, B. J. *Methods in Biology, New Protein Techniques*; Humana: Clifton, NJ, 1988.

(72) Frude, M. J.; Read, A.; Kennedy, L. *Biotech Lett* **1993**, *15*, 797.

(73) Beavis, R. C.; Chait, B. T.; Creel, H. S.; Fournier, M. J.; Mason, T. L.; Tirrell, D. A. J Am Chem Soc. **1992**, *114*, 7584.

(74) Cantor, E. J.; Cooper, S. J.; Atkins, E. D. T.; Mason, T. L.; Fournier, M. J.; Trrell, D. A. *J Biochem* **1997**, *In Press*.

(75) Williams, S. K.; Schneider, T.; Kapelan, B.; Jarrell, B. E. *J Elec Micr Tech* **1991**, *19*, 439.

(76) Yannas, I. V. *Angew Chem Int Ed Engl* **1990**, *29*, 20.

(77) Clowes, A. W.; Kohler, T. *J Vasc Surg* **1991**, *13*, 734.

(78) Pasic, M.; Muller-Glauser, W.; Segesser, L. v.; Odermatt, B.; Lachat, M.; Turina, M. *Eur J Cordio-Thorac Surg* **1996**, *10*, 372.

(79) Leseche, G.; Ohan, J.; Bouttier, S.; Palombi, T.; Bertrand, P.; Andreassian, B. *Ann Vacs Surg* **1995**, *9*, S15.

(80) Urry, D. W.; Gowda, C.; Parker, T. M.; Luan, C.-H.; Reid, M. C.; Harris, C. M.; Pattanaik, A.; Harris, R. D. *Biopolymers* **1992**, *32*, 1243.

(81) *Current Protocols in Molecular Biology*; Ausubel, F. M.; Brent, R.; Kingston, R. E.; Moore, D. M.; Sideman, J. G.; Smith, J. A.; Struhl, K., Eds.; John Wiley & Sons, Inc.: USA, 1995; Vol. 2, pp 15.1.1.

(82) Masumoto, A.; Hemler, M. E. *J Cell Biol* **1993**, *123*, 245.

(83) Peluso, G.; Petillo, O.; Anderson, J. M.; Ambrosio, L.; Nicolais, L.; Melone, M. A. B.; Eschbach, F. O.; Huang, S. J. *J Biomed Mat Res* **1997**, *34*, 327.

(84) Lee, J. H.; Jung, H. W.; Kang, I.-K.; Lee, H. B. *Biomaterials* **1994**, *15*, 705.

(85) Bouaziz, A.; Richert, A.; Caprani, A. *Biomaterials* **1997**, *18*, 107.

(86) Urry, D. W. *J Protein C* **1988**, *7*, 1.

(87) Urry, D. W.; Parker, T. M.; Reid, M. C.; Gowda, D. C. *J Bioact and Comp Pol* **1991**, *6*, 263.

(88) Urry, D. W.; Long, M. M. In *Elastin and Elastic Tissue*, 1976; Vol. 79; pp 685.

(89) Burridge, K.; Faith, K. *BioEssays* **1989**, *10*, 104.

(90) Burridge, K.; Fath, K.; Kelly, T.; Nuckolls, G.; Turner, C. *Ann Rev Cell Biol* **1988**, *4*, 487.

(91) Urry, D. W.; Trapane, T. L.; Prasad, K. U. *Biopolymers* **1985**, *24*, 2345.

(92) Khor, E. *Biomaterials* **1997**, *18*, 95.

(93) Solomons, T. W. *Organic Chemistry*; 6 ed.; John Wiley & Sons, Inc.: New York, 1996.

(94) Hynes, R. *Ann Rev Cell Biol* **1985**, *1*, 67.

(95) Kornblihtt, A. R.; Umezawa, K.; Vibe-Pedersen, K.; Baralle, F. E. *EMBO J* **1985**, *4*, 1755.

(96) Mould, A. P.; Humphries, M. J. *EMBO J* **1991**, *10*, 4089.

(97) Kleinman, H. K.; Weeks, B. S.; Schnaper, H. W.; Kibbey, M. C.; Yamamura, K.; Grant, D. S. *Vitamins and Hormones* **1993**, *47*, 161.

(98) Mecham, R. *Ann Rev Cell Biol* **1991**, *7*, 71.

(99) Charonis, A. S.; Skubitz, A. P. N.; Koliakos, G. G.; Reger, L. A.; Dege, J.; Vogel, A. M.; Wohlhueter, R.; Furcht, L. T. *J Cell Biol* **1988**, *107*, 1253.

(100) Woods, A.; Couchman, J. R.; Johansson, S.; Hook, M. *EMBO J* **1986**, *5*, 665.

(101) Clowes, A. W.; Reidy, M. A. J of Vasc Surg 1991, *13*, 885.

(102) Lotz, B.; Wittmann, J. C. *J Polym Sci Polym Phys Ed* **1986**, *24*, 1559.